EXPRESSION OF ARGONAUTE PROTEIN OF *PENAEUS MONODON* AND CHARACTERIZATION OF ITS BIOCHEMICAL FUNCTION

NARAKORN KHUNWEERAPHONG

A THESIS SUBMITTED IN PARTIAL FULFILLMENT
OF THE REQUIREMENTS FOR
THE DEGREE OF MASTER OF SCIENCE
(MOLECULAR GENETICS AND GENETIC ENGINEERING)
FACULTY OF GRADUATE STUDIES
MAHIDOL UNIVERSITY
2006

ISBN 974-04-7670-8

Thesis

Entitled

EXPRESSION OF ARGONAUTE PROTEIN OF *PENAEUS MONODON* AND CHARACTERIZATION OF ITS BIOCHEMICAL FUNCTION

Narakorn Khunweeraphong

Miss Narakorn Khunweeraphong
Candidate

Apinunt Udomkit

Asst. Prof. Apinunt Udomkit, Ph.D.
Major-Advisor

Sakol Panyim

Prof. Emeritus Sakol Panyim, Ph.D.
Co-Advisor

Chalermporn Ongvarrasopone

Lect. Chalermporn Ongvarrasopone, Ph.D.
Co-Advisor

Prof. M.R. Jisnuson Svasti, Ph.D.
Dean
Faculty of Graduate Studies

V. Akkarapatumwong

Asst. Prof. Varaporn Akkarapatumwong, Ph.D.
Chair
Master of Science Programme in
Molecular Genetics and Genetic Engineering
Institute of Molecular Biology and Genetics

Thesis

Entitled

EXPRESSION OF ARGONAUTE PROTEIN OF *PENAEUS MONODON* AND CHARACTERIZATION OF ITS BIOCHEMICAL FUNCTION

was submitted to the Faculty of Graduate Studies, Mahidol University
for the degree of Master of Science (Molecular Genetics and Genetic Engineering)
on
25 September, 2006

Narakorn Khunweeraphong
Miss Narakorn Khunweeraphong
Candidate

U. Akkarapatumwong
Asst. Prof. Varaporn Akkarapatumwong, Ph.D.
Chair

Apinunt Udomkit
Asst. Prof. Apinunt Udomkit, Ph.D.
Member

Sakol Panyim
Prof. Emeritus Sakol Panyim, Ph.D.
Member

Plearnpis Luxananil
Miss Plearnpis Luxananil, Ph.D.
Member

Chalermporn Ongvarrasopone
Lect. Chalermporn Ongvarrasopone, Ph.D.
Member

Prof. M.R. Jisnuson Svasti, Ph.D.
Dean
Faculty of Graduate Studies
Mahidol University

C. Krittanai
Asst. Prof. Chartchai Krittanai, Ph.D.
Acting Director
Institute of Molecular Biology and Genetics
Mahidol University

ACKNOWLEDGEMENTS

This M.Sc. thesis will never be successful without the valuable helps from these people to whom I would like to express my deepest and sincere gratitude.

My advisor, Asst. Prof. Apinunt Udomkit, for his kindness, valuable advice, encouragement, support, every helpfulness and being so nice throughout this study.

Prof. Emeritus Sakol Panyim, for his valuable comments, helpful guidance, supervision and teaching me to think scientifically. I am equally grateful to Dr. Chalermporn Ongvarrasopone and Dr. Plearnpis Luxananil for their valuable advices, discussion and recommendations that have greatly assisted the completion of this study. Asst. Prof. Witoon Tirasophon for his helpfulness for anti-PAZ antibody, providing materials and valuable suggestion.

I am really grateful for the assistance given by Ms. Supattra Treerattrakool for her kindness, encouragement and helpfulness. My appreciation is also expressed to all my lab members for warming and making my laboratory work delightful.

Special thanks are also expressed to Mrs. Busaba Powthongchin from Assoc. Prof. Chanan Angsuthanasombat lab for kindly providing pET-15b vector including recombinant T-CyaA, Miss Nipawan Nuemket from Asst. Prof. Surapon Piboonphokanun lab for recombinant Der p3.1, Mr. Teva Panaksri from Asst. Prof. Witoon Tirasophon lab for given anti-FMDV antibody and Mr. Tawin Iempridee for his knowledge and training technical skill in protein purification.

My sincere appreciation is expressed to all my lecturers for giving knowledge, keen interest and valuable suggestion through all the years at IMBG.

I am greatly indebt to all staffs and my friends for assistance, their precious and memorable friendship. Especially to Miss Nipawan Nuemket and Mr. Chalongrat Noree for their helpfulness, suggestion, support, spirit and discussion in my works.

Finally, I am grateful to express my deepest appreciation and thankfulness to my parents and my family for their entirely care, endless love, support and encouragement throughout my study and my life. They are behind all of my successfulness.

Narakorn Khunweeraphong

EXPRESSION OF ARGONAUTE PROTEIN OF *PENAEUS MONODON* AND CHARACTERIZATION OF ITS BIOCHEMICAL FUNCTION

NARAKORN KHUNWEERAPHONG 4737243 MBMG/M

M.Sc. (MOLECULAR GENETICS AND GENETIC ENGINEERING)

THESIS ADVISORS : APINUNT UDOMKIT, Ph.D., SAKOL PANYIM, Ph.D., CHALERMPORN ONGVARRASOPONE, Ph.D.

ABSTRACT

Argonaute protein is the core component of RISC (RNA-induced silencing complex) that plays a critical role in post-transcritptional silencing of gene expression resulting in sequence-specific mRNA cleavage (siRNA pathway) or translation suppression (miRNA pathway). This mechanism is known as RNA interference (RNAi) which is responsible for antiviral mechanism in eukaryotes. The understanding of RNAi in shrimp is essential for development of an effective viral defense strategy in the future.

Argonaute proteins are defined by the presence of 2 conserved regions, RNA-binding PAZ domain and the endonuclease-like PIWI domains. This study emphasizes the expression of the recombinant Argonaute (Pem-AGO) and PAZ domain proteins of *P. monodon* and characterizes their biochemical function in the RNAi pathway. Recombinant PAZ domain protein was firstly expressed in *Pichia pastoris* expression system. However, the recombinant protein could not be observed in either the intracellular or extracellular compartment. Accordingly, the expression system was altered to *Escherichia coli* (BL21(DE3)pLysS) by utilizing pET-15b as an expression vector to produce the recombinant Pem-AGO and PAZ domain protein as N-terminal hexahistidine fusion-tagged proteins with the molecular weight 108 kDa for Pem-AGO and 19 kDa for PAZ domain protein. The soluble fractions were further purified by Ni^{2+} column affinity chromatography.

The RNA binding activity of the recombinant PAZ domain was investigated by Electrophoretic Mobility Shift Assay (EMSA) with ^{32}P-labeled ssRNA. By using ssRNA, dsRNA or ssDNA as competitors, the result revealed that the PAZ domain binds preferentially to RNA, either single- or double-stranded, rather than to DNA. The function of Argonaute protein in sequence-specific mRNA cleavage was characterized by mRNA cleavage assay. However, the primary attempt on mRNA cleavage assay to determine the function of Argonaute protein has not been successful. The results implied that Pem-AGO should participate in RNAi pathway as it possesses preferential RNA binding activity of the PAZ domain. Nevertheless, it cannot be concluded at this point whether Pem-AGO functions in the siRNA or miRNA pathway.

KEY WORDS: ARGONAUTE/ RNA INTERFERENCE/ RISC/ PAZ/ PENAEUS MONODON

195 P. ISBN 974-04-7670-8

การแสดงออกและการศึกษาคุณลักษณะหน้าที่ทางชีวเคมีของโปรตีน Argonauteในกุ้งกุลาดำ
(EXPRESSION OF ARGONAUTE PROTEIN OF *PENAEUS MONODON* AND CHARACTERIZATION OF ITS BIOCHEMICAL FUNCTION)

นรากร คุณวีระพงศ์ 4737243 MBMG/M

วท.ม. (อณูพันธุศาสตร์และพันธุวิศวกรรมศาสตร์)

คณะกรรมการควบคุมวิทยานิพนธ์ : อภินันท์ อุดมกิจ, Ph.D., สกล พันธุ์ยิ้ม, Ph.D.,
เฉลิมพร องศ์วรโสภณ, Ph.D.

บทคัดย่อ

โปรตีน Argonaute เป็นองค์ประกอบหลักของโมเลกุล RISC ซึ่งทำหน้าที่ควบคุมยีน ทำให้เกิดการตัดสาย mRNA แบบจำเพาะใน siRNA pathway หรือการยับยั้งการสร้างโปรตีนใน miRNA pathway กระบวนการนี้เรียกว่า RNA interference (RNAi) ซึ่งมีบทบาทในการป้องกันไวรัสในสิ่งมีชีวิตหลายชนิด การศึกษาความเข้าใจกระบวนการ RNAi ในกุ้งกุลาดำจึงมีประโยชน์ต่อการพัฒนาวิธีป้องกันโรคไวรัสของกุ้งในอนาคต

โปรตีน Argonaute มี 2 บริเวณอนุรักษ์ ได้แก่ บริเวณ PAZ ที่ใช้จับกับ RNA และ บริเวณ PIWI ที่มีโครงสร้างเหมือน endonuclease งานวิจัยนี้มีวัตถุประสงค์เพื่อทำการแสดงออกและวิเคราะห์หน้าที่ของโปรตีนลูกผสม Argonaute ของกุ้งกุลาดำ (Pem-AGO) และ PAZ domain ในการทดลองนี้ไม่ประสบความสำเร็จในการแสดงออกของโปรตีนลูกผสม PAZ domain ในยีสต์ *Pichia pastoris* ทั้งในรูปของโปรตีนภายในเซลล์และโปรตีนที่หลั่งออกนอกเซลล์ ด้วยเหตุนี้จึงทำการแสดงออกของโปรตีนใน *Escherichia coli* สายพันธุ์ BL21(DE3)pLysS แทน โดยใช้พลาสมิด pET-15b เพื่อสร้างโปรตีนลูกผสมของ Pem-AGO และ PAZ domain ในรูปที่เชื่อมต่อกับ histidine ทางปลายอะมิโน โปรตีนลูกผสมที่แสดงออกมาในรูปที่ละลายน้ำได้ถูกทำให้บริสุทธิ์ก่อนนำไปทดสอบความสามารถในการจับกับ RNA โดยวิธี Electrophoretic Mobility Shift Assay (EMSA) โดยใช้ RNA สายเดี่ยวที่ทำการติดฉลากด้วยสารกัมมันตรังสี พบว่าโปรตีน PAZ สามารถจับกับ RNA สายเดี่ยวและสายคู่ได้ดีกว่าการจับกับ DNA ส่วนหน้าที่ของโปรตีน Argonaute ที่ทดสอบโดยวิธี mRNA cleavage assay เพื่อศึกษาการตัดสาย mRNA แบบจำเพาะ อย่างไรก็ตามการทดลองเบื้องต้นยังไม่ประสบผลสำเร็จ กล่าวโดยสรุป ผลการทดลองจากงานวิจัยนี้แสดงให้เห็นว่า Pem-AGO น่าจะมีบทบาทในกระบวนการ RNAi เนื่องจากมี PAZ domain ที่จับกับ RNA อย่างจำเพาะ ซึ่งเป็นคุณลักษณะอย่างหนึ่งของโปรตีน Argonaute ในกระบวนการ RNAi อย่างไรก็ตามยังไม่สามารถสรุปได้ว่า Pem-AGO ทำหน้าที่ในกระบวนการตัดสาย RNA แบบจำเพาะ (siRNA pathway) หรือ กระบวนการยับยั้งการสร้างโปรตีน (miRNA pathway)

195 หน้า. ISBN 974-04-7670-8

CONTENTS

	Page
ACKNOWLEDGEMENTS	iii
ABSTRACT	iv
LIST OF TABLES	xv
LIST OF FIGURES	xvi
LIST OF ABBREVIATIONS	xx
CHAPTER	
I INTRODUCTION	1
II OBJECTIVES	5
III LITERATURE REVIEW	6
1. RNA Interference Pathway Discovery and Classification	6
2. siRNA Pathway	9
2.1 Mechanism of siRNA Pathway	9
2.1.1 The Initiation Step: Generation of siRNA	9
2.1.2 The Effector Step: Degradation of Target mRNA	10
2.1.3 Amplification of siRNA	10
2.2 Biological Function of siRNA Interference Pathway	11
3. MicroRNA (miRNA)	12
4. The Difference of siRNA and miRNA Pathway	13
5. Machinery of the RNA Interference Pathway	15
5.1 Initiator Machinery: The RNase III Endonuclease Family	15
5.1.1 Drosha: The Initiator Machinery in miRNA Pathway	17
5.1.2 Dicer: The Initiator Machinery in RNA Interference Pathway	17
5.2 Effector Machinery: RISC	20

CONTENTS (Cont.)

6. Argonaute Family Proteins 20
6.1 Biological Function of Argonaute Protein 20
6.2 Argonaute Protein in RNA Interference Pathway 21
6.3 PAZ Domain: RNA Binding Domain 24
6.4 PIWI Domain: Catalytic RNase-H Structure 26

IV MATERIALS 30
4.1 Chemicals 30
4.2 Miscellaneous Materials 30
4.3 Enzymes and Accessory Buffers 31
4.4 Antibodies 32
4.5 Bacterial Strains 32
4.6 Yeast Strains 34
4.7 Vectors and Recombinant Plasmids 34
4.8 Synthetic Oligonucleotides 38
4.8.1 PCR Primers for Amplification of cDNA Encoding *P. monodon*'s *Argonaute* (Pem-AGO) for *Pichia pastoris* Expression System 38
4.8.2 PCR Primers for Amplification of the *P. monodon*'s *PAZ* Region for *Pichia pastoris* Expression System 38
4.8.3 PCR Primers for Amplification of the *P. monodon*'s *Argonaute* cDNA *(Pem-ago)* for *E. coli* Expression System 39
4.8.4 PCR Primers for Amplification of the *P. monodon*'s *PAZ* Region for *E. coli* Expression System 39
4.8.5 PCR Primers for Analyzing of Genome Integration 39
4.8.6 PCR Primers for DNA Sequencing Reactions 40
4.8.7 PCR Primers for Amplification of the GFP Sense-stranded 41
4.8.8 Sense and Anti-sense GFP-siRNA 41
4.8.9 Synthetic Single-stranded DNA 41

CONTENTS (Cont.)

4.9 Culture Media 42
4.9.1 Culture Media for Yeast Expression System 42
4.9.1.1 Bacterial Culture Medium 42
4.9.1.2 Yeast Culture Medium 42
4.9.2 Culture Media for *Escherichia coli* Expression System 43

V METHODS 44
5.1 Plasmid DNA Extraction by Cetyltrimethylammonium Bromide (CTAB) Minipreparation Method 44
5.2 Agarose Gel Electrophoresis 45
5.3 Restriction Endonuclease Digestion 45
5.4 DNA Amplification by Polymerase Chain Reaction (PCR) 46
5.4.1 PCR Amplification of the Coding Region of *Penaeus monodon*'s Argonaute (*Pem-ago*) and the *PAZ* Domain for *Pichia pastoris* Expression System 46
5.4.2 PCR Amplification of the Coding Region of *Penaeus monodon*'s Argonaute (*Pem-ago*) and the *PAZ* Domain for *Escherichia coli* Expression System 47
5.4.3 PCR Amplification of GFP Sense-strand Template 48
5.5 Recovery and Purification of DNA Fragments 49
5.5.1 Purification of DNA from Agarose Gel by QIAquick® Gel Extraction Kit 49
5.5.2 Purification of DNA from PCR and Enzymatic Reactions by QIAquick® PCR Purification Kit 50
5.6 Dephosphorylation of Linearlized Plasmid 50
5.7 DNA Ligation 50
5.8 Transformation of Recombinant Plasmids by Heat-shock Method 51
5.8.1 Preparation of Competent Cells by the $CaCl_2$ Method 51
5.8.2 Transformation of Plasmid DNA into Competent Cells 51
5.9 Screening for the Recombinant Clones 52

CONTENTS (Cont.)

5.9.1 Screening by Rapid Size-Screening 52
5.9.2 Screening by Restriction Digestion Analysis 52
5.10 DNA Sequencing 52
5.11 *Pichia pastoris* Expression System 52
5.11.1 Preparation of *P. pastoris* Competent Cells 52
5.11.2 Preparation of Linearized Recombinant Plasmid 53
5.11.3 Transformation of *P. pastoris* Competent Cells by Electroporation 53
5.11.4 Total DNA Isolation from *P. pastoris* 54
5.11.5 PCR Analysis of *P. pastoris* Integrants 54
5.11.6 Screening of the *P. pastoris* Integrants by Colony PCR Method 55
5.11.7 Expression of Recombinant Proteins in *P. pastoris* System (Small Scale) 56
5.11.8 Protein Sample Preparation from *P. pastoris* Expression 56
5.11.8.1 TCA Precipitaiton for Extracellular Expression Analysis 56
5.11.8.2 Sample Preparation for Intracellular Protein Expression 57
5.12 *Escherichia coli* Expression System 57
5.12.1 Small Scale Expression of Recombinant Protein in *E. coli* 57
5.12.2 Large Scale Expression of Recombinant Protein in *E. coli* 58
5.13 Purification of the Soluble Recombinant Histidine-tagged Proteins 58
5.14 Determination of Protein Concentration 59
5.15 SDS-Polyacrylamide Gel Electrophoresis (SDS-PAGE) 60
5.15.1 Sample Preparation from Crude Cell Extract 60
5.15.2 Sample Preparation from Fractionated Purified Protein 60

CONTENTS (Cont.)

5.15.3 Sample Preparation for Dot Blot Analysis 60
5.15.4 Seperation of Protein Samples (Protein Electrophoresis) 61
5.16 Western Blot Analysis 62
5.16.1 Electrotransfer of Protein from SDS-PAGE to Nitrocellulose Membrane by Semi-Dry Blot 62
5.16.2 Electrotransfer of Protein from SDS-PAGE to Nitrocellulose Membrane by Wet Blot 62
5.16.3 Detection of the Recombinant Hexahistidine Tagged Protein by Colorimetric Method 63
5.17 Synthesis of Single-stranded RNA by *In vitro* Transcription Reaction using Ribomax™ Large Scale RNA Production System-T7 RNA Polymerase (Promega) 64
5.18 Determination of RNA Concentration and Visualization by Electrophoresis 65
5.19 Electrophoresis of RNA 65
5.19.1 Gel Preparation 65
5.19.2 RNA Sample Preparation for Electrophoresis 65
5.20 Labeling at 5' End of Single-stranded RNA 66
5.20.1 Dephosphorylation of 5' End by Alkaline Phosphatase 66
5.20.2 Labeling of [γ-^{32}P]ATP to the 5' End of ssRNA by T4 Polynucleotide Kinase 67
5.21 Electrophoretic Mobility Shift Assays (EMSA) 67
5.21.1 Non-Denaturing Polyacrylamide Gel Electrophoresis 67
5.21.2 Electrophoretic Mobility Shift Assay Reaction 68
5.22 RISC Activity Assay 69
5.22.1 Formaldehyde Gel Electrophoresis 69
5.22.2 mRNA Cleavage Assay Reaction 69

VI RESULTS PART I 70
6.1 Restriction Analysis of pUC19/*Pem-ago* Recombinant Plasmid 70

CONTENTS (Cont.)

6.2 Construction of pPICZαA/*Pem-ago* and pPICZαA/*PAZ* Expression Recombinant Plasmid for *P. pastoris* Expression System 72

6.2.1 Amplification of cDNA Encoding Pem-AGO and PAZ Domain for *Pichia pastoris* Expression System 72

6.2.2 Cloning of DNA Fragments into pPICZαA Vector 76

6.2.3 Screening of the Recombinant Clones 76

6.3 Nucleotide and Deduced Amino Acid Sequence Analysis of cDNA Encoding Argonaute and PAZ Domain of *Penaeus monodon* 84

6.4 Transformation and Integration of *PAZ* Fragment into *P. pastoris* Genome 88

6.4.1 Transformation of *PAZ* Fragment into *P. pastoris* Genome 88

6.4.2 Determination of *PAZ* cDNA in *P. pastoris* Genome 88

6.5 Expression of the Recombinant PAZ Domain in *P. pastoris* 90

6.5.1 Expression of Secreted Recombinant PAZ Protein in Culture Medium 90

6.5.2 Optimization of the Expression Conditions for the Recombinant PAZ Domain Protein in *P. pastoris* Expression System 90

VII RESULTS PART II 96

7.1 Construction of pET-15b/*Pem-ago* and pET-15b/*PAZ* Expression Recombinant Plasmids for *E. coli* Expression System 96

7.1.1 Amplification of cDNA Encoding *P.monodon*'s Pem-AGO and PAZ Domain for *E. coli* Expression System 97

CONTENTS (Cont.)

7.1.2 Cloning of DNA Fragments into pET-15b Vector 100

7.1.3 Screening of the Recombinant Clones 100

7.2 Nucleotide and Deduced Amino Acid Sequence Analysis of the cDNA Encoding Argonaute and PAZ Domain of *Penaeus monodon* 103

7.3 Expression of the Recombinant Pem-AGO Protein in *E. coli* Strain BL21(DE3)pLysS 107

7.3.1 Pem-AGO Protein Expression of the Positive Clone No. 1 to 6 107

7.3.2 Optimization of Recombinant Pem-AGO Expression from pET-15b/*Pem-ago* Recombinant Plasmid in *E. coli* Strain BL21(DE3)pLysS 109

7.3.3 Optimization of the Expression Temperature and IPTG Concentration Induction of the Pem-AGO Protein in *E. coli* Strain BL21(DE3)pLysS 109

7.3.4 Determination of the Recombinant Pem-AGO Protein in Inclusion and Soluble Fractions 112

7.4 Expression of the Recombinant PAZ Domain in *E. coli* Strain BL21(DE3)pLysS 115

7.4.1 Optimization of the Expression Period of the PAZ Domain Protein from pET-15b Recombinant Plasmid in *E. coli* Strain BL21(DE3)pLysS 115

7.4.2 Optimization of the Expression Temperature and IPTG Concentration of the Pem-PAZ Domain in *E. coli* Strain BL21(DE3)pLysS 115

7.4.3 Determination of the Recombinant PAZ Domain Protein in Inclusion and Soluble Fractions 118

CONTENTS (Cont.)

7.5 Purification of the Recombinant Pem-AGO and Recombinant PAZ Domain Proteins 121

7.5.1 Purification of Recombinant AGO Fusion Protein Under Native Condition by Immobilized Affinity Column (IMAC) 121

7.5.2 Purification of Recombinant PAZ domain Under Native Condition by Immobilized Affinity Column (IMAC) 124

7.6 Stability of the Recombinant Proteins When Exposed to Different Temperatures 127 127

7.7 Electrophoretic Mobity Shift Assay (EMSA) 129

7.7.1 Optimization of the Amount of PAZ Protein in the Reaction 129

7.7.2 Determination of Specific RNA-Binding Activity of the Recombinant PAZ Domain Protein 131

7.7.3 Determination of the Protein that Binds to RNA by Supershift EMSA 133

7.8 Determination of RISC Activity of Recombinant Pem-AGO by mRNA Cleavage Assay 135

VIII DISCUSSION 138

1. Expression in *Pichia pastoris* System 138

1.1 Construction of *P. monodon*'s Argonaute (Pem-ago) and PAZ Domain Protein in pPICZαA Vector 139

1.2 Expression of the Recombinant *PAZ* in *P. pastoris* System 140

2. Expression in *Escherichia coli* System 142

2.1 Expression of the Recombinant Pem-AGO Protein in *E. coli* Strain BL21(DE3)pLysS 142

CONTENTS (Cont.)

2.2 Expression of the Recombinant PAZ Domain in *E. coli* Strain BL21(DE3)pLysS 143

2.3 Purification of the Recombinant Pem-AGO and Recombinant PAZ Domain Proteins 144

2.4 Functional Characterization of the Recombinant *P. monodon*'s PAZ Domain by Electrophoretic Mobility Shift Assay 145

2.5 Functional Characterization of Recombinant *P. monodon*'s Argonaute Protein 148

IX CONCLUSION 152

REFERENCES 155

APPENDIX 169

BIOGRAPHY 173

LIST OF TABLES

Tables		Page
3.1	Different types of endogeneous small RNA	8
4.1	Restriction enzymes used in this thesis with their recognition sites, incubation temperature, recommendation reaction buffers and manufacturers	31
5.1	PCR profile for amplification of the coding region of *Penaeus monodon*'s Argonaute (*Pem-ago*) and the *PAZ* domain for *Pichia pastoris* expression system	47
5.2	PCR profile for amplification of the coding region of *Penaeus monodon*'s Argonaute (*Pem-ago*) and the *PAZ* domain for *Escherichia coli* expression system	47
5.3	PCR profile for amplification of GFP sense-strand	48
5.4	PCR parameter profile for screening of *P. pastoris* integrants	55
5.5	Preparation of SDS-PAGE gel	62

LIST OF FIGURES

Figures		Page
1.1	Lateral view of the external morphology of *Penaeus monodon*	2
3.1	The model for the biogenesis and post-transcriptional suppression of microRNAs and small interfering RNAs	14
3.2	Schematic structures illustrate three classes of RNase III endonuclease enzyme	16
3.3	Crystal structure of *Giardia* Dicer	18
3.4	Model for Dicer catalysis process by Zhang *et al.*, 2004	19
3.5	Crystal structure of *Pyrococcus furiosus* Argonaute	23
3.6	Stereo ribbon diagram shows the structure of *Drosophila* Ago2-PAZ	25
3.7	Stereo ribbon diagram shows the structure of *Archaeoglobus fulgidus* PIWI	27
3.8	Comparison tertiary structure between domain B of *Archaeoglobus fulgidus* PIWI domain and RNase HII from *Methanococcus jannaschii*	28
3.9	Ribbon diagrams of the PIWI domain, *Escherichia coli* RNase HI and *Methanococcus jannaschii* RNase HII	29
4.1	Physical map of pLysS plasmid	33
4.2	Physical map of pPICZαA vector	35
4.3	Physical map and cloning region of plasmid pET-15b	37
6.1	Restriction digestion analysis of pUC19/Argonaute recombinant plasmid	71
6.2	A schematic diagram represents the cDNA encoding Pem-AGO containing the regions of PAZ and PIWI domains and the binding sites of primers for cloning into pPICZαA vector	73
6.3	Amplification of *Pem-ago* cDNA for *P. pastoris* expression system	74
6.3	Amplification of *Pem-ago* cDNA for *P. pastoris* expression system	75
6.5	Screening of the recombinant pPICZαA/*Pem-ago* clones by rapid size screening	77

LIST OF FIGURES (Cont.)

6.6	Screening of the recombinant pPICZαA/*Pem-ago* clones by restriction enzyme digestion with *Xho* I & *Sal* I (cloning sites)	78
6.7	Screening of the recombinant pPICZαA/*Pem-ago* clones by internal digestion with *Xmn* I and *Dra* I	79
6.8	Screening of the recombinant pPICZαA/*PAZ* by rapid size screening	80
6.9	Screening of the recombinant pPICZαA/ *PAZ* by restriction cloning enzyme digestion with *Xho* I & *Sal* I (cloning sites)	81
6.10	Screening of the recombinant pPICZαA/ *PAZ* by internal digestion with *Dra* I & *Bgl* II	82
6.11	Screening of the recombinant pPICZαA/*PAZ* by PCR amplification analysis	83
6.12	The alignment of nucleotide sequences at the 5'end of the recombinant pPICZαA/Pem-AGO of five individual clones	85
6.13	The alignment of nucleotide sequences at the 3'end of the recombinant pPICZαA/Pem-AGO of five individual clones	86
6.14	The alignment of nucleotide sequences of the recombinant pPICZαA/PAZ from three individual clones	87
6.15	Colony PCR screening for integration of pPICZαA/*PAZ* recombinant plasmid into the genome of *P. pastoris* transformants	89
6.16	SDS-PAGE analysis of the recombinant PAZ protein expression in the culture medium under 1% (v/v) methanol induction for 5 days	91
6.17	Western Blot analysis of expressed intracellular recombinant PAZ domain protein from crude cell lysate	92

LIST OF FIGURES (Cont.)

6.18	SDS-PAGE analysis of the recombinant PAZ protein expression that was induced with 3% (v/v) methanol for 0 to5 days	94
6.19	SDS-PAGE and Western Blot analysis of the recombinant PAZ protein expression from supernatant and crude cell lysate under 0 to 5 % (v/v) methanol induction for 2 days	95
7.1	A schematic diagram represents the binding sites of primers on Pem-AGO cDNA template	97
7.2	Amplification of *Pem-ago* cDNA for construction in *E. coli* expression system	98
7.3	Amplification of *P.monodon*'s PAZ domain for construction in *E. coli* expression system	99
7.4	Screening of the recombinant pET-15b/*Pem-ago* clones by restriction enzyme digestion with *Nde* I and *Bam*H I (cloning sites)	101
7.5	Screening of the recombinant pET-15b/*PAZ* by restriction cloning enzyme digestion with *Nde* I and *Bam*H I (cloning sites)	102
7.6	The alignment of nucleotide sequences of pET-15b/Pem-AGO from clone no. 116	105
7.7	The alignment of nucleotide sequences of pET-15b/PAZ from clone no. 1 and 2 respectively	106
7.8	SDS-PAGE and Western blot analysis of the Pem-AGO from BL21(DE3)pLysS/pET-15b/Pem-AGO expression clones	108
7.9	Western Blot analysis of recombinant Pem-AGO expression from clone no.3 at various periods of induction	110
7.10	SDS-PAGE and Western Blot analysis of Pem-AGO expession from clone no.3 expression at various temperatures and IPTG concentrations	111
7.11	SDS-PAGE and Western Blot analysis of Pem-AGO fusion protein in inclusion and soluble fractions	113

LIST OF FIGURES (Cont.)

7.12	Dot Blot analysis of Pem-AGO fusion protein form	114
7.13	SDS-PAGE and Western Blot analysis of recombinant PAZ domain expression at different period of incubation time	116
7.14	SDS-PAGE and Western Blot analysis of recombinant PAZ domain expression at the various temperature and IPTG concentration	117
7.15	SDS-PAGE and Western Blot analysis of recombinant PAZ domain fusion protein in inclusion and soluble fractions	119
7.16	Dot Blot analysis of recombinant PAZ domain fusion protein	120
7.17	SDS-PAGE analysis of purification profile of the recombinant Pem-AGO under native condition by Ni^{2+} affinity chromatography	122
7.18	Western Blot analysis of the Ni^{2+} affinity chromatography purified recombinant Pem-AGO	123
7.19	SDS-PAGE analysis of purification profile of the recombinant PAZ under native condition by Ni^{2+} affinity chromatography	125
7.20	Western Blot analysis of the Ni^{2+} affinity chromatography purified recombinant Pem-PAZ	126
7.21	Western Blot analysis with anti-His antibody of the recombinant Pem-AGO after incubating at various temperatures for 4 hours	127
7.22	Western Blot analysis with anti-His antibody of the recombinant Pem-PAZ after incubating at various temperatures for 4 hours	128
7.23	RNA Electrophoretic Mobility Shift Assay of *P. monodon*'s PAZ domain protein	130
7.24	RNA electrophoretic mobility shift assay assessing RNA binding of *P. monodon's* PAZ domain in the presence of competitors	132
7.25	Supershift of RNA electrophoretic mobility shift assay assessing RNA binding of *P. monodon's* PAZ domain in the presence of antibodies	134
7.26	*In vitro* Transcription of sense-GFP	136
7.27	mRNA cleavage assay	137

LIST OF ABBREVIATION

AGO	Argonaute
AOX	alcohol oxidase gene
A. aeolicus	*Aquifex aeolicus*
A. fulgidus	*Archaeoglobus fulgidus*
BCIP	5-bromo-4-chloro-3-indolyl phosphate
bp	base pair
BM	Buffered minimal complex medium
BMGY	Buffered minimal glycerol complex medium
BSA	bovine serum albumin
^{o}C	degree Celsius
cDNA	complementary DNA
C. elegans	*Caenorhabditis elegans*
CTAB	cetyltrimethylammoniumbromide
C-terminal	carboxy terminal
DNA	deoxyribonucleic acid
dNTP	deoxyribonucleotide triphosphate
D. melanogaster	*Drosophila melanogaster*
ds	double stranded
DTT	1, 4-dithiothreitol
E. coli	*Escherichia coli*
FMDV	foot mouse disease virus
g	gram
G. lamblia	*Giardia lamblia*
hr	hour
IPTG	isopropyl-β-D-thiogalactopyranoside
kb	kilobase pair (s)
kDa	kilodalton (s)

LIST OF ABBREVIATIONS (Cont.)

LB	Luria-Beriani (medium)
M	molar
mA	milliampere
mg	milligram
min	minute (s)
ml	milliliter
mM	millimolar
MOPS	4-morpholinepropanesulfonic acid
µg	microgram
µl	microliter
µM	micromolar
NaCl	sodium chloride
ng	nanogram
NBT	nitroblue tetrazolium
nM	nanomolar
nm	nanometer (s)
nt	nucleotide (s)
N-terminal	amino terminal
miRNA	microRNA
OD	optical density
PAZ	Piwi/Argonaute/Zwille
PCR	polymerase chain reaction
Pem-AGO	*Penaeus monodon*'s Argonaute
P. furiosus	*Pyrocuccus furiosus*
pM	picomolar
P. monodon	*Penaeus monodon*
P. pastoris	*Pichia pastoris*
p.s.i.	pounds per square inch
PBS	phosphate buffer saline
PTGS	post-transcriptional gene silencing

LIST OF ABBREVIATIONS (Cont.)

RdRP	RNA-dependent RNA polymerase
RISC	RNA-induced silencing complex
RNA	ribonucleic acid
RNAi	RNA interference
RNase	ribonuclease
RNasein	RNase inhibitor
rpm	revolutions per minute
SDS	sodium dodecyl sulfate
SDS-PAGE	sodium dodecyl sulfate-polyacrylamide gel electrophoresis
sec	second (s)
siRNA	small interfering RNA
ss	single stranded
TEMED	N, N, N', N' tetramethylenediamine
TGS	transcriptional gene silencing
T_m	melting temperature
T4 PNK	T4 polynucleotide kinase
U	unit (s)
UV	ultraviolet
V	volt
v/v	volume / volume
w/v	weight / volume
WSSV	white spot syndrome virus
YEPD	yeast extract peptone dextrose
YHV	yellow head virus

CHAPTER I
INTRODUCTION

The black tiger shrimp or *Penaeus monodon* (Figure 1.1) is the economically important marine animal which is widely distributed through tropical and subtropical areas of South-East Asia including Thailand. The shrimp industrial activity provides high commercial exported value per year. Within the past decade, the shrimp industry developed rapidly with a little increase in scientific knowledge to support the new farming techniques and management that caused many consequent problems in shrimp aquaculture, for instance, ecological problem, agricultural pollution, the retardation of gonad maturation and, particularly, the outbreak of several diseases. The deteriorate infectious diseases in shrimp farming are mainly caused by viruses including yellow head virus (YHV) and white spot syndrome (WSSV) and bacteria belonging to Vibrionacea family. These situations are critical problems that resulting in the reduction of the quality and outcome of prawn products and high economic losses.

In order to overcome these problems, the study in molecular knowledge in shrimp pathology including the functional, biochemical and genetic characterization of defense mechanism is required in shrimp aquaculture to improve the application method for efficient detection and diagnosis (Bachere, 2000). Moreover, the prevention and control of diseases are now the priority for the durability of this industry (website: http://www.ifremer.fr/incodc/).

Figure 1.1 Lateral view of the external morphology of *Penaeus monodon* or Black tiger shrimp (Taken from website: http://www.ifremer.fr/incodc/)

The taxonomy definition of the black tiger shrimp (*Penaeus monodon*) is as follows (Bailey-Brock and Moss, 1992)

Phylum	:	Arthropoda
Class	:	Crustacea
Subclass	:	Malacostraca
Order	:	Decapoda
Suborder	:	Natantia
Superfamily	:	Penaeoidea
Family	:	Penaeidae Rafinesque
Genus	:	*Penaeus Fabricius*
Subgenus	:	*Penaeus*
Species	:	*Penaeus monodon*

The living things respond to the invading pathogenic agents by induction of the immune system from host cell. The defense mechanisms in invertebrate animals do not possess an adaptive immune response that involves immunologic memory and specificity. Instead, it relies on innate immune system which consists of cellular response via phagocyte, an inducible antibacterial peptides and phenoloxidase cascade through melanin production (Englemann *et al*., 2005, Little *et al*., 2005, Soderhall and Thornqvist, 1997). Due to the lack of information of acquire immune system that employs B cell, T cell and major histocompatibility complex molecule as the cores, the immune system in invertebrate animals including *Penaeus monodon* may lose the ability of memory and specificity (Destoumieux-Garzon *et al*., 2001). However, there are evidences revealing that invertebrate animals possess the property of memory in immunity (Kurtz *et al*., 2003; Wittlveldt *et al*., 2004)

RNA interference (RNAi) is a highly conserved mechanism that functions in many different cellular pathways to regulate gene expression, control gene activity, be involved in development and act as adaptive immune system to defense viral infection (Geley and Muller, 2004) by degrading target mRNA in a sequence-specificity manner (Williums and Rubin, 2002) as well as translation suppression. This mechanism is mediated by ribonucleoprotein complex called RISC or RNA-induced silencing complex that contains Argonaute family protein as a key component. The

understanding of RNAi may then shed light on genome defense and endogeneous developmental pathway (Williums and Rubin, 2002; Yan *et al.*, 2003) which may be applied for the prevention of viral infection.

At present, RNAi pathway in *Drosophila* (Phylum: Arthopoda) was discovered and characterized (Pham and Sontheimer *et al*., 2005; Kavi *et al*., 2005). There are many evidences that support the existing of RNAi mechanism in Phylum Arthopoda. However, the understanding of this pathway in shrimp is still obscured and the study in shrimp is required.

In previous study in our laboratory, the cDNA encoding Argonaute protein of *Penaeus monodon* which contains PAZ and PIWI domains had been cloned into pUC19 vector in *E. coli*. The goal of this project is to elucidate the biochemical function of Argonaute protein of *Penaeus monodon* in RNAi pathway. The cDNA encoding Argonaute protein as well as PAZ domain will be cloned into expression vector. The recombinant Argonaute proteins will be characterized for the functions of siRNA-dependent RNA endonuclease by mRNA cleavage assay, whereas the recombinant PAZ domain was characterized for the function of RNA-binding domain by Electrophoretic Mobility Shift Assay (EMSA).

In mammalian system, an understanding of how siRNA acts is important for refining this gene silencing technology and for producing gene-specific therapeutic agent in the future (Martinez *et al.*, 2002; Ito *et al.*, 2005; Uprichard *et al.*, 2005). Similarly, the study of RNAi mechanism especially the key component including RISC, in shrimp is preliminarily required with the anticipation that RNA interference (RNAi) is one of the techniques in molecular mechanisms that is being developed with an attempt to be applied for inhibition the viral infection in this economically important animal.

CHAPTER II
OBJECTIVES

1. Rationale

Black tiger shrimp (*Penaeus monodon)* is an economically important aquatic animal which provides high exported value annually. However, the major problem in shrimp farming is the viral infection that resulting in low quality and high mortality of shrimp products. Nowadays, there is no effective prevention method available to protect the shrimp for these diseases. As it has been known that RNA interference is responsible for viral defense mechanism in many organisms, the knowledge of this mechanism will be an alternative application for shrimp viral defense strategy in the future. However, the understanding of this mechanism in shrimp is still insufficient. Accordingly, the study of the function mechanisms as well as machinery components is need.

2. Hypothesis

The recombinant Argonaute protein and PAZ domain of *Penaeus monodon* play functional role in RNA interference pathway.

3. Objectives

The objectives of this project are:

- To express the recombinant *Penaeus monodon*'s Argonaute protein and to characterize its function in siRNA-dependent RNA cleavage.
- To express the recombinant PAZ domain of *Penaeus monodon* and to characterize the function of RNA-binding domain.

CHAPTER III
LITERATURE REVIEW

Many organisms possess various mechanisms that are responsible for their living in order to apply to all natural processes. Gene silencing is an evolutionarily conserved phenomenon that regulates gene expression at either transcriptional or post-transcriptional level (Pal-Bhadra *et al.*, 2002). The transcriptional gene silencing (TGS) occurs during transcriptional process through heterochromatin formation, programmed genome rearrangement, RNA-directed DNA methylation, meiotic silencing by unpaired DNA and histone modification by suppression of transcription (Cerutti *et al.*, 2006). In contrast, post-transcriptional gene silencing (PTGS) mechanism regulates gene expression at the level of mRNA stability and protein translation through degradation of target mRNA as well as translational suppression in a sequence-specific manner. These phenomena are known as RNA interference or RNAi (Agrawal *et al.*, 2003; Chicas and Macino *et al.*, 2001).

1. RNA Interference Pathway Discovery and Classification

RNA interference or post-transcriptional gene silencing is an ancient regulatory phenomenon that is conducted by small regulatory RNAs approximately 21-23 nucleotides in length, which are derived from the processing of long double-stranded RNA (dsRNA) in order to regulate sequence-specific gene expression in post-transcriptional level (Hannon , 2002). The RNA silencing phenomena was first discovered in 1990 in plants by the scientists who tried to enhance the color of petunia flower by introducing numerous copies of a gene encoding enzyme for deep purple flower. However, not as expected, many petunia flowers did not show the darker color but rather presented in white or patchy flowers (Napoli *et al.*, 1990). Until in 1998, Fire *et al.* discovered that the injection of dsRNA mixture into the nematode *Caenorhabditis elegans* was more potent for homology-dependent gene silencing than sense or antisense RNAs alone. This sequence-specific gene silencing mechanism that

is triggered by double-stranded RNA (dsRNA) was named RNA interference or RNAi (Fire *et al*., 1998). Since the discovery of this phenomenon, the study of RNAi has emerged in many organisms. This RNAi mechanism has been demonstrated to be an evolutionarily conserved gene regulation pathway in a variety of organisms from yeast to human including protozoa, nematodes, parasites, insects, invertebrates, vertebrates, mouse and human (Tuschl and Meister, 2004; Cogoni and Macino,2000) with the crucial function as an innate immunity containing the properties of sequence-specificity against the viral RNA (Waterhouse *et al*.,2001) or mobile genetic elements (Ketting *et al*., 1999) by the cleavage or translational repression of complementary single-stranded target mRNAs (Geley and Muller, 2004). In addition, some small RNAs play an important role in the developmental control in eukaryote. The classification of RNAi pathway was based on the origin and function of small RNAs that are distinct in the RNA silencing effector complex in different organisms. Currently, the small RNAs are classified into 4 types, microRNA (miRNA), siRNA, rasiRNA and tncRNA as illustrated in table 3.1 (Aravin and Tuschl, 2005). The gene silencing effects from dsRNA exhibit at least four different types of responses, chromosomal rearrangement, inhibition of transcription, degradation of mRNAs and protein translation inhibition and (Agami *et al*.,2002) depend on the type of small regulatory RNA. SiRNA and miRNA are well characterized small regulatory RNA that seems similar in their biogenesis, molecular characteristics, effector functions. These two types of small RNA also share some related RNAi mechinery to each other. The RNA interference pathways are named according to the type of small regulatory RNA, for example siRNA or miRNA pathway for the silencing pathways mediated by siRNA or miRNA, respectively. The model for microRNA and siRNA is illustrated in figure 3.1.

Table 3.1 Different types of endogenous small RNA (Aravin and Tuschl, 2005)

Class of small RNA	Size of mature form (nt)	Structure of precursor	Biogenesis	Mechanism of action	Organism
miRNA	20-23	Imperfect hairpin	Successive cleavage by Drosha and Dicer resulting in a mature form with defined sequence	Translational repression, mRNA cleavage	*C. elegans* *D. melanogaster* *X. laevis* *D. rerio* *Mammals* *Plants* *Viruses*
rasiRNA	23-28	Long dsRNA	Processing of long dsRNA by Dicer resulting in multiple short RNAs	Regulation of chromatin structure, transcriptional silencing	*S. pombe* *T. brucei* *C. elegans* *D. melanogaster* *D. rerio* *A. thaliana*
Endogenous siRNA	20-23	Long dsRNA	Processing of long dsRNA by Dicer. Biogenesis requires RdRP activity	mRNA cleavage	*C. elegans* *A. thaliana*
tncRNA	19-23	Unknown	Unknown. Mature forms have defined sequence	Unknown	*C. elegans*

2. siRNA Pathway

2.1 Mechanism of siRNA Pathway

The RNA interference (RNAi) pathway is triggerred by the presence of double-stranded RNA (dsRNA) that is either an RNA duplex or extended hairpin, experimentally introduced RNA duplex, naturally generated dsRNA, product synthesized from RNA-dependent RNA polymerase (RdRp) (in plants, fungi and nematode), mobile transposable genetic elements or viral RNA (Denli and Hannon, 2003). The long dsRNAs are processed into small fragment RNAs called small interfering RNA or siRNA which is defined as a short RNA duplex, 21-23 nt in length with 19-21 basepair RNA core duplex that harbors 5' phosphate and 2 nucleotides overhang at 3' hydroxyl termini (Zamore *et al*., 2000). The mechanism of RNAi can be divided into two main steps: the first step is initiation step which is the processing of long dsRNA into siRNA by RNase III family enzyme namely Dicer, and the second step is effector step that is involved in the repression of target mRNA after the assembly of siRNA into effector complex, RISC (RNA-induced silencing complex) that contains Argonaute family protein as a core component, leading to cleavage of homologous mRNA.

2.1.1 The Initiation Step: Generation of siRNA

The long double-strand RNA or primary transcripts that present in the cell was recognized and stepwise processed by Dicer, a member of RNase III family (Bernstein *et al*., 2001; Meister *et al*., 2004; Sontheimer, 2005; Tomari and Zamore, 2005) that cleaves long dsRNA into small RNA duplexes approximately 21-23 nucleotides in length harboring 5' phosphate and 2 nucleotide overhang at 3' end which is the characteristic of the cleavage product from the function of RNase III family endonuclease (Blaszczyk *et al*., 2001). The *in vivo* and *in vitro* experiments in *Drosophila* have revealed that this step required ATP and the rate of siRNA formation was also controlled by the ATP level (Lee *et al*., 2004; Liu *et al*., 2003; Nykanen *et al*., 2001). However, in human Dicer, ATP-dependent process has not been observed (Provost *et al*., 2002; Zhang *et al*., 2002). Therefore the necessary of utilizing ATP for the activity of Dicer is still unclear.

2.1.2 The Effector Step: Degradation of Target mRNA

The effector step is a multiple step processes that is crucial for a variety of silencing pathways (Almeida and Allshire *et al*., 2005). The small dsRNA duplex is unwound in an ATP-dependent process (Nykanen *et al*., 2001) and one of the RNA strand is incorporated into the multiprotein complex called RNA-induced silencing complex or RISC (Hammond *et al*., 2000; Tang, 2005; Martinez *et al*., 2002). The determination of selective siRNA strand to be incorporated into RISC depends on the relative stability of the two ends (Aza-Blanc *et al*., 2003; Khvorova *et al*., 2003). RISC contains Argonatue family protein as a core component. Argonaute family proteins are characterized by the presence of 2 conserved regions named PAZ and PIWI domains that are responsible in different functions. The activated RISC functions as multiple-turnover enzyme to recognize and cleave cognate RNA which is complementary to the incorporated single-stranded siRNA. This activity is called "slicer" activity (Meister *et al*., 2004; Sontheimer, 2005; Tomari and Zamore, 2005). The mRNA is cleaved between the nucleotides paired to the position of 10 and 11 of siRNA (Elbashir *et al*., 2001). The cleavage is magnesium-dependent that requires a divalent metal ion for their activity (Martinez and Tuschl, 2004; Schwarz *et al*., 2004). The PAZ domain of Argonaute possesses the function of RNA-binding domain that interacts with 3' end of siRNA and uses this siRNA as a guide to select the binding to sequence-specific target mRNA by Watson-Crick base pairing whereas the PIWI domain that illustrates RNase H-like structure is responsible for the degradation or translation repression of the homologous mRNA. The formation of the effector complex leads to the cleavage of sequence-specific mRNA at the specific site by the RNase-H like activity of the PIWI domain and, accordingly, produces the cleavage products that can be recognized by the cell as an aberrant transcript before being destroyed by nucleases within the cell.

2.1.3 Amplification of siRNA

In plants, fungi and nematode but not mammals, there is an interesting phenomenon that a few dsRNA can efficiently degrade target transcripts for a long time and extend to the next generation and wide spread from cells to cells. Therefore it has been suspected that RNAi pathway may also involve amplification step. In plants, the aberrant RNA can serve as a template for RNA-dependent RNA polymerase

(RdRP) (Wassenegger *et al*., 2006) to generate dsRNA from single-stranded transcripts *de novo* (Cerutti *et al*., 2006) without priming and then be as substrate for Dicer. In fungi and nematode, the amplification of siRNA is beginning by using siRNAs as a primer to synthesize RNA complementary to the target mRNA. The binding of single-stranded siRNA to their target mRNA in a sequence-specific manner and amplification of dsRNA will enhance the RNAi response (Baulcombe, 2004). This amplification of siRNA leads to spreading between cells.

2.2. Biological Function of siRNA Interference Pathway

RNA interference is activated through the induction of dsRNA resulting in sequence-specific transcript degradation as well as transcriptional repression. This silencing phenomenon is evolutionarily conserved that has been observed in various organisms with the critical function in antiviral mechanism (Ye K *et al*., 2003), described as an adaptive cellular immune system defense against viral infection, that is conserved among eukaryotes to protect organisms from invading nucleic acid including viral RNA (Plasterk, 2002). The transposition of transposable elements which produces aberrant RNA or dsRNA in the host cell is silenced by RNAi mechanism as has been revealed in *C. elegans* germ line after exposure to homologous dsRNA (Sijen and Plasterk, 2003). Recently, there is the evidence illustrated that gene silencing may induce the antiviral immunity system through either sequence-dependent or sequence-independent pathway to protect yellow head virus (YHV) infection in *Penaeus monodon* (Yodmuang *et al*., 2006). This knowledge is a perspective sign in the future application for antiviral mechanism in invertebrate animals. Although RNA interference was previously described as post-transcription gene silencing mechanism that regulates gene expression in the level of post-transcription through the induction of small RNA, there are evidences revealed that the components in RNAi machinery can regulate gene expression in transcription level by nuclear processing through heterochromatin formation resulting in transcription gene silencing (TGS) (Wassenegger, 2005; Holmquist, 2006; Grewal and Rice, 2004). The study in yeast *Schizosaccharomyces pombe* showed that siRNA or miRNA are required for methylation of lysine 9 on histione H3 and then for the recruitment of the remodelling factor HP1; a silencing process in heterochromatin, that regulates proper

centromere and telomere function to maintain the centromeric heterochromatin (Volpe *et al*., 2002; Provost *et al*., 2002; Hall, 2003). However, the effector complex of transcriptional level gene silencing, namely RITS (RNA-induced initiation of transcriptional gene silencing), is distinct from RISC (Sigova *et al*., 2004; Verdel *et al*., 2004)

3. MicroRNA (miRNA) (He and Hannon, 2004; Bartel, 2004)

MicroRNA (miRNA) is a class of small non-coding RNA with 21-25 nt in length that functions in RNA interference pathway to negatively regulate gene expression by inhibiting the sequence-specific protein translation (Ambros, 2003; Meister *et al*., 2004; Bartel, 2004). They were initially discovered as small temporal RNAs (stRNAs) in *C. elegans* that function in the regulation of larval developmental transitions and physiology (Pasquinelli *et al*., 2002; Bartel, 2004; Carringtom *et al*., 2003). In addition, the control of cell proliferation, cell apoptosis and fat metabolism in *Drosophila melanogaster*, neuronal patterning in nematodes, modulation of haematopoietic lineage differentiation in mammals, organ development and the control of leaf and flower development in plants were also reported to be regulated by miRNA (He and Hannon, 2004; Wienholds and Plasterk, 2005; Kim, 2005; Baulcombe, 2004). MicroRNA was first identified in *Caenorhabditis elegans* (Chalfie *et al*., 1981) and it also has been founded as the most abundant family of small RNAs in various organisms including plants, mammals and metazoans (Pasquinelli *et al*., 2000). The precursor of miRNA is derived from the nascent miRNA transcripts (pri-miRNA) after the transcription by RNA polymerase II and form an imperfect complementary hairpin stem loop within nucleus. The pri-miRNA is processed into miRNA precursor (pre-miRNA) in the length of 60-70 nt stem loop containing 5' phosphate and 2 nt overhang at 3' end at one end by RNase III endonuclease enzyme called Drosha (Lee *et al*., 2003; Basyuk *et al*., 2003). Subsequently, the pre-miRNA is transported from nucleus to the cytoplasm through Ran-GTP dependent nucleo/cytoplasmic cargo transporter and the Exportin-5 (Lund *et al*., 2004; Yi *et al*., 2003). In cytoplasm, another end of mature miRNA is mediated by another RNase III endonuclease enzyme called Dicer (Lee *et al*., 2003) which is the similar machinery to that involved in siRNA biogenesis (Bernstein *et al*., 2001). The PAZ domain of Dicer recognizes the 2

nt at 3' end overhang to generate mature miRNA which is characterized as an imperfect match RNA duplex of 21-25 nt in length that possesses 5' phosphate and 2 nt overhang at 3'end. However, in plants that lack Drosha homologues, the pri- and pre-miRNA may be executed by the function of Dicer-like protein 1 (DCL-1) that takes place in the nucleus before transported into cytoplasm by HASTY which is the exportin-5 homologue (Kim, 2005). In effector step, miRNA share effector complex RISC that also contains Argonaute family protein as a core component with siRNAs. However, the effect of miRNA is different from siRNA. In animal, miRNAs are usually imperfect complementary binding at 3' untranslated region (UTR) of target mRNA whereas in plants they are usually complementary to the coding regions and lead to protein translation inhibition without the degradation of target mRNA, but sometimes also causes mRNA cleavage (He *et al*., 2004). Moreover, the binding of imperfect complementary siRNA to target mRNA can induce the translational suppression process as miRNA mechanism (Doench *et al*., 2003).

4. The Difference of siRNA and miRNA Pathway

MiRNAs and endogenous siRNA are rather similar in that they have a shared central biogenesis and can perform interchangeable biochemical function. They cannot be clearly distinguished by either chemical composition or mechanism of action. However, one of the main difference is their origin. Precursor of siRNAs is generated from mRNAs, transposons, viruses or heterochromatic DNA that form long dsRNA duplex or extended hairpins whereas miRNAs are derived from genetic loci distinct from other recognized gene that form RNA hairpin structure. A majority of miRNA loci are found in intronic regions of protein-coding or non-coding transcription units, whereas the others are found in exonic regions of non-coding transcription units (Kim, 2005). Each strand of miRNA:miRNA duplex is generated from the same precursor hairpin whereas a multitude of siRNA duplexes are generated from different single-stranded RNA precursor. Additionally, regarding the evolutionarily conservation, the sequences of miRNA are rather conserved in related organisms whereas sequences of siRNA are rarely conserved.

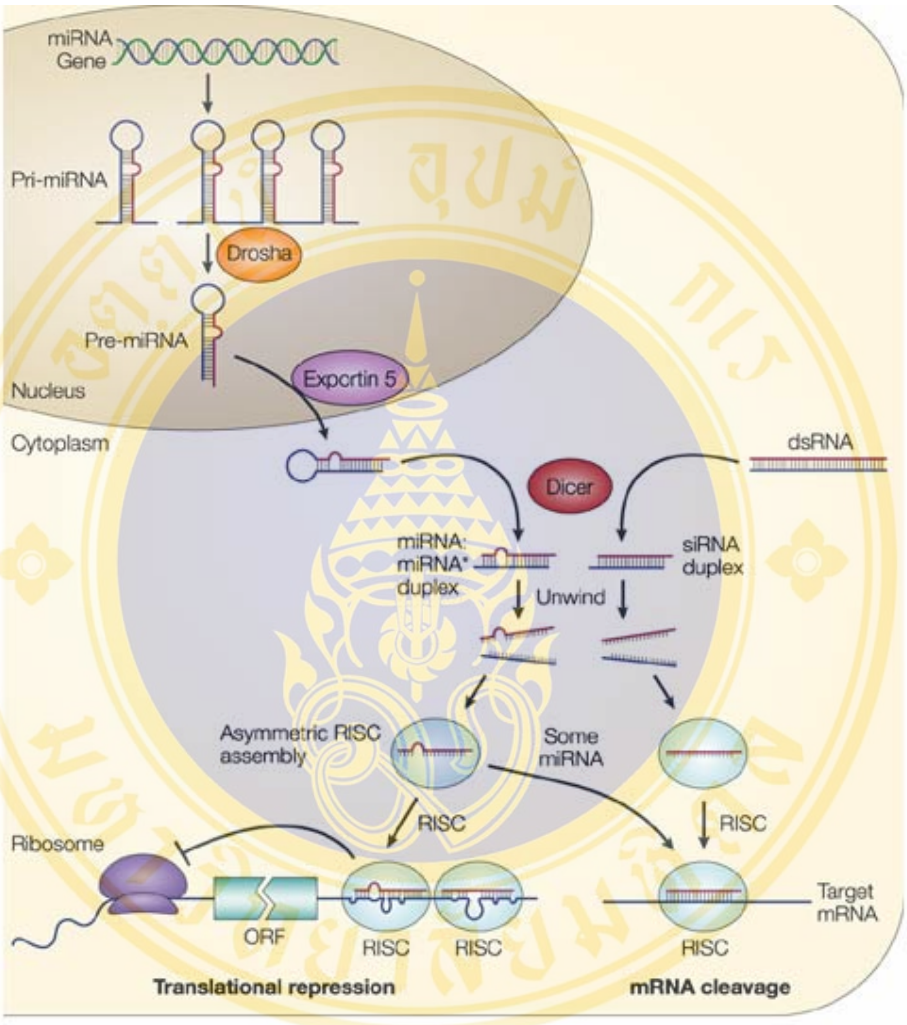

Figure 3.1 The model for the biogenesis and post-transcriptional suppression of microRNAs and small interfering RNAs (He and Hannon, 2004)

5. Machinery of the RNA Interference Pathway

5.1 Initiator Machinery: The RNase III Endonuclease Family

The initiation step of RNA interference mechanism is triggered by the presence of double-stranded RNA which is subsequently processed into small duplex RNA products with 21-23 nucleotides in length containing 5' phosphate and 2 nucleotides overhang at 3' end which is the characteristic of the cleavage product generated by ribonuclease (RNase) III endonuclease family. Generally, RNase III family endonuclease can be classified into 3 classes. The first class is represented as *Escherichia coli* RNase III that is involved in maturation of rRNA, mRNA, tRNA and can initiate mRNA degradation in *E. coli* and yeast, the second class is indicated as Drosha that plays role in microRNA pathway and the third class is illustrated as Dicer that involve in producing of siRNA or miRNA (Carmell *et al*., 2004). The structural domain of RNase III family is demonstrated in figure 3.2.

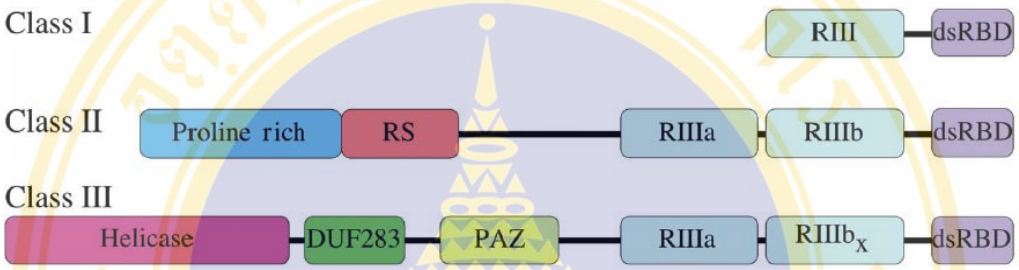

Figure 3.2 Schematic structures illustrate three classes of RNase III endonuclease enzyme. Class I is represented by *E. coli* RNase III, Class II by *Drosha* and Class III by Dicer (Carmell *et al*., 2004).

RIII boxes represent RNase III catalytic domain

dsRBD boxes represent double-stranded RNA binding domain

Proline rich box represents proline rich region

RS box represents arginine-serine rich region

Helicase box represents helicase domain

DUF283 box represents unknown function domain

PAZ box represents PAZ domain

5.1.1 Drosha: The Initiator Machinery in miRNA Pathway

Drosha is a ribonuclease (RNase) III class II enzyme harboring N-terminal proline rich region (PRR) followed by a serine-arginine rich region (RS) which is suspected to be involved in protein-protein interaction region. Additionally, it also contains two RNase III domains and C-terminal double-stranded RNA binding domain (dsRBD) (Carmell *et al*., 2004). In microRNA pathway, Drosha assumes a pseudo-dimer catalytic core that plays a critical role in miRNA maturation by recognizing the hairpin stem-loop (Han *et al*., 2004). The size of stem-loop is important for this recognition. Subsequently, pri-miRNA is processed into pre-miRNA (Zeng *et al*., 2005) by the pseudo-dimer catalytic core of Drosha that is similar to Dicer (Han *et al*., 2004) before nuclear export through an exportin-5 in a RAN-GTP dependent manner. The 3' end of this product can be recognized by the PAZ domain of Dicer and proceed in the same way of siRNA pathway. The recognition process is still unclear although the conserved sequences have been found (Ohler *et al*., 2004)

5.1.2 Dicer: The Initiator Machinery in RNA Interference Pathway

Dicer is also a ribonuclease (RNase) III class III enzymes about 200 kDa in size composing of multi-domains: N-termimal helicase domain, PAZ domain, two RNase III catalytic domains and double-stranded RNA binding domain at C-terminus (Carmell *et al*., 2004) which is a machinery in both siRNA and microRNA pathway (Hutvagner *et al*., 2001; Grishok Bass 2001; Knight and Bass, 2001; Ketting *et al*., 2001). Dicer is responsible for the generation of siRNA and miRNA from long dsRNA and pre-miRNA, respectively. Dicer functions as monomer by utilizing two endonucleolytic reactions to generate one new termini (Zhang *et al*., 2002; 2004). The crystal structure of Dicer has been characterized in *Giardia lamblia* (figure 3.3) (Macrae *et al*., 2006). The crystal of RNase III from *Aquifex aeolicus* which is the RNase III class I containing one RNase III catalytic domain has been revealed and studied as a model (Blaszczyk *et al*., 2001). The model of Dicer function was proposed that two domains of RNase III domains associate intramolecularly as pseudo-dimer which then cut a single strand of the duplex to generate one new terminus with 2 nucleotides overhang which is measured by dimer alignment whereas 21 nucleotides is measured by the distance between the terminal binding PAZ domain

and the active site (figure 3.4) (Hammond, 2005) Zhang *et al.* have proposed that the distance between the combination of Dicer's PAZ and RNase III catalytic domain act as a molecular ruler to generate the precise approximately 21 nucleotides siRNA (Zhang *et al*., 2004). Due to the similarity between Dicer and Drosha that contain two tandem RNase-III domains, it is probable that both Dicer and Drosha share the closely related processing to generate siRNA or miRNA.

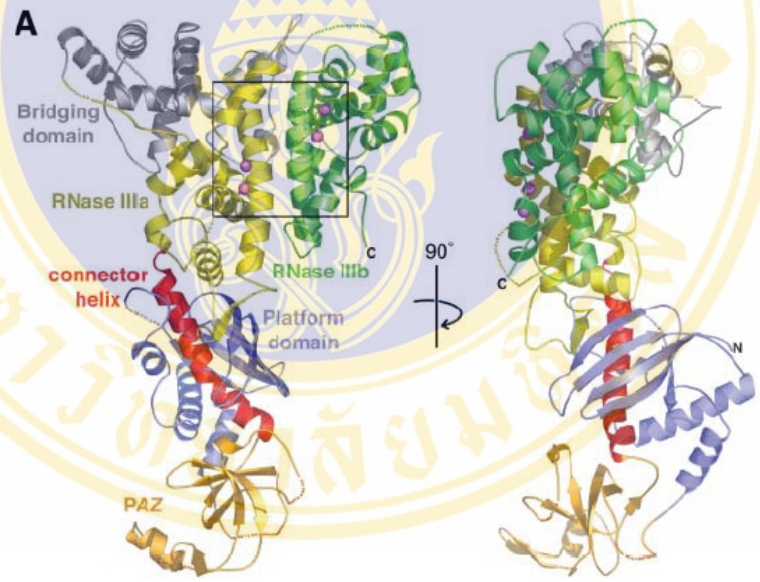

Figure 3.3 Crystal structure of *Giardia* Dicer (Macrae *et al*., 2006)

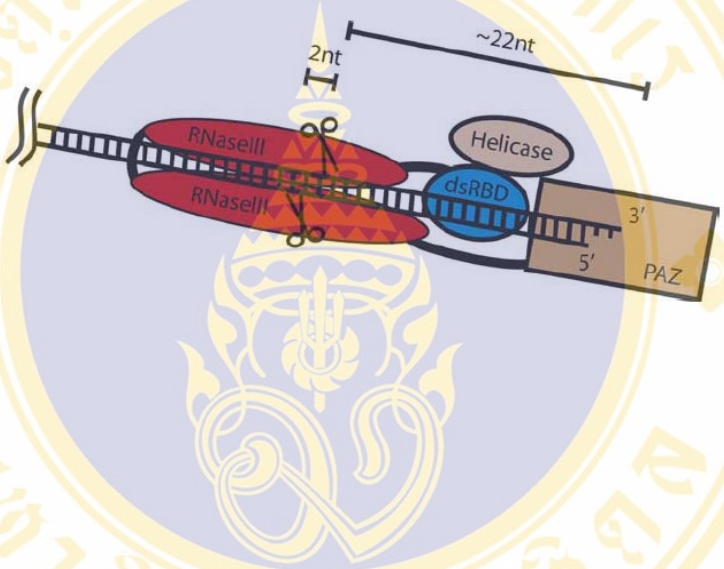

Figure 3.4 Model for Dicer catalysis process by Zhang *et al.*, 2004

The Dicer that contains two RNase III catalytic domains function as monomer by using PAZ domain to recognize the 3' end and two catalytic domains form a pseudo-dimer. (Picture taken from Hammond, 2005)

5.2 Effector Machinery: RISC

The phenomenon of RNA interference pathway is executed by the induction of dsRNA that leads to mRNA cleavage (siRNA pathway) or repression of protein translation (microRNA pathway) in a sequence-specific manner. This activity is mediated by the multiprotein complex called RNA-induced silencing complex or RISC that contains Argonaute family protein as a major constituent (Song *et al*., 2003). The nuclease activity of RISC in the presence of siRNA was first reported in *Drosophila* culture cells (Tuschl *et al*., 1999; Hammond *et al*., 2000). RISC utilizes short interfering RNA (siRNA) or microRNA (miRNA) as a guide to target the sequence-specific mRNA destruction.

The incorporation of small RNA into RISC requires 5' phosphate (Nykanen *et al*., 2001; Martinez *et al*., 2002). The modification at 5' phosphate by an amino-methylene linkage showed the decreased in the binding capacity (Martinez *et al*., 2002). Although the loss of 5' phosphate showed similar pattern of activity, however, the activity was further reduced. Therefore the presence of 5' phosphate of siRNA is important for the RISC-siRNA complex stability and the fidelity of the enzyme (Rivas *et al*., 2005).

6. Argonaute Family Proteins

6.1 Biological Function of Argonaute Protein

Argonaute family proteins are multidomain proteins (approximately 100 kDa) that are highly conserved and found in various organisms from prokaryote to eukaryote (Traci M and Tanaka H, 2005). Argonaute gene family members are scattered on several different chromosomes in the genome. Argonautes are the protein component to all RISC-related complexes (Parker *et al*., 2004). They play important biological roles including regulation of development, maintenance of germ-line stem cell and are also involved in a variety of RNA silencing pathways (Miyoshi *et al*., 2005; Sasaki *et al*., 2003). For instance, in plants, the mutation of Argonaute gene impairs gene silencing pathway leading to susceptible for virus infection (Morel *et al*., 2002). In Drosophila, *Ago1* mutant also affected developmental control that exhibited the numerous phenotypic abnormalities (Williams RW and Rubin GM, 2002; Carmell and Hannon, 2004; Sigova *et al*., 2004). In mammals, Ago 2-mutant embryos showed

a variety of development defects in mouse suggesting that Argoanute 2 is essential for mouse development (Liu *et al*., 2004). In *Drosophila*, Argonaute2 (AGO2) is shown to be presented as the component for RNAi response and is required for the unwinding of siRNA duplex. In contrast, Argonaute1 (AGO1) is involved in miRNA biogenesis. Therefore distinct Argonaute proteins are responsible for different small RNA silencing mechanisms (Okamura *et al*., 2004).

Argonaute proteins are conserved but different in number among species, not all members are involved in RNAi pathway. *Drosophila* genome contains at least four Argonaute family members, AGO1, AGO2, Piwi, and Sting, which have been linked both to gene silencing phenomena and to the control of development in diverse species. Only AGO2 is shown biochemically to be a component of RISC (Liu J *et al.*, 2004; Hammond SM *et al.,* 2001; Rand TA *et al.,* 2004; Rivas *et al*., 2005; Rand TA *et al.*, 2005). Whereas human contain 8 Argonaute proteins that are classified into two subfamilies based on the sequence comparison. The PIWI subfamily consists of 4 members, *PIWIL1/HIWI, PIWIL2/HILI, PIWIL3* and *PIWIL4/HIWI2* and the eIF2C/AGO subfamily consists of 4 members of *EIF2C1/hAGO1, EIF2C2/hAGO2, EIF2C3/hAGO3* and *EIF2C4/hAGO4* (Sasaki *et al.*, 2003). It has been demonstrated recently that hAgo2 can function to cleave siRNA-specific mRNA target (Hammond, 2004; Rivas *et al*., 2005).

6.2 Argonaute Protein in RNA Interference Pathway

Double-stranded RNA triggered-cleavage or translation inhibition of cognate mRNA is mediated by the effector complex named RISC or RNA-induced silencing complex by using siRNAs or miRNAs to guide to the complementary target mRNA. Several reports showed that the presence of human Argonaute 2 together with siRNA is sufficient for slicer activity (Rivas *et al*., 2005; Rand *et al*., 2004; Liu *et al*., 2004). The components of RISC were first identified from *Drosophila* cell culture in 2001 by Hammond *et al.* They found that RISC associated with ribosome in cell-free extract. In order to obtain the components of RISC, the ribosome associated complex RISC protein was collected by high speed centrifugation. Subsequently, the soluble RISC was recovered from the ribosome pellet by performing high salt extraction. Size fractions that contained RISC activity were approximately 500 kDa. The expected

RISC protein was then excised from SDS-PAGE and further analyzed by microsequencing using tandem mass spectroscopy and identified as a member of the Argonaute protein family. In addition, Argonaute protein was the only protein present in a highly purified active form of *Drosophila* RISC (Rand *et al*., 2004). The genetic analysis and knockout data illustrated that Argonaute proteins were required for RISC-mediated mRNA cleavage (Okamura *et al*., 2004; Meister *et al*., 2004; Liu *et al*., 2004) and displayed biochemical function catalytic activity that was similar to RNase H-type enzyme. (Martinez amd Tuschl, 2004; Schwarz *et al*., 2004)

Proteins in the Argonaute family are characterized by the presence of two conserved regions of PAZ and PIWI domains. Argonaute protein generally comprises of four major domains, N-terminal, PAZ domain, middle and PIWI domain. At present, the crystal structure of Argoanute from *Pyrococcus furiosus* (figure 3.5) and *Aquifex aeolicus* have been identified (Song *et al*., 2004; Yuan *et al*., 2005). Moreover, the structure of PAZ domain from *Drosophila* (Song *et al*., 2004) and PIWI domain from *Archaeoglobus fulgidus* (Parker *et al*., 2004) have also been illustrated. The structural information enhance the understanding the biological functions of both domains that mediate the role in RNA silencing pathway. The tertiary structure of PAZ domain represented the RNA binding domain whereas the PIWI domain's structure is similar to that of RNase H structure harboring the active site residues. The structure and function of the PAZ and PIWI domains implicated that Argonaute acts as "Slicer" by itself that can cleave target mRNA by the RNase H like function of PIWI domain that guided by the siRNA strand binding at PAZ domain (Song *et al*., 2004).

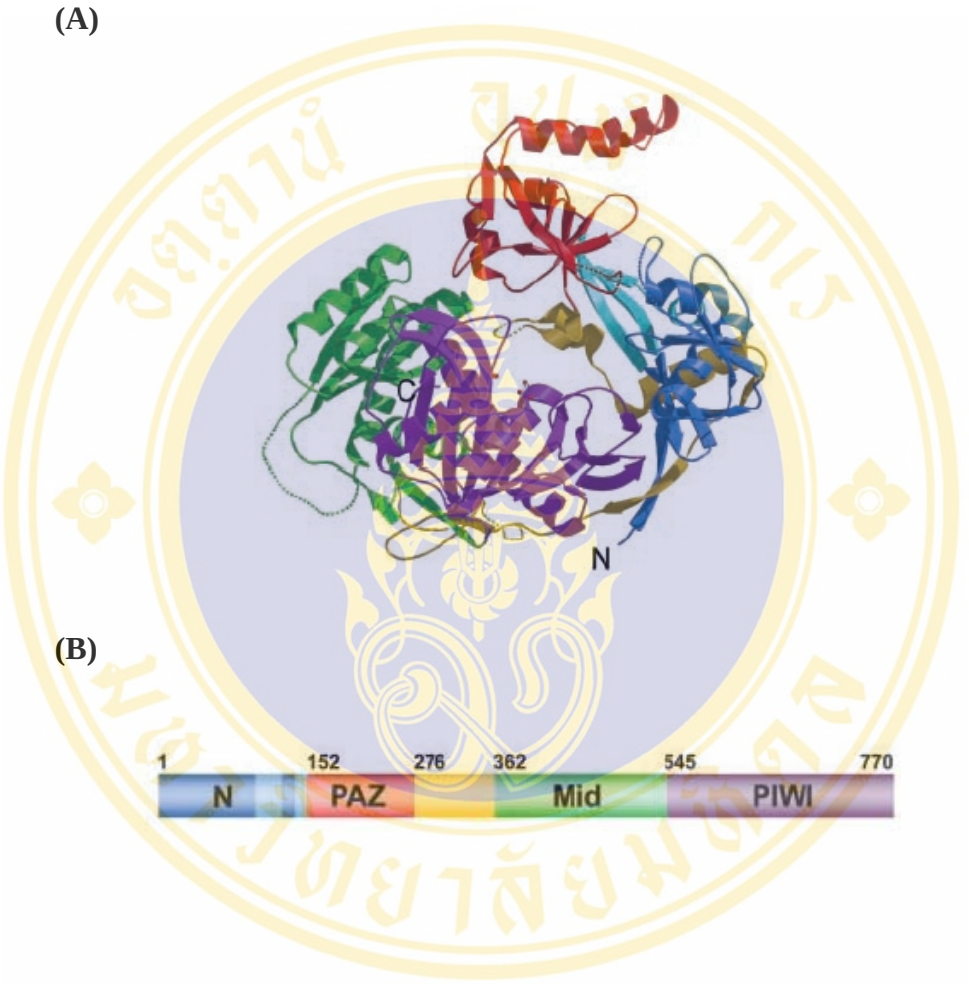

Figure 3.5 Crystal structure of *Pyrococcus furiosus* Argonaute (Song *et al*., 2004)

(A) Stereoview ribbon represents the full-length of *Pyrococcus furiosus* Argonaute protein

(B) Schematic diagram of the domain regions in Argonaute protein

6.3 PAZ Domain: RNA Binding Domain

PAZ (Piwi/Argonaute/Zwille) domain is the 130 amino acids conserved region that presented in both Dicer and Argonaute family proteins which are the key components in RNAi pathway (Yan *et al*., 2003). The tertiary structure of PAZ domain, as illustrated by nuclear magnetic resonance (NMR), in *Drosophila melanogaster* Argonaute 1 and Argonaute 2 have revealed an oligo-binding (OB) fold as a left-handed twisting β-barrel of 5 or 6 β-stranded (figure 3.6) . This β-structure at the central clef is capped at one end by two α-helices with the conserved sub-domain consisting of β-hairpin followed by a short helix inserted into a loop between two strands of the β-barrel. In addition, the N- and C-termini form an anti-parallel β-sheet with a highly positive electrostatic potential and groove for RNA binding (Yan *et al*., 2003). The NMR titration technique with mutation analysis in the PAZ cleft and electrophoretic mobility shift assay (EMSA) demonstrated that the central cleft region lined with conserved aromatic residues which are responsible for nucleic binding region that specifically binds to 3' end of siRNA with the electrostatic interaction (Lingel *et al*., 2003; Song *et al*.,2003; Yan *et al*., 2003). The 3' end of siRNA binds deep into a conserved hydrophobic pocket (Collin *et al*., 2005). The PAZ domain recognizes and interacts with ssRNA and RNA duplex at 2 nucleotides overhang at 3' end with low affinity and dissociation constant in the micromolar range (Song *et al*., 2003; Ma *et al*., 2004; Carmell and Hannon, 2004). In addition, the binding of PAZ domain is independent of sequence. Ago1 PAZ domain is able to interact with ssRNA oligonucleotides preferentially over ssDNA and it also bind to ssRNA better than dsRNA without the requirement of the unstructured C-terminal region (Yan *et al*., 2003). The crystal structure of *Drosophila* Argonaute 2 was identified and the binding properties of PAZ domain was analyzed by using UV-crosslinking and illustrated that the PAZ domain could efficiently bind both ssRNA and dsRNA in the presence of dTdT overhang at 3' whereas the binding could not competed with blunt ended dsRNAs (Song *et al*., 2003). Additionally, two nucleotides overhang at 5' end were also unable to compete the binding. This indicated that the PAZ domain can bind to the two nucleotides overhang at 3' end of ssRNA which is the characteristic of the cleavage products from Dicer and Drosha in RNAi pathway. The results suggested the interaction model of the PAZ domain in Dicer and Argonaute proteins to the 3' end

terminal of siRNAs and pre-miRNAs (Song *et al*., 2003). However, the research group of Lingel *et al.* showed that the PAZ domain can bind ssRNA equally to ssDNA (Lingel *et al*., 2004). Moreover, the function of thePAZ domain as a protein-protein interaction motif have also been reported (Cerutti *et al.,* 2000). Therefore the PAZ domain may be involved in the interaction between Argonaute and Dicer proteins (Hammond *et al.,* 2001).

Figure 3.6 Stereo ribbon diagram shows the structure of *Drosophila* Ago2-PAZ (Song *et al.,* 2003)

6.4 PIWI Domain: Catalytic RNase-H Structure

PIWI domain is approximately 300 amino acid residues located at the C-terminus of Argonaute protein. Tertiary structure of the PIWI domain from *Archaeoglobus fulgidus* (figure 3.7) and *Pyrococcus furiosus* Argonaute is similar to RNase H family enzyme with two conserved aspartate residues (Park *et al.,* 2004, Song *et al.,* 2004) and prominent positively charged channel reminiscent of RNA-binding protein. (Park *et al.,* 2004)

The study in *A. fulgidus* PIWI (AfPiwi) domain by Parker *et al*., 2004, divided AfPiwi into two domains, domain A and B and one sub-domain called the N-sub-domain. Domain A is like the sugar-binding portion of the *lac* repressor. Whereas domain B shares the structure similarity to RNase H family enzyme with two conserved catalytic aspartate residues implying the slicer activity of Argonaute in RISC. However, RNase H cleaves RNA strand in an RNA-DNA heteroduplex by the guidance of DNA strand, whereas RISC cleaves the RNA in RNA-RNA duplex by siRNA guide strand. In addition, RNase H-related family enzymes contain three highly conserved catalytic residues, aspartate-aspartate-glutamate motif. The mutagenesis analysis of conserved two aspartate residues in the PIWI domain showed that they are required as catalytic residues but the mutation at the third carboxylate, glutamate, did not affect the endonuclease activity. As the mechanism revealed that the metal ion coordinated with two aspartates as well as another histidine residue. It might suggest that histidine, rather than glutamate is the third active site residue of the PIWI domain. This implied that Argonaute employs a unique aspartate-aspartate-histidine motif for metal ion coordination as catalytic site. There is a report showing that siRNAs that lost the 5’ phosphate group could not be incorporated into RISC complex (Nykanen *et al.,* 2001, Chiu *et al.,* 2002).

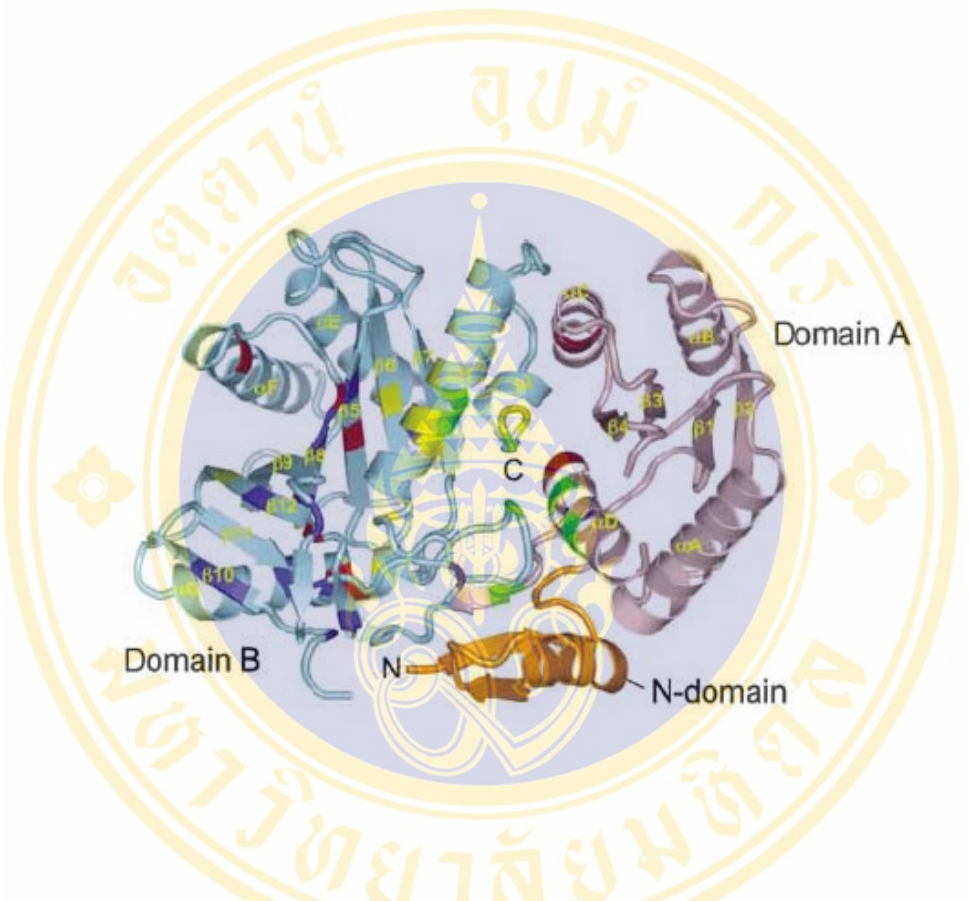

Figure 3.7 Stereo ribbon diagram shows the structure of *Archaeoglobus fulgidus* PIWI (Park *et al.*, 2004)

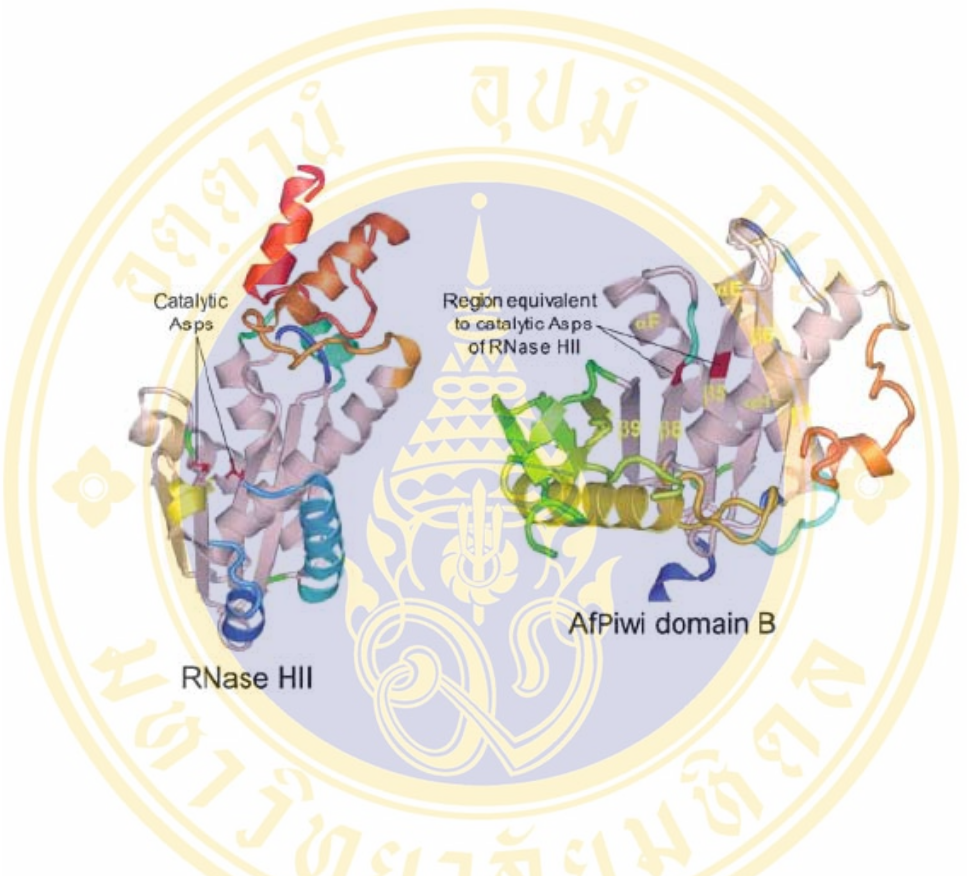

Figure 3.8 Comparison of tertiary structure between domain B of *Archaeoglobus fulgidus* PIWI domain and RNase HII from *Methanococcus jannaschii*

The figures reveal the catalytic aspartate residues on the equivalent positions of β5 and β8 (Park *et al.*, 2004)

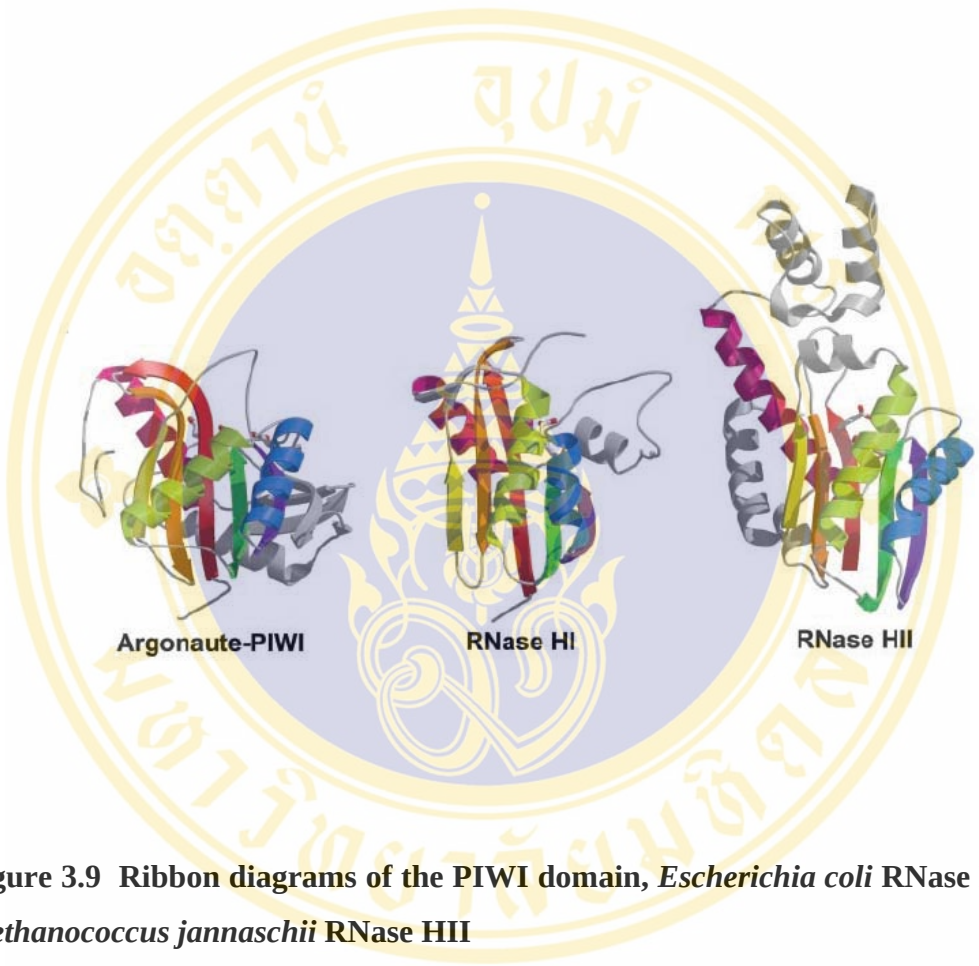

Figure 3.9 Ribbon diagrams of the PIWI domain, *Escherichia coli* RNase HI and *Methanococcus jannaschii* RNase HII

The figures illustrate the similar view with the secondary structure elements of the canonical RNase H fold (Song *et al.*, 2004).

CHAPTER IV
MATERIALS

4.1 Chemicals

All chemicals used in this thesis were analytical grade purchased from a variety of reliable suppliers, such as BIO-RAD, Bio Basic Inc., Fluka, Gibco BRL, Merck, Sigma, Promega, Invitrogen, USB Corporation, BDH Laboratory Supplies, Research Organics, Amersham Pharmacia Biotech, Fermentas, and so on.

4.2 Miscellaneous Materials

Deoxyribonucleotide triphosphate (dNTPs)	Amersham Pharmacia Biotech
Standard DNA markers	Fermentas, Biolabs, GibcoBRL
QIAquick® gel purification kit	QIAGEN
QIAquick® PCR purification kit	QIAGEN
Zeocin™	Invitrogen
Ampicillin	Sigma
Chloramphenicol	Bio Basic
Standard Broad Range Protein Marker	BIO-RAD
Bio-RAD Bradford Protein Assay	BIO-RAD
Standard Bovine Serum Albumin	Pierce
HisTrap™ FF crude column	Amersham Pharmacia Biotech
RiboMAX ™ Large Scale RNA Production System	Promega
1, 4-dithiothreitol (DTT)	Merck
5-bromo-4-chloro-3-indolyl phosphate (BCIP)	Sigma
Nitro Blue Tetrazolium (NBT)	Sigma
Isopropyl-β-D-thiogalactopyranoside (IPTG)	Carl Roth
DEPC	USB corporation
MicroSpin™ G-50 columns	Amersham Pharmacia Biotech
SIGMACOTE	Sigma

Tri-Reagent LS	Molecular Research Center
RNasein	Promega
Protease inhibitor cocktail	Roche

4.3 Enzymes and Accessory Buffers

Cloned *Pfu* polymerase	Promega
Taq DNA polymerase	Promega
Ribonuclease A	Sigma
Lysozyme	Sigma
T4 DNA ligase	Gibco BRL
Calf Intestine Alkaline phosphatase (CIAP)	Promega
T4 Polynucleotide kinase (PNK)	Bio Labs

Table 4.1 Restriction enzymes used in this thesis with their recognition sites, incubation temperature, recommendation reaction buffers and manufacturers

Restriction Enzymes	Recognition sequence	Incubation temperature	Reaction buffer*	Suppliers
Xho I	C↓TCGAG	37°C	Buffer D	Promega
Sal I	G↓TCGAC	37°C	Buffer D	Promega
Dra I	TTT↓AAA	37°C	Buffer B	Promega
Nde I	CA↓TATG	37°C	Buffer D	Promega
*Bam*H I	G↓GATCC	37°C	Buffer E	Promega
EcoR I	G↓AATTC	37°C	Buffer D	Promega
Xba I	T↓CTAGA	37°C	Buffer D	Promega
Pst I	CTGCA↓G	37°C	Buffer D	Promega
Bgl II	A↓GATCT	37°C	Buffer D	Promega

↓ indicates the cleavage site

* Manufacturers recommended reaction buffers.

10X buffer B: 6 mM Tris-HCl (pH 7.5), 50 mM NaCl, 6 mM $MgCl_2$ and 1 mM DTT

10X buffer D: 60 mM Tris-HCl (pH7.9), 1.5M NaCl, 60 mM $MgCl_2$ and 10 mM DTT

10X buffer E: 6 mM Tris-HCl (pH 7.5), 100 mM NaCl, 6 mM $MgCl_2$ and 1 mM DTT

4.4 Antibodies

Mouse anti-His antibody	Amersham Pharmacia Biotech
Anti-mouse IgG, alkaline phosphatase conjugated	Promega
Anti-mouse IgG, peroxidase conjugated	Amersham Pharmacia Biotech
Mouse Anti-PAZ IgG	This study by the helpfulness from Asst. Prof. Witoon Tirasophon
Anti-FMDV-3Cprotease	Kindly provided by Asst. Prof. Witoon Tirasophon

4.5 Bacterial Strains

***Escherichia coli* strain DH5α** [*supE*44, Δ*lac*U169 (ϕ80 *lacZ* ΔM15), *hsdR*17, *recA*1, *endA*1, *gyrA*96, *thi*-1, *relA*1], obtained from GIBCO BRL, was employed as a host cell for recombinant plasmid propagation.

***Escherichia coli* strain BL21(DE3)pLysS** [*E.coli* B F^- *dcm ompT hsdS*($r_B^-m_B^-$) *gal* λDE3) pLysS(Cam^R)], obtained from Stratagene, was kindly provided by Mrs. Busaba Powthongchin from Assoc. Prof. Chanan Angsuthanasombat's laboratory. This strain is high-stringency expression host for expression of recombinant proteins in *E. coli* which is deficient in the *lon* protease and lacks the *ompT* outer membrane protease that can degrade proteins during purification. Moreover it also contained pLysS plasmid that provides chloramphenicol antibiotic resistance marker. Cell carrying this plasmid accumulates much lower level of lysozyme and useful for the stability of the expressed recombinant protein. The unique sites of pLysS plasmid are shown on the circle map in figure 4.1.

***Escherichia coli* strain BL21(DE3)pLysS/pET-15b/T-CyaA** is the *E. coli* expression host containing the recombinant plasmid of 130 kDa Truncated-CyaA protein used as positive control for soluble protein expression in *E. coli*. This host was kindly provided by Mrs. Busaba Powthongchin from Assoc. Prof. Chanan Angsuthanasombat's laboratory.

***Escherichia coli* strain BL21(DE3)pLysS/pET-15b** is the *E. coli* expression host containing the pET-15b used as negative control of protein expression was generated in this study.

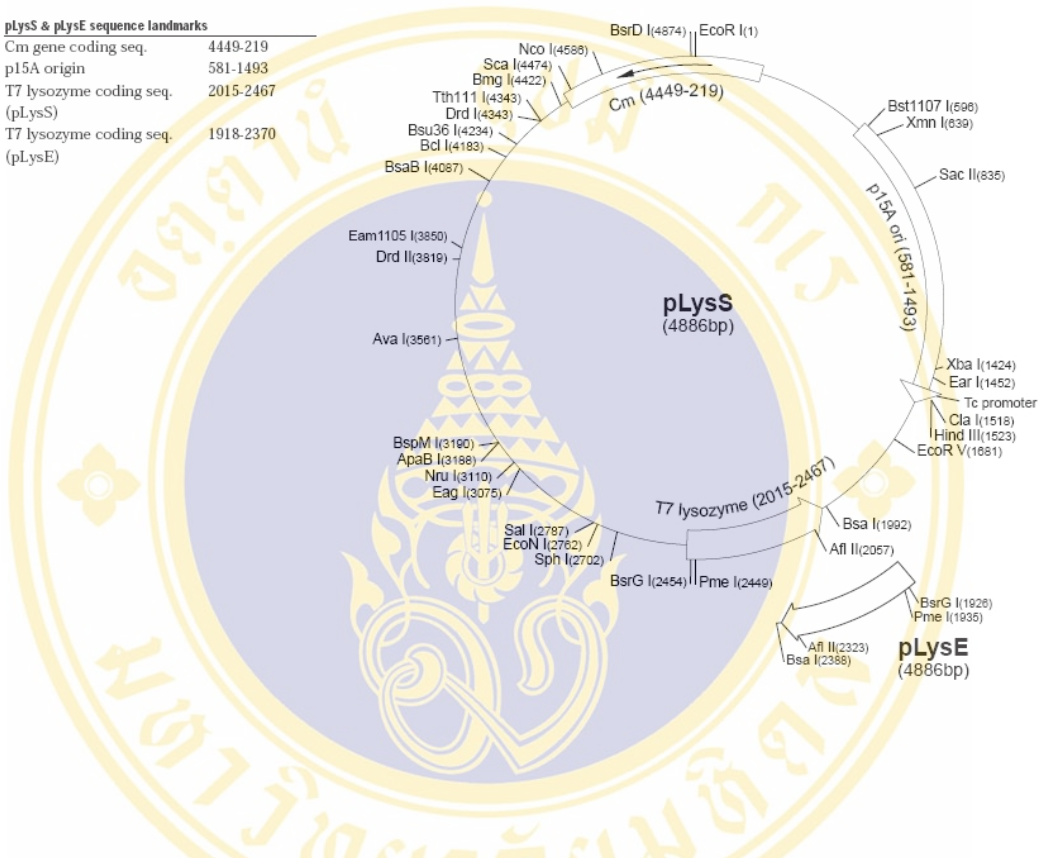

Figure 4.1 Physical map of pLysS plasmid (Novagen)

The figure represents the physical map of pLysS (4,886 bp) from Novagen. This plasmid harboring T7 lysozyme gene that is useful to suppress basal expression from the T7 promoter in λDE3 lysogenic hosts and chloramphenicol antibiotic resistance gene as a selectable marker.

4.6 Yeast Strains

***Pichia pastoris* strain KM71** (*arg4, his4, aox1::Arg4*) was employed as a host cell for gene integration into host genome and expression of the recombinant protein in yeast expression system.

***Pichia pastoris* strain KM71/pPICZαA/Der p3.1** was kindly provided by Miss Nipawan Nuemket from Asst. Prof. Surapon Piboonphokanun's laboratory. This yeast strain is *Pichia* recombinant strain harboring pPICZαA/Der p3.1 integrated in its genome and was used as a positive control for secreted extracellular protein expression.

4.7 Vectors and Recombinant Plasmids

pUC19/*Pem-ago* is the recombinant plasmid containing the cDNA encoding Argonaute cDNA of *P. monodon* (Pem-AGO) that was used as a template for amplification of the Argonaute and PAZ domain regions in the cloning steps. This recombinant plasmid was constructed by Miss Manasave Dechkla (M.Sc. Thesis, Mahidol University, 2006).

pPICZαA (3,593 kb) vector obtained from Invitrogen (figure 4.2). This plasmid is *Pichia* secretion expression vector containing the *sh ble* gene (*Streptoalloteichus hindustanus bleomycin* gene) from *Streptoalloteichus* conferring the Zeocin™ resistance gene, *AOX*1 promoter for induction under the control of methanol and act as the region of recombinant plasmid integration to *AOX*1 locus of yeast genome, α-factor secretion signal derived from *Saccharomyces cerevisiae* to allow the extracellular secretion of the expressed recombinant protein into the culture medium, multiple cloning sites for insertion of the target gene, polyhistidine (6xHis) tag for expression as C-terminus hexa-histidine tag fusion protein that is useful for detection and purification steps followed by *AOX*1(TT), transcription termination and polyadenylation signal from *AOX*1 gene that increase the stability and efficiency of 3' mRNA processing, *TEF1* promoter that controls the expression of *Sh ble* gene for Zeocin™ resistance in *P. pastoris, EM7* promoter which is a constitutively synthetic promoter to control the expression of *Sh ble* gene *in E. coli, CYC1*, 3' end of the *Saccharomyces cerevisiae CYC1* gene which increase a stability and efficiency of 3' mRNA processing of the *Sh ble* gene and *ColE1* to allow replication and maintenance of the recombinant plasmid in *E. coli.*

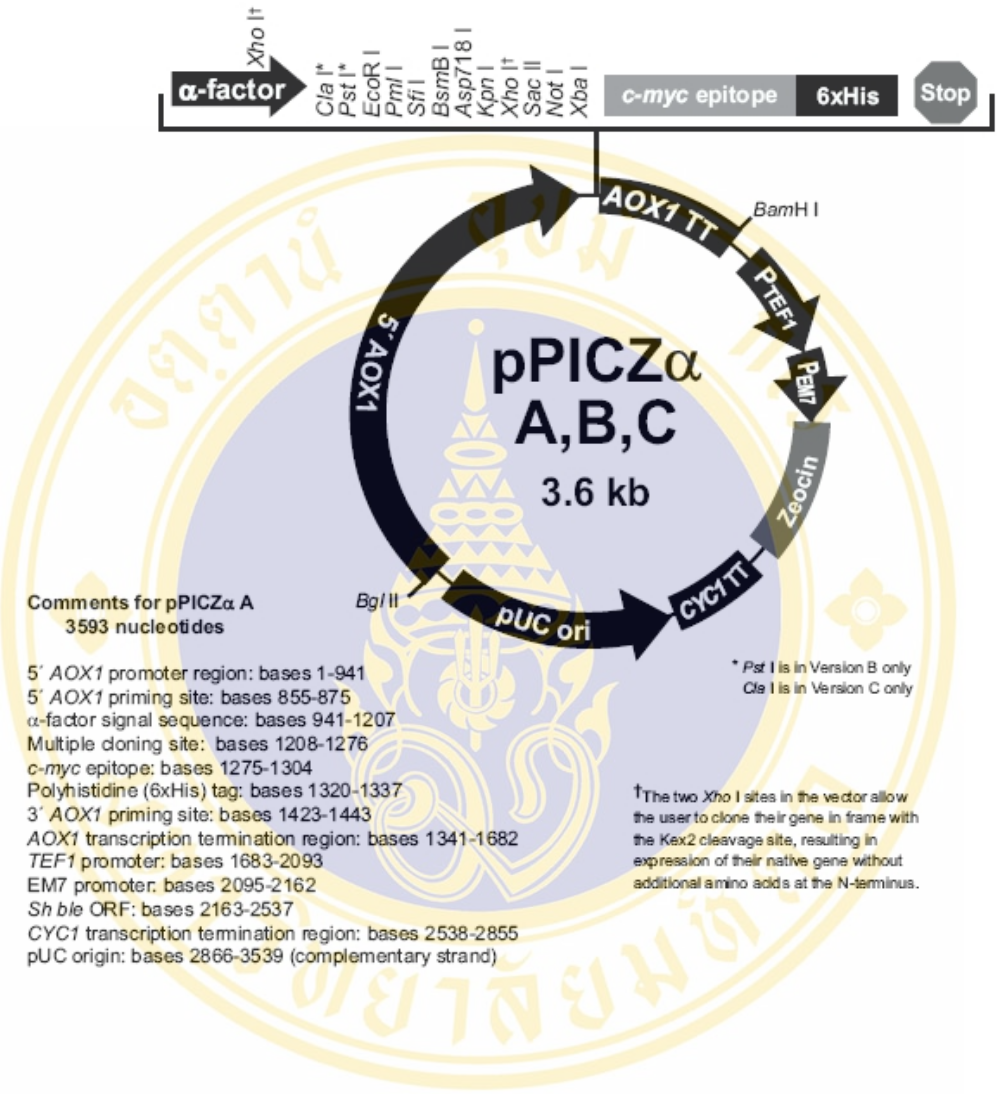

Figure 4.2 Physical map of pPICZαA vector (Invitrogen)

The figure illustrates the physical map of pPICZαA vector, reproduced from pPICZα A, B, and C (version E) manual (Invitrogen), containing 5' *AOX1* promoter, α-factor secretion signal (MFα-1) from *Saccharomyces cerevisiae*, multiple cloning site, C-terminal polyhistidine (6xHis) tag, *AOX1* transcription termination (TT), *TEF1* promoter, *EM7* promoter, Zeocin^{TM} resistance gene (*Sh ble), CYC1* transcription termination region and pUC origin of replication in *E. coli*.

pET-15b (5,708 bp) plasmid obtained from Novagen (figure 4.3) was kindly provided by Mrs. Busaba Powthongchin form Assoc. Prof. Chanan Angsuthanasombat's laboratory. This vector is designed for expression of the recombinant protein in *E. coli* system as fusion N-terminus hexa-histidine tag protein. The variety of expression level can be controlled by T7 promoter under the induction of IPTG. It also provides *bla* gene conferring the ampicillin resistance gene as an antibiotic selectable marker, the thrombin cleavage site that is useful for minimization the extra-amino acid residues followed by multiple cloning sites for insertion of the target gene.

pBluescript/GFP sense-strand is the recombinant plasmid given by Miss Niramon Thammaviriyasati (the original constructs from Asst. Prof. Witoon Tirasophon) used as template for amplification of GFP-sense stranded template for *in vitro* transcription reaction by using specific primers that contain T7 sequences in the forward primer.

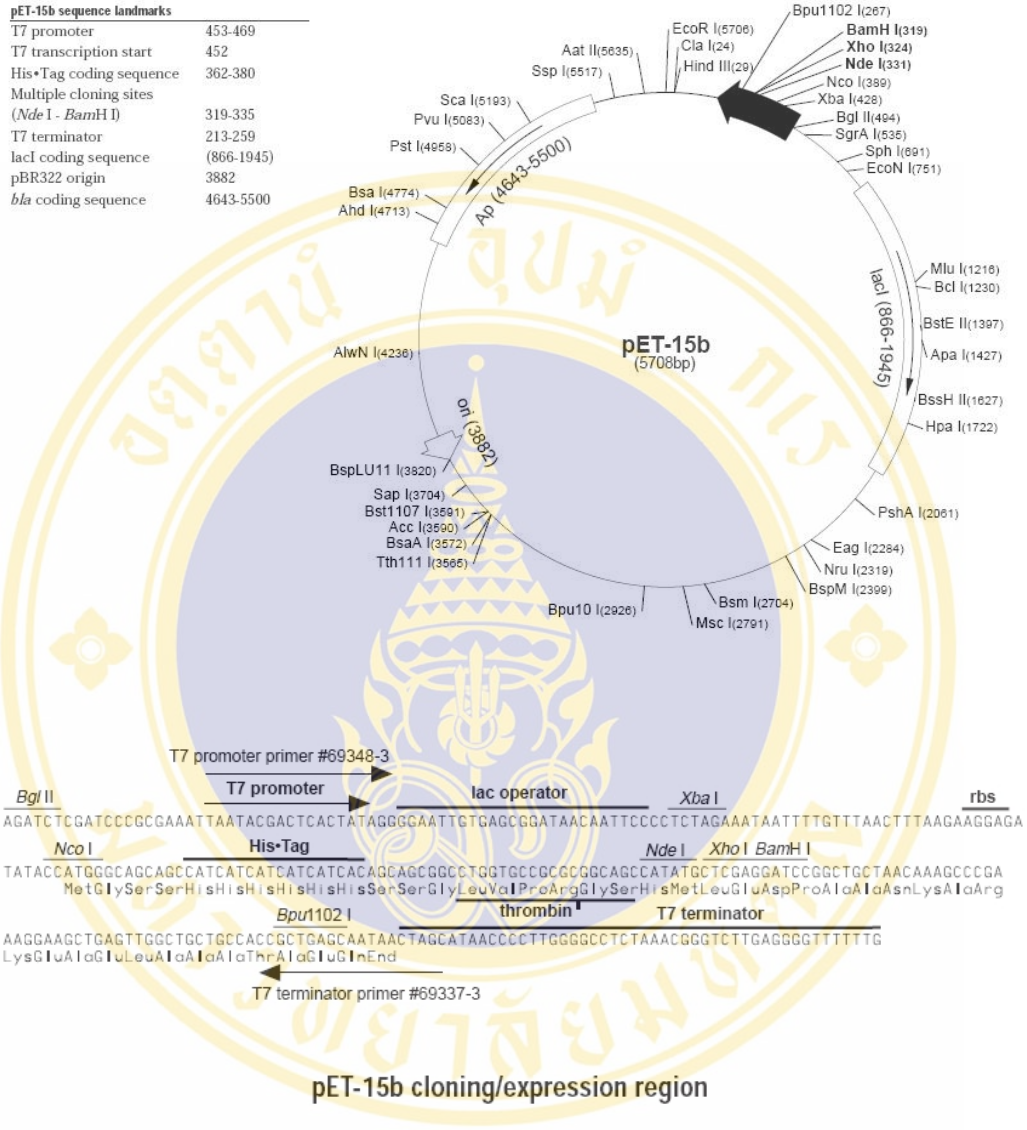

Figure 4.3 Physical map and cloning region of plasmid pET-15b (Novagen)

The figure indicates the physical map of pET-15b vector, reproduced from Novagen. The vector contain T7 promoter, T7 transcription start site, polyhistidine (6xHis) tag, multiple cloning sites (*Nde* I, *Xho* I, *Bam*H I), T7 terminator and ampicillin resistance gene.

4.8 Synthetic Oligonucleotides

The synthetic oligonucleotides used in this study were purchased from Proligo Singapore Pte Ltd. All primers were specifically designed based upon nucleotide sequences of the desired regions with melting temperature (T_m), %GC, dimers and hairpin loops by VectorNTI program.

4.8.1 PCR Primers for Amplification of cDNA Encoding *P. monodon*'s Argonaute (Pem-AGO) for *Pichia pastoris* Expression System

The pUC19/*Pem-ago* recombinant plasmid was used as a template in the PCR reaction to amplify *Pem-ago* cDNA corresponding to the nucleotide position 1 to 2,829 by using specific primers containing Kex2 cleavage site sequence on the forward primer as shown below:

Primers	Sequences	Size (bp)	T_m (^oC)
Argo-F	*Xho* I Kex2 5'-CCGCTCGAGAAAAGAATGTACCCTGTTGGGCAGCC-3'	35	64
Argo-R	*Sal* I 5'-ACGCGTCGACAGCAAAGTACATGACTCTGTTTG-3'	33	64

4.8.2 PCR Primers for Amplification of the *P. monodon's PAZ* Region for *Pichia pastoris* Expression System

To amplify the *PAZ* region corresponding to nucleotide position 865 to 1,281, the specific primers were designed. The *Xho* I recognition site and the Kex2 cleavage site sequence were introduced into the forward primer whereas *Sal* I recognition site was added to the reverse primer.

Primers	Sequences	Size (bp)	T_m (^oC)
PAZex-F	*Xho* I Kex2 5'-CCGCTCGAGAAAAGATTTATGTGTGAAGTGTTAGATATTC -3'	40	64
PAZex-R	*Sal* I 5'-ACGCGTCGACAGATCTAGCTGTTGCCTTGATC-3'	32	64

4.8.3 PCR Primers for Amplification of the *P. monodon*'s *Argonaute* cDNA (*Pem-ago*) for *E. coli* Expression System

For *E. coli* expression system, the recombinant plasmids were constructed using pET-15b as expression vector. To amplify *Pem-ago* cDNA according to the nucleotide position 1 to 2,829, the restriction sites were designed corresponding to the cloning site on the vector as shown below by using pUC19/ *Pem-ago* as a template in the PCR reaction.

Primers	Sequences	Size (bp)	T_m (^oC)
EX-AGO-F	*Nde* I 5' -GGAATTCCATATGATGTACCCTGTTGGGCAGC- 3'	32	60
EX-AGO-R	*Bam*H I 5' -CGGGATCCTTAAGCAAAGTACATGACTCTG- 3'	30	60

4.8.4 PCR Primers for Amplification of the *P. monodon's PAZ* Region for *E. coli* Expression System

The *PAZ* was amplified form nucleotide position 865 to 1,281, with specific primers with appropriate recognition sites as shown below.

Primers	Sequences	Size (bp)	T_m (^oC)
EX-PAZ-F	*Nde* I 5' -GGAATTCCATATGTTTATGTGTGAAGTGTTAGATATT- 3'	37	64
EX-PAZ-R	*Bam*H I 5' -CGGGATCCAGATCTAGCTGTTGCCTTGAT- 3'	29	64

4.8.5 PCR Primers for Analyzing of Genome Integration

In order to check the stable integration of the DNA fragments into *P. pastoris* genome, the primers bind to the sequences located in 5'*AOX*1 and 3'*AOX*1 promoter region were used in the amplification reaction. The sequences are shown as follows:

Primers	Sequences	Size (bp)	T_m (^oC)
5'*AOX*1	5'-GACTGGTTCCAATTGACAAGC-3'	21	62
3'*AOX*1	5'-GCAAATGGCATTCTGACATCC-3'	21	62

4.8.6 PCR Primers for DNA Sequencing Reactions

In order to verify the sequences of the recombinant plasmids, sequencing primers that located on the vector are indicated as follows

Sequencing primers on pPICZαA vector are:

Primers	Sequences	Size (bp)	T_m (^oC)
5'*AOX*1	5'-GACTGGTTCCAATTGACAAGC-3'	21	62
3'*AOX*1	5'-GCAAATGGCATTCTGACATCC-3'	21	62

Sequencing primers on pET-15b vector are:

Primers	Sequences	Size (bp)	T_m (^oC)
T7 promoter	5' -TAATACGACTCACTATAGGG- 3'	20	56
T7 terminator	5' -GCTAGTTATTGCTCAGCGG- 3'	20	58

Since the large size of *Pem-ago* (2.8 kb), therefore in order to obtain the entire sequences, the internal sequencing primers were designed corresponding to the *Pem-ago* cDNA sequence as illustrated below:

Primers	Sequences	Size (bp)	T_m (^oC)
dsAgo-R3	5'-TGTATTGCATCATAAGGAATGGTTC-3'	25	68
dsAgo-F3	5'-ACGTGACAGGGTGTTCAAGGTAG-3'	23	70
PAZ-R	5'-CATGGTAGATGTCTGCATGTCTGT-3'	24	70
5'RACE4	5'-CCCTTAATTTCTTTTGTGAACTTGA-3'	25	66
dsAgo-R2	5'-TGAGCAGCTCCTTCACCATAG-3'	21	64
PIWI-F	5'-CAGCTTGTATGTGTTGTTCTACCAGG-3'	26	76
PIWI-R	5'-GAGATGATAACGAGCCCTGAAGG-3'	23	70
dsAgo-F2	5'-AGACAGAATGGATCAACAACAC-3'	22	62
5'RACE –Ago1	5'-GACAGTGTTTGAGGTGAGGT-3'	20	60

4.8.7 PCR Primers for Amplification of the GFP Sense-stranded

GFP sense-strand containing T7 promoter that was used as template for *in vitro* transcription reaction could be amplified by using the specific primers as show:

Primers	Sequences	Size (bp)	T_m (^{0}C)
T7 GFP-F	T7 promoter 5’ -TAATACGACTCACTATAGGGAGAATGGTGAGCAAGGGCGAGGAGC- 3’	45	72
GFP-R	5’ -AGGTCGTGCTGCTTCATGTGG- 3’	43	68

4.8.8 Sense and Anti-sense GFP-siRNA

The function of PAZ domain and Pem-AGO involved in RNA interference pathway were investigated by utilizing GFP gene. Sense and anti-sense stranded siRNA were commercially synthesized with the length of 21 nucleotides.

siRNA	Sequences
SenseGFP	5’ –rArArGrCUrGrArCrCrCUrGrArArGUUrCrAUrC- 3’
antisenseGFP	5’ –rCrArGrAUrGrArArCUUrCrArGrGrGUrCrArGrC- 3’

4.8.9 Synthetic Single-Stranded DNA

Substrate specific of PAZ domain was characterized by employing 21 nt of single-strand DNA as a competitor in the reaction. The sequence of 5’-MIH3gr2-3 as show:

ssDNA	Sequences
5’-MIH3gr2-3	5’ –AAGGATTGGGTCCTTCCGGAT- 3’

4.9 Culture Media

4.9.1 Culture Media for Yeast Expression System

The recombinant plasmid for yeast expression system, pPICZαA, contains *Sh ble* gene which is responsible for Zeocin™ resistance. The growth condition should be culture in low salt medium.

4.9.1.1 Bacterial Culture Medium

Escherichia coli transformants harboring pPICZαA plasmid was cultured in LB (Luria-Bertani) low salt medium consisting of 1% (w/v) tryptone or peptone, 0.5% (w/v) yeast extract, and 0.5% (w/v) NaCl. The pH of the medium was adjusted to 7.5 with NaOH. For LB agar, 1% (w/v) of bacto-agar was added into LB broth medium. The *E. coli* transformants were grown in low salt LB medium containing 25 μg/ml Zeocin™.

4.9.1.2 Yeast Culture Medium

Culture and Selective Media

Pichia pastoris strain KM71 was grown in enriched medium YEPD broth [2% (w/v) peptone, 1% (w/v) yeast extract and 2% (w/v) glucose]. The *P. pastoris* transformants bearing *Sh ble* gene from the recombinant plasmid integration were cultured under selective condition of YEPD containing 100 μg/ml Zeocin™.

Expression Medium

Expression in *P. pastoris* system comprises two culture mediums, BMGY and BMMY, which are different in the nutritional source component.

Buffered minimal glycerol complex medium (BMGY) is composed of 2% (w/v) peptone, 1% (w/v) yeast extract, 0.67% (w/v) yeast nitrogen base, 100 mM potassium phosphate, pH 6.0, 0.00004% (w/v) biotin and 1% (w/v) glycerol.

Buffered minimal methanol complex medium (BMMY) is composed of 2% (w/v) peptone, 1% (w/v) yeast extract, 0.67% (w/v) yeast nitrogen base, 100 mM potassium phosphate, pH 6.0, 0.00004% (w/v) biotin and methanol was added to final concentration of 1-5% (v/v) to induce the expression of the recombinant protein in *P. pastoris* expression system.

4.9.2 Culture Media for *Escherichia coli* Expression System

LB (Luria-Bertani) medium for the culture of *Escherichia coli* expression system consists of 1% (w/v) tryptone or peptone, 0.5% (w/v) yeast extract and 1% (w/v) NaCl. The pH of the medium was adjusted to 7.5 with NaOH. For LB agar, 1% (w/v) of bacto-agar was added into LB broth medium. Under selective condition, antibiotics were added into the culture medium according to the characteristics of the recombinant plasmids. Ampicillin was added into final concentration of 100 μg/ml whereas chloramphenicol was 34 μg/ml.

CHAPTER V
METHODS

5.1 Plasmid DNA Extraction by Cetyltrimethylammonium Bromide (CTAB) Minipreparation Method (Sal *et al*., 1988)

A single colony of bacteria was inoculated into 3 ml of LB broth (1% (w/v) tryptone, 0.5% (w/v) yeast extract, and 1% NaCl, pH 7.5) containing 100 µg/ml ampicillin and the culture was incubated overnight at 37°C with 250 rpm shaking. The bacterial cell suspension was transferred to a 1.5 ml microtube and the cells were harvested by centrifuged at 13,000 rpm for 1 min at room temperature. The supernatant was then discarded before resuspending the pellet in 200 µl of STET buffer (8% (w/v) sucrose, 50 mM Tris-HCl pH 8.0, 50 mM EDTA and 0.1% (v/v) Triton X-100) followed by adding 10 µl of freshly prepared lysozyme (50 mg/ml). The mixture was thoroughly mixed, incubated at room temperature for 10 min and boiled for 45 sec. Subsequently, the cells debris was packed by centrifugation at 13,000 rpm for 15 min at room temperature. The white pellet containing chromosomal DNA was removed by a sterile toothpick. Plasmid DNA and residual low molecular weight RNA were recovered from the supernatant by adding 1/10 volume of 5% (w/v) CTAB. The mixture was immediately mixed and centrifuged at 13,000 rpm for 5 min at room temperature. The DNA pellet was dissolved in 300 µl of 1.2 M NaCl by vigorously vortex. RNA was eliminated by adding 10 µl of RNaseA (10 mg/ml) and incubated at 37°C for 30 min. In order to remove residual proteins, the mixture was extracted with an equal volume of chloroform:isoamyl alcohol (24:1) by vortexing and centrifugation at 13,000 rpm for 5 min at room temperature. The clear upper aqueous phase was transferred to a new 1.5 ml microtube. Subsequently, two volumes of absolute ethanol were added to precipitate the DNA. The mixture was mixed and incubated at -20°C for 30 min. The DNA was collected by centrifugation at 13,000 rpm for 15 min at room

temperature. The DNA pellet was rinsed with 200 µl of 70% (v/v) ethanol and centrifuged at 13,000 rpm for 5 min at room temperature. Finally, the DNA pellet was air dried and dissolved in sterile distilled water.

5.2 Agarose Gel Electrophoresis (Sambrook J., *et al*.,1989)

The analysis of DNA fragments was performed by submarine agarose gel electrophoresis. The concentration of agarose is referred to as a percentage of agarose to a volume of buffer (w/v) and normally in the range of 0.3-3% depended on the size of DNA fragments to be separated. The agarose gel was prepared by dissolving agarose powder in either 1X TAE buffer (40 mM Tris-HCl, 40 mM acetic acid, 2.5 mM EDTA, pH 8.0) or 1X TBE buffer (89 mM Tris-HCl, 89 mM boric acid, 2.5 mM EDTA, pH 8.0) at boiling temperature. After cooling down to 50-60°C, the gel mixture was then poured into the mold. A comb was inserted in the molten gel. After the gel was completely solidified (approximately 30-45 min at room temperature), the comb was carefully removed and the gel was installed on the platform in the electrophoresis chamber containing appropriate buffer. The DNA samples were mixed with 4X gel loading dye (0.25%(w/v) Bromophenol Blue, 25% (w/v) glycerol, 60 mM EDTA) to give a final concentration of 1X gel loading dye before loading into the slot of the gel which was submerged in the buffer. After the electrophoresis was completed, the gel was stained in 2 µg/ml ethidium bromide solution for 3 min followed by destaining in sterile distilled water for 15 min. The DNA patterns were visualized under UV light and recorded by photography.

5.3 Restriction Endonuclease Digestion (Sambrook, *et al.*, 1989)

Restriction endonucleases are site-specific DNA cutting enzymes which recognize and cleave the DNA molecules in specific positions. In a typical reaction, an appropriate amount of the enzyme was added to achieve complete digestion. Generally, 1 µg of DNA can be digested with 1 unit of the enzyme in the recommended buffer at optimum temperature in 2-3 hr. After the digestion reaction had been completed, the digested products were analyzed by agarose gel electrophoresis.

5.4 DNA Amplification by Polymerase Chain Reaction (PCR)

5.4.1 PCR Amplification of the Coding Region of *Penaeus monodon*'s Argonaute (*Pem-ago*) and the *PAZ* domain for *Pichia pastoris* Expression System

DNA amplification was carried out by using pUC19 containing full-length cDNA encoding *P. monodon*'s Argonaute (*Pem-ago*) as a template with specific primers. The PCR reaction was performed by using automated thermal cycler GeneAmp® PCR system model 2400 (Perkin Elmer Cetus,USA) according to the condition shown in table 5.1.

The PCR reaction of *Pem-ago* (100 µl) contained		
DNA template	50	ng
10X cloned *Pfu* buffer	10	µl
dNTP mix	200	µM each
Argo-F primer	0.5	µM
Argo-R primer	0.5	µM
Cloned *Pfu* DNA polymerase	2.5	unit

The PCR reaction of *PAZ* domain (100 µl) contained		
DNA template	50	ng
10X cloned *Pfu* buffer	10	µl
dNTP mix	200	µM each
PAZex-F primer	0.5	µM
PAZex-R primer	0.5	µM
Cloned *Pfu* DNA polymerase	2.5	unit

Table 5.1 PCR profile for amplification of the coding region of *Penaeus monodon*'s Argonaute (*Pem-ago*) and the *PAZ* domain for *Pichia pastoris* expression system

Segment	Step	Temperature (°C)	Time (min)	Number of cycles
1	Pre-denaturation	94	2	1
2	Denaturation	94	1	30
	Annealing	64	1	
	Extension	72	4	
3	Final extension	72	7	1

5.4.2 PCR Amplification of the Coding Region of *Penaeus monodon*'s Argonaute (*Pem-ago*) and the *PAZ* domain for *Escherichia coli* Expression System

DNA amplification was carried out by using pUC19 containing full-length cDNA encoding Pem-AGO as a template with specific primers that designed by in-frame with N-terminal histidine tag. The PCR reaction was performed by using automated thermal cycler GeneAmp® PCR system model 2400 (Perkin Elmer Cetus,USA) according to the condition shown in table 5.2. The PCR reactions were set up as described in 5.4.1 except that EX-AGO-F and EX-AGO-R primers were used to amplify *Pem-ago* coding region whereas EX-PAZ-F and EX-PAZ-R primers were introduced to amplify the *PAZ* domain.

Table 5.2 PCR profile for amplification of the coding region of *Penaeus monodon*'s Argonaute (*Pem-ago*) and the *PAZ* domain for *Escherichia coli* expression system

Segment	Step	Temperature (°C)	Time (min)	Number of cycles
1	Pre-denaturation	94	2	1
2	Denaturation	94	1	30
	Annealing	62	1	
	Extension	72	5.5	
3	Final extension	72	7	1

5.4.3 PCR Amplification of GFP Sense-Strand Template

In this thesis, the function of Pem-AGO protein in RNA interference pathway was determined by study the cleavage of the target mRNA that contain the complementary sequences to the siRNA. Therefore, mRNA cleavage assay experiment was performed and the sequence of GFP was selected to apply in this experiment. The GFP DNA template for transcription of sense-stranded RNA was amplified by PCR reaction by using pBluescript/GFP plasmid as a template with specific primers containing the T7 RNA polymerase promoter at the 5' end. The PCR reaction was performed by using automated thermal cycler GeneAmp® PCR system model 2400 (Perkin Elmer Cetus,USA) according to the condition shown in table 5.3.

The PCR reaction of GFP sense-stranded template (50 µl) contained

DNA template	50	ng
10X PCR buffer	5	µl
25 mM $MgCl_2$	1.5	mM
dNTP mix	200	µM each
GFP-F primer	0.2	µM
GFP-R2 primer	0.2	µM
Taq DNA polymerase (Promega)	1.25	unit

Table 5.3 PCR profile for amplification of GFP sense-strand

Segment	Step	Temperature (°C)	Time (min)	Number of cycles
1	Pre-denaturation	94	3	1
2	Denaturation	94	0.5	5
	Annealing	57-53*	0.5	
	Extension	74	1	
3	Denaturation	94	0.5	30
	Annealing	57	0.5	
	Extension	74	1	
4	Final extension	74	7	1

* touch down steps ; the annealing temperature was decreased for 1°C in each cycle.

After completion, the PCR products were analyzed by agarose gel electrophoresis.

5.5 Recovery and Purification of DNA Fragments

5.5.1 Purification of DNA from Agarose Gel by QIAquick® Gel Extraction Kit

QIAquick® Gel Extraction kit (QIAGEN) is designed to extract and purify DNA of 70 bp to 10 kb in length from standard or low-melting point agarose gels in TAE or TBE buffer. Purification of DNA from agarose gel electrophoresis was performed by using QIAquick® gel extraction kit based on the method according to the manufacturer's protocol. After gel electrophoresis, the expected DNA fragment was excised from the gel under low intensity, long wavelength UV light. The gel slice was transferred into a eppendorf and weighted. Three volumes of buffer QG were added to 1 volume of the gel (100 mg ~ 100 µl). The mixture was incubated at 50°C for 10 min with vortex every 2-3 min to dissolve the gel. After the gel was completely dissolved, one volume of isopropanol was added to the sample and mixed thoroughly, this step will help increase the yield of DNA fragments of size <500 bp and >4 kb. The sample mixture was then applied to the QIAquick column that had been placed in a 2 ml collection tube and centrifuged at 13,000 rpm for 1 min. At pH lower than 7.5 and high salt concentration, DNA was adsorbed on the silica-gel membrane while unwanted impurities passed through the column into the flow-through which was then discarded. Salts were washed away by adding 0.75 ml of buffer PE to the column, then centrifuged at 13,000 rpm for 1 min. After the flow-through was discarded, residual ethanol was removed by an additional centrifuge at 13,000 rpm for 1 min. The column was placed into a new microcentrifuge tube air dry and the DNA was eluted from the column under basic conditions and low salt concentration by adding 30 µl of buffer EB (10mM Tris-HCl, pH 8.5) or sterile MilliQ water. The column was incubated at room temperature for 5-10 min followed by centrifugation at 13,000 rpm for 1 min. The elution step might be repeated for higher yield of DNA. Finally, the concentration of the eluted DNA was determined by analyzing on agarose gel electrophoresis.

5.5.2 Purification of DNA from PCR and Enzymatic Reactions by QIAquick® PCR Purification Kit

Purification of DNA in aqueous solution was performed by using QIAquick PCR Purification Kit based on the method described in the manufacture's instructions. In order to purify PCR products or DNA from enzymatic reactions with high purity, five volumes of buffer PB was added to one volume of samples (which is the PCR reaction or enzymatic reactions containing DNA to be purified). The mixture was applied to a QIAquick spin column, centrifuged at 13,000 rpm for 30-60 seconds and the flow-through was discarded. Then the column was proceeded to next steps as described in 5.5.1 to obtain the purified DNA.

5.6 Dephosphorylation of Linearlized Plasmid

Linearlized plasmid DNA was dephosphorylated by the method described in Sambrook *et al*., 1989. In order to phosphorylate 1 pmole of 5'-terminal phosphate, 1unit of Calf intestinal alkaline phosphatase (CIAP) was added to the reaction mixture containing 1X dephosphorylation buffer (Gibco BRL) twice at 30 min interval. After the reaction was completed, the enzyme was inactivated by incubated at 75ºC for 10 min in the presence of 5 mM EDTA. The dephosphorylated DNA was purified by phonol:chloroform extraction and precipitated by ethanol.

5.7 DNA Ligation

The appropriate amount of linearlized DNA vector and DNA insert fragment in the ligation reaction was calculated from the molar ratio of vector to DNA insert. Normally, the molar ratio could be varied from 1:1 to 1:7 depending on the size of the vector compared to the insert DNA. The lower ratio could be applied when the size of DNA vector and DNA insert were not greatly different whereas the higher amount of insert was increased if the size of vector was larger than DNA insert. Molar of DNA can be calculated by the following equation:

$$\text{Molar of DNA} = \frac{\text{amount of DNA (g)}}{660 \times \text{DNA size (bp)}}$$

The plasmid vector and DNA fragment were digested with appropriate restriction enzymes and purified by QIAquick Purification Kit. The digested vector and DNA insert were mixed and incubated at 45°C for 90 seconds then immediately placed on ice for 2 min before adding the ligation buffer (50mM Tris-HCl pH 7.8, 10 mM $MgCl_2$, 10 mM DTT, 25 µg/ml BSA and 1 mM ATP) and T4 DNA ligase to final concentration of 1X and 2 units, respectively in the total volume of 20 µl. The reaction mixture was then incubated overnight at 16°C.

5.8 Transformation of Recombinant Plasmids by Heat-shock Method (Sambrook J., et al., 1989)

5.8.1 Preparation of Competent Cells by the $CaCl_2$ Method

A single colony of *E.coli* was inoculated into 3 ml of LB broth and incubated overnight (12-16 hr) at 37°C with shaking at 250 rpm. The overnight culture was diluted 1:100 in new LB broth and incubated at 37°C with shaking at 250 rpm until OD_{600} reached 0.3-0.4. The culture was chilled on ice for 10 min prior to centrifugation at 3,000 rpm for 10 min at 4°C. The supernatant was decanted and the pellet was resuspended in 10 ml of ice-cold 0.1 M $CaCl_2$ and stored on ice for 15 min. After centrifugation at 3,000 rpm for 10 min at 4°C, the pellet was resuspended in 10 ml of ice-cold 0.1 M $CaCl_2$, placed on ice for 10 min followed by centrifugation at 3,000 rpm for 10 min at 4°C. Then the pellet was resuspended in 2 ml of ice-cold 0.1 M $CaCl_2$ for each 50 ml of original culture. For storage as frozen cells, glycerol was added to the solution with gently swirling to make a 30% final concentration. Aliquots of the competent cells (100 µl) were stored at -80°C until required.

5.8.2 Transformation of Plasmid DNA into Competent Cells

An aliquot of 100 µl *E.coli* competent cells was mixed with 5-10 ng of ligated products. The mixture was gently mixed and chilled on ice for 30 min. Subsequently, the mixture was subjected to heat-shock at 42°C for 90 seconds and immediately placed on ice for an additional 5 min. The transformed cells were mixed with 800 µl of LB medium and incubated at 37°C for 1-2 hr with shaking at 250 rpm. After centrifugation at 3,000 rpm for 2 min, 400 µl of the supernatant was discarded. The cells were resuspended in the remaining medium and an aliquot of 250 µl was spread

on the LB agar plate containing ampicillin (100 µg/ml) and incubated overnight at 37°C.

5.9 Screening for the Recombinant Clones

5.9.1 Screening by Rapid Size-Screening

A colony (1mm in diameter) was transferred into 30 µl of pre-warmed lysis buffer (5 mM EDTA, 10% (w/v) sucrose, 0.25% (w/v) SDS, 100 mM NaOH, 100 mM KCl , 0.1% (w/v) Bromophenol Blue). After vigorously vortex, the homogenate was then incubated at 37°C for 5 min, then chilled on ice for an additional 5 min. Subsequently, the mixture was centrifuged at 12,000 rpm for 3 min. A 25 µl of supernatant was analyzed by agarose gel electrophoresis. The recombinant clone that contained the insert DNA fragment would present the shifted bands of plasmid DNA when compared with plasmid vector alone.

5.9.2 Screening by Restriction Digestion Analysis

The recombinant clones were screened by analyzing the pattern of restriction enzyme digested plasmid constructs. The extracted plasmids were digested with the restriction enzymes, whose recognition sites were introduced into the 5' end of the primers. Internal sites digestion within the inserts was then performed to confirm correct orientation of the inserts.

5.10 DNA Sequencing

The DNA sequencing reactions were performed by using an ABI PRISM™ Dye Terminator Cycle Sequencing Ready Reaction Kit (Perkin Elmer). Sequencing reactions were run on ABI PRISM™ Model 377 DNA Sequencer (Perkin Elmer).

5.11 *Pichia pastoris* Expression System

5.11.1 Preparation of *P. pastoris* Competent Cells

A single colony of *P. pastoris* was grown in 50 ml of YEPD medium in a conical flask at 30°C with shaking at 250 rpm until OD_{600} reached 1.3-1.5. The yeast cells were harvested by centrifugation at 3,000 rpm for 10 min at 4°C. The cell pellet was resuspended in 5 ml of ice-cold sterile water and centrifuged at 6,000 rpm for 5 min at

4°C. Then the cell pellet was resuspended in 1 ml of 1 M ice-cold sorbital and centrifuged at 6,000 rpm for 5 min at 4°C. The supernatant was subsequently discarded, and the cell pellet was finally resuspended in 1 ml of ice-cold 1 M sorbitol. A 40 µl aliquot was dispended into microcentrifuge tube for one transformation reaction.

5.11.2 Preparation of Linearized Recombinant Plasmid

In order to transform the recombinant construct into yeast genome, the recombinant plasmid was first linearized by digesting with appropriate restriction enzyme that was not present in the inserted gene. For the pPICαA/PAZ and pPICαA/Argonaute constructs, 1 µg of the recombinant plasmids was digested with *Dra* I at 37°C. Then the linearlized plasmids were precipitated with 60 µl of absolute ethanol in the presence of 3 µl of 3 M sodium acetate and 1.5 µl of tRNA. After incubation at -80°C for 15 min, the mixture was centrifuged at 10,000 rpm at 4°C for 10 min. The DNA pellet was washed with 70% (v/v) ethanol. After the pellet was air-dried, it was resuspended in 5 µl of sterile distilled water.

5.11.3 Transformation of *P. pastoris* Competent Cells by Electroporation

The reaction mixture was composed of 40 µl of *P. pastoris* competent cells and 5 µl (300 ng) of linearized recombinant plasmid DNA. The mixture was transferred to an ice-cold 0.2 cm electro-cuvette and incubated on ice for 5 min. The cells were pulsed by using BIO-RAD Gene Pulser according to the conditions of 1.5 kV, 25 µF and 200 Ω (time constant should be 4.5). Then 1 ml of 1 M sorbitol was added immediately to the cuvette and the mixture was transferred into a sterile microcentrifuge tube. The tube was incubated at 30°C without shaking for 1 hr, before 1 ml of YEPD medium was added. The culture was further incubated at 30°C with shaking for another 2 hr. The cells were then harvested by centrifugation at 3,000 rpm at 4°C for 5 min and the supernatant was discarded. After that, 800 µl of YEPD medium was added to resuspend the cell pellet. Then 100 µl of transformed cell was spread on YEPD agar plate containing 100 µg/ml Zeocin™. The plate was incubated at 30 °C for 2-3 days until visible colonies were formed.

5.11.4 Total DNA Isolation from *P. pastoris*

The recombinant and wild-type *P. pastoris* were grown in YEPD containing 100 µg/ml Zeocin™ at 30°C with shaking at 250 rpm until OD_{600} reached 5-10. The cells were collected by centrifugation at 3,000 rpm for 5 min at room temperature. The cell pellet was washed with 1 ml sterile water and resuspended in 200 µl of SCED buffer, pH 7.5 (1 M sorbitol, 10 mM sodium citrate pH 7.5, 10 mM EDTA, 10 mM DTT). Then, 5 µl of lyticase (25U/ µl) was added and the cells were kept at 30°C for 3-4 hr. After that 100 µl of 2% (w/v) SDS was added, mixed gently, and the mixture was chilled on ice for 5 min. Next, 150 µl of 5 M potassium acetate pH 8.9 was added to the cell mixture and centrifuged at 10,000 rpm for 5-10 min at 4°C. The supernatant was collected and transferred into a new microcentrifuge tube. Subsequently, one volume of absolute ethanol was added to the supernatant and incubated at 4°C for overnight. After centrifugation at 10,000 rpm for 20 min at 4°C, the supernatant was removed and the cell pellet was resuspended gently in 500 µl of TE buffer (10 mM Tris-HCl pH 7.4, 1 mM EDTA pH 8.0). The DNA solution was incubated with 10 µl of 5 mg/ml RNase A at 37 °C for 1 hr. An equal volume of phenol was added, mixed gently and centrifuged at 14,000 rpm for 5 min. The aqueous layer containing the nucleic acid was transferred into a new micro centrifuge tube. An equal volume of chloroform:isoamyl alcohol (24:1) was added before gently mixed and centrifuged at 14,000 rpm for 5 min. The aqueous was collected into a new micro centrifuge tube. This step was then repeated once. After transferring the aqueous phase to a new tube, half volume of 7.5 M ammonium acetate pH 7.5 and two volumes of absolute ethanol were added and the tube was subsequently kept at -80 °C for 10 min. The solution was centrifuged at 10,000 rpm for 20 min at 4 °C. The pellet was washed with 70% (v/v) ethanol, air-dried and the DNA was resuspended in 40 µl of sterile distilled water or TE buffer pH 7.5 and stored at -20 °C until ready to use.

5.11.5 PCR Analysis of *P. pastoris* Integrants

Pichia transformants containing chromosomal integrations of the expression plasmid were analyzed by hot start PCR as follows. The PCR reactions consisting of 1X reaction buffer (10 mM Tris-HCl pH 8.3, 50 mM KCl), 25 mM $MgCl_2$, 2 mM of dNTP, 10 pmole of each primer (5' *AOX*1 forward primer and 3'

*AOX*1 reverse primer), 2 units of *Taq* DNA polymerase (Promega) (5u/µl), 50-100 ng of gemonic DNA was adjusted to a total volume of 25 µl with sterile distilled water The reactions were operated in the automated thermal cycler GeneAmp® PCR system model 2400 (Perkin Elmer Cetus,USA) according to the condition shown in table 5.4. The PCR products were analyzed on agarose gel electrophoresis.

Table 5.4 PCR parameter profile for screening of *P. pastoris* integrants

Segment	Step	Temperature (°C)	Time (min)	Number of cycles
1	Pre-denaturation	94	2	1
2	Denaturation	94	0.5	30
	Annealing	43	0.5	
	Extension	72	1	
4	Extra extension	72	7	1

5.11.6 Screening of the *P. pastoris* Integrants by Colony PCR Method

Another rapid and convenient strategy for screening the chromosomal integrants is colony PCR. A colony (1 mm in diameter) of transformed clones from a master plate was picked by a sterile toothpick and resuspended in the mixture of PCR reaction consisting of 1X reaction buffer (10mM Tris-HCl pH8.3 and 50 mM KCl), 25 mM $MgCl_2$, 2 mM dNTP, 10 pmole of each primer (5' *AOX1* forward primer and 3' *AOX1* reverse primer) and 2 units of *Taq* DNA polymerase (Promega) (5 U/µl). The total volume was adjusted to 25 µl with sterile distilled water. The *P. pasteris* colonies transformed with pPICZαA/Der p3.1 and pPICZαA alone were used as positive and negative control for expression, respectively. The reactions were operated in the automated thermal cycler GeneAmp® PCR system model 2400 (Perkin Elmer Cetus,USA) according to the condition shown in table 5.4. The PCR products were analyzed on agarose gel electrophoresis.

$MgCl_2$, 2 mM of dNTP, 10 pmole of each primer (5' *AOX*1 forward primer and 3' *AOX*1 reverse primer), 2 units of *Taq* DNA polymerase (Promega) (5u/µl), 50-100 ng of gemonic DNA was adjusted to a total volume of 25 µl with sterile distilled water The reactions were operated in the automated thermal cycler GeneAmp® PCR system model 2400 (Perkin Elmer Cetus,USA) according to the condition shown in table 5.4. The PCR products were analyzed on agarose gel electrophoresis.

Table 5.4 PCR parameter profile for screening of *P. pastoris* integrants

Segment	Step	Temperature (°C)	Time (min)	Number of cycles
1	Pre-denaturation	94	2	1
2	Denaturation	94	0.5	30
	Annealing	43	0.5	
	Extension	72	1	
4	Extra extension	72	7	1

5.11.6 Screening of the *P. pastoris* Integrants by Colony PCR Method

Another rapid and convenient strategy for screening the chromosomal integrants is colony PCR. A colony (1 mm in diameter) of transformed clones from a master plate was picked by a sterile toothpick and resuspended in the mixture of PCR reaction consisting of 1X reaction buffer (10mM Tris-HCl pH8.3 and 50 mM KCl), 25 mM $MgCl_2$, 2 mM dNTP, 10 pmole of each primer (5' *AOX1* forward primer and 3' *AOX1* reverse primer) and 2 units of *Taq* DNA polymerase (Promega) (5 U/µl). The total volume was adjusted to 25 µl with sterile distilled water. The *P. pasteris* colonies transformed with pPICZαA/Der p3.1 and pPICZαA alone were used as positive and negative control for expression, respectively. The reactions were operated in the automated thermal cycler GeneAmp® PCR system model 2400 (Perkin Elmer Cetus,USA) according to the condition shown in table 5.4. The PCR products were analyzed on agarose gel electrophoresis.

5.11.7 Expression of Recombinant Proteins in *P. pastoris* System (Small Scale)

A single colony of positive recombinant clones from PCR integration analysis of *P. pastoris KM71* was incubated in 3 ml of YEPD broth containing 100 μg/ml Zeoin™ with 250 rpm shaking at 30°C for approximately 2 days, and the OD_{600} of the cell culture was measured. The cells were harvested by centrifugation at 5,000 rpm for 5 min and transferred into fresh BMGY medium that contained glycerol as a nutritional source to the final OD_{600} of 0.1-0.2. The culture was grown under the conditions as mentioned earlier until the OD_{600} reached 5-6. For the induction step, the cell pellet was harvested by centrifugation at 5,000 rpm for 5 min at room temperature. The supernatant was discarded and the cell pellet was resuspended in BMMY medium using 1/5 volume of the original culture or 25-30 OD_{600} per 1 ml of BMMY medium by using the container that provided the aeration space ratio (volume of culture per volume of the container) of approximately 1:20. The container was covered with 2 layers of sterile gauze. In order to maintain the induction, the absolute methanol was added to a final concentration that varied from 0-5% (v/v) every 24 hr. One ml of BMMY induction cultures were collected at the following time points of 0, 24, 48, 72, 96 and 120 hr to determine the period of expression that provided the highest recombination protein expression level. The cell cultures were collected by centrifugation at 13,000 rpm for 5 min at room temperature. To prove the extracellular expression whether the recombinant protein could be secreted into the medium, the supernatant medium was collected and transferred to a new microcentrifuge tube. The proteins presented in the cell pellet and the culture medium were maintained at –80°C until analyzed by SDS-PAGE as described in 5.1.4.

5.11.8 Protein Sample Preparation from *P. pastoris* Expression

5.11.8.1 TCA Precipitaiton for Extracellular Expression Analysis

In order to analyze the expressed soluble proteins that were secreted into the supernatant, the culture medium was concentrated by TCA (Trichloro Acetic Acid) precipitation (Hames, 1981). A 100 μl of 100% (w/v) TCA was added into 1 ml of the supernatant, and mixed by vortex. Proteins were precipitated by incubation of the mixture on ice for 30 min then centrifugation at 14,000 rpm for 10 min to obtain the

protein pellet. The supernatant was discarded immediately. The remaining of TCA could be completely removed by washing the protein pellet twice with 200 µl of ice-cold acetone and the acidic condition of protein was neutralized by resuspended in 10-50 µl of 0.1 N NaOH.

The protein sample was then mixed with 4X sample buffer (200 mM Tris-HCl pH 7.5, 4 mM EDTA pH 8.0, 4% (w/v) SDS, 40% glycerol, 0.1% (w/v) Bromophenol Blue and 100 mM DTT) to a final concentration of 1X sample buffer. The sample was boiled at 100^{o}C for 5 min and centrifuged at 14,000 rpm for 5 min before subjected to SDS-PAGE analysis.

5.11.8.2 Sample Preparation for Intracellular Protein Expression

In order to analyze the protein that expressed intracellularly, the cells were collected by centrifugation at 14,000 for 1 min at room temperature. The cell pellet was subsequently resuspended with 50 µl of distilled water and mixed with 4X sample buffer (200 mM Tris-HCl pH 7.5, 4 mM EDTA pH 8.0, 4% (w/v) SDS, 40% glycerol, 0.1% (w/v) Bromophenol Blue and 100 mM DTT) in the ratio 3:1 followed by boiling for 5 min and centrifugation. The cell amount equivalent to 0.6 OD_{600} was subjected to SDS-PAGE.

5.12 *Escherichia coli* Expression System

5.12.1 Small Scale Expression of Recombinant Protein in *E. coli*

Recombinant plasmids containing the Pem-*ago* and PAZ domain cDNA were transformed into *E. coli* BL21(DE3)pLysS for protein expression. A single colony of *E. coli* harboring the recombinant plasmids was inoculated in 3 ml of LB broth containing 100 µg/ml Ampicillin. The culture was incubated overnight at 37^{o}C with 200 rpm shaking. The overnight culture was diluted at 1:100 in the appropriate volume of LB broth containing selective antibiotics as mention earlier and the culture was grown for an additional time at 37^{o}C with shaking at 250 rpm until OD_{600} reached 0.5-0.6. Subsequently, the expression of the recombinant protein was induced by IPTG under the control of T7-promoter at a final concentration of 0.1-0.4 mM. The culture was further incubated at 25^{o}C with shaking. An aliquot of the induced culture containing 1X10^{8} cells (1 OD_{600} of *E. coli* is approximately 10^{8} cells) were collected at

different time points and then centrifuged at 13,000 rpm for 1 min. The cells were resuspended in a final concentration of 1X sample buffer, and the pattern of protein expression was analyzed by SDS-PAGE.

5.12.2 Large Scale Expression of Recombinant Protein in *E. coli*

A single colony of the *E. coli* BL21(DE3)pLysS harboring the recombinant plasmid was inoculated into 10 ml of LB broth containing 100 μg/ml ampicillin and incubated overnight at 37°C with 250 rpm shaking. The overnight culture was transferred to new LB broth containing 100 μg/ml ampicillin to yield the final dilution of 1:100 followed by incubation at 37°C for an additional time until OD_{600} of the culture reached 0.5-0.6. To express the recombinant protein under the control of T7-promoter, IPTG was added into the culture at a final concentration of 0.1 mM. The induced culture was incubated at 25°C with shaking at 250 rpm for 2 hr for expression of recombinant Pem-AGO and 7 hr for expression of recombinant PAZ protein. The cell culture was harvested by centrifugation at 4,000 rpm for 15 min at 4°C and analyzed by SDS-PAGE.

5.13 Purification of the Soluble Recombinant Histidine-tagged Proteins

Cell pellet harvested from 1 liter expression culture was resuspended with 20 ml of lysis buffer (50 mM Tris-HCl pH 8.0, 100 mM NaCl, 5% glycerol, 10 mM imidazole, 1 mM PMSF and 0.1 mg/ml lysozyme). Cell pellet was mixed thoroughly with lysis buffer by sonication with the power level 3 for total sonication time of 3 min before lysis the cell by using Cell press (French Press) with 10,000 psi twice. The inclusion protein pellet was separated from the soluble part by centrifugation at 10,000 rpm for 40 min at 4°C. The supernatant was centrifuged with the same condition one more time in order to remove residual debris and preserved under 4°C all the time and then immediately purified by using HisTrap™ FF crude column (Amersham). Before starting the purification step, all of the reagents including purification buffer (buffer H composed of 50 mM Tris-HCl pH 8.0, 100 mM NaCl, 5% glycerol) must be filtrated by using filter paper size of 0.2 μm before applied to the column. Moreover, every step and all equipments were chilled and performed under cold condition. The recombinant histidine-tagged proteins were purified according to the charge interaction between

histidine residues that located on the N-terminus of the recombinant proteins and Ni^{2+} that was immobilized in the column. The column was connected to the pump. The preservative agent of 20% ethanol that filled in the column was removed with 10 ml of milliQ water at 1 ml/min flow rate followed by equilibration with 10 ml of binding buffer (buffer H containing 20 mM imidazole). In order to improve the purity of the purified protein, the blank run step was performed as recommended by the instruction manual with 5 ml of binding buffer followed by 3 ml of eluting buffer (buffer H containing 500 mM imidazole) before equilibrating the column with 15 ml of binding buffer. For protein purification step, supernatant sample was applied into the column with 1 ml/min flow rate for two times to allow efficient binding between the recombinant histidine-tagged protein and Ni^{2+} on the surface of the prepacked beads in the column. To remove the recombinant protein and reduce the non-specific proteins that bind to the Ni^{2+} column with weak interaction, the column was washed with 15 ml of washing buffer (buffer H containing 30 mM imidazole). For eluting step, in order to enhance the specificity of the eluted protein, the gradient of imidazole in elution buffer was gradually increased from 100, 200, 300, 400 and 500 mM, respectively. The proteins were eluted with 2 ml at each concentration and an additional 10 ml of 500 mM imidazole. The eluted solution was collected as a 1 ml fraction. After finishing the elution step, the column was washed with 15 ml of milliQ water followed by 5 ml of 20% ethanol to preserve the column from microorganism growth. Finally the column was sealed with parafilm to prevent the evaporation of ethanol before stored at $4^{o}C$. Every fraction was analyzed on SDS-PAGE or by Western Blot analysis.

5.14 Determination of Protein Concentration

The concentration of the protein samples was determined by using Bio-Rad Protein Assay dye reagent with a microtiter plate reader based on the method described by Bradford Protein Assay kit. The working Bradford reagent was prepared by diluting 1 part Dye Reagent Concentrate with 4 parts of distilled water and filtered through a Whatman #1 filter to remove particulates. The standard protein calibration curve was constructed using bovine serum albumin (BSA). The BSA standards were prepared at the concentration of 0.1, 0.2, 0.3, 0.4 and 0.5 mg/ml. A volume of 200 µl of Bio-Rad dye reagent was mixed with 10 µl of sample solution then the reactions

were incubated at room temperature for at least 5 min. The protein concentration was measured at OD_{595} by SPECTRA MAX 190 (Molecular Devices) after comparing to the standard curve.

5.15 SDS-Poly Acrylamide Gel Electrophoresis (SDS-PAGE)

5.15.1 Sample Preparation from Crude Cell Extract

The 1 OD_{600} cell culture was harvested by centrifugation at 15,000 rpm for 1 min. The pellet was resuspended by adding 50 µl of distilled water and 20 µl of 4X sample buffer (200 mM Tris-HCl pH 7.5, 4 mM EDTA pH 8.0, 4% (w/v) SDS, 40% glycerol, 0.1% (w/v) bromophenol blue and 100 mM DTT) in the ratio of 3:1 and vortex. The mixture sample was heated at 95^{o}C for 5 min followed by centrifugation at 13,000 rpm for 5 min. The sample equivalent to 0.1 OD_{600} would be loaded onto the SDS-PAGE.

5.15.2 Sample Preparation from Fractionated Purified Protein

Protein sample corresponding to 5-10 µg or 10 µl from eluted fraction was mixed with 4X sample buffer into final 1X sample buffer. The sample was subsequently boiled for 5 min followed by centrifugation for 5 min and placed on ice until the SDS-PAGE had been set up.

5.15.3 Sample Preparation for Dot Blot Analysis

Cell culture corresponding to 0.2 OD_{600} was harvested by centrifugation at 13,000 rpm for 1 min. The cell pellet was resuspended in 500 µl of lysis buffer (50 mM Tris-HCl pH 8.0, 100 mM NaCl, 5% glycerol, 10 mM imidazole, 1 mM PMSF and 0.1 mg/ml lysozyme). The cells were subsequently sonicated at level 3 for total sonication time of 2 min. The inclusion was collected by centrifugation at 13,000 rpm for 10 min. The soluble protein was collected by tranferring the supernatant into a new micro centrifuge tube and concentrated by TCA precipitation before dissolved in 5 µl of distilled water. The pellet of the inclusion proteins and the TCA precipitated proteins were resuspended in 5 µl of loading buffer (200 mM Tris-HCl pH 7.5, 4 mM EDTA pH 8.0, 4% (w/v) SDS, 40% glycerol and 100 mM DTT) then vortex throughly. After completely dissolved, the sample mixtures were heated for 5 min

followed by centrifugation at 13,000 rpm for 3 min. Before apply the samples, PVDF membrane was pre-wet with methanol. The samples corresponding to 0.2 OD_{600} were spotted on the membrane and air-dried. The membrane was then blocked in 5% skim milk followed by incubation with anti-His antibody as primary antibody and anti-mouse conjugated with alkaline phosphatase as secondary antibody before the detection step as described in method 5.15.3.

5.15.4 Seperation of Protein Samples (Protein Electrophoresis)

Electrophoresis of protein was performed according to the protocols for Mini Protein II electrophoresis (BIO-RAD). The SDS-PAGE gel was prepared as described in table 5.5 The recombinant Argonaute protein (approximately 100 kDa) was analyzed on 8-10% of separating gel whereas the recombinant PAZ domain (approximately 19 kDa) was analyzed on 15% separating gel. After the stacking and separating gel were allowed to polymerized at room temperature for 30 min, the comb was removed and wells were flushed with distilled water to remove unpolymerized acrylamide solution. The electrophoresis was carried out in a descending direction in Tris-glycine buffer (25 mM Tris-HCl pH 8.3, 192 mM glycine, 0.1% (w/v) SDS) at a constant voltage of 120 volts until the dye front reached the bottom edge of the gel. The electrophoresis equipments were then disassembled. The protein bands on the gel were visualized by staining with Coomassie staining solution (0.1% Coomassie Brilliant Blue R250, 50% methanol, 10% glacial acetic acid) with gentle shaking at room temperature for at least 2 hr. The background was removed by soaking the gel in a destaining solution (10% methanol and 10% glacial acetic acid) with gentle shaking at room temperature overnight or until the protein bands were clearly visible. The protein molecular weight was predicted by comparing the migration distance of the band of interest to the standard protein marker.

Table 5.5 Preparation of SDS-PAGE gel

Solution	5% Stacking gel	8% Separating gel	10% Separating gel	15% Separating gel
30% Acrylamide solution (ml) [29% (w/v)acrylamide + 1% (w/v) bis-acrylamide]	0.17	1.3	1.7	2.5
1.5 M Tris-HCl pH 8.8 (ml)	-	1.3	1.3	1.3
1.0 M Tris-HCl pH 6.8 (ml)	0.13	-	-	-
Distilled water (ml)	0.68	2.3	1.9	1.1
10% (w/v) SDS (ml)	0.01	0.05	0.05	0.05
10% (w/v) Ammonium persulphate (ml)	0.01	0.05	0.05	0.05
TEMED (ml)	0.001	0.003	0.02	0.002

5.16 Western Blot Analysis

5.16.1 Electrotransfer of Protein from SDS-PAGE to Nitrocellulose Membrane by Semi-Dry Blot

After electrophoresis, The SDS-PAGE gel was soaked in transfer buffer (25 mM Tris-HCl pH 9.2, 192 mM glycine, 20% (v/v) methanol) for 10 min. The nitrocellulose membrane and 4 pieces of filter paper were cut to the same size as the gel and immersed in transfer buffer for 10 min. The blotting apparatus was assembled by put two soaked filter papers in the center of the platinum anode of the Trans-Blot SD Semi-Dry Electrophoresis Transfer cell (BIO-RAD) followed by a nitrocellulose membrane, the polyacrylamide gel and the other two pieces of wet filter papers. Electroblotting was carried out at constant current calculated by multiplying the gel size (cm^2) by 3 (mA) for 1.5 hr.

5.16.2 Electrotransfer of Protein from SDS-PAGE to Nitrocellulose Membrane by Wet Blot

After electrophoresis, The SDS-PAGE gel was soaked in transfer buffer (25 mM Tris-HCl pH 9.2, 192 mM glycine, 20% (v/v) methanol) for 10 min. The nitrocellulose membrane and 4 pieces of filter paper were cut to the same size as the

gel and immersed in transfer buffer for 10 min. The blotting apparatus was assembled by putting two soaked filter papers on the buffer soaked spong that placed on the white side of the set followed by putting a nitrocellulose membrane, the polyacrylamide gel, the other two pieces of wet filter papers and another spong. The set was then placed into the container by face the black side of the set to the same color in the container. Electroblotting was carried out at constant voltage at 50 volts for 3 hr in the cold room

5.16.3 Detection of the Recombinant Hexa-histidine Tagged Protein by Colorimetric Method

Detection is based on the affinity of hexa-histidine tag of the fusion recombinant protein. After Western Blotting processing according to standard protocols, the nitrocellulose membrane was stained with Ponceau S (2% Ponceau S and 3% Trichloroacetic acid) at room temperature for 5 min and washed with distilled water to remove the excess staining solution. Subsequently, the standard protein marker bands were marked by pencil. After completely remove Ponceau S solution by washing with 1X TBS buffer (25 mM Tris-HCl pH 8.3, 192 mM glycine, 20% (v/v) methanol) for 5 min at room temperature, the membrane was pre-blocking by immersing in blocking solution (5% (w/v) skim milk in 1X TBS buffer) at room temperature for 2 hr or 4^{o}C overnight. The membrane was incubated with a new blocking solution containing 1:10.000 dilution of mouse anti-His antibody for 2 hr at room temperature with shaking. The membrane was washed twice with TBS-T buffer (1X TBS containing 0.1% (v/v) Tween 20) for 10 min each, followed by TBS buffer for another 10 min. Subsequently, the membrane was incubated with the alkaline phosphatase conjugated anti-mouse IgG (1:10,000 dilution) in blocking solution for 1 hr at room temperature with shaking. The membrane was washed twice with TBS-T buffer for 10 min each and with TBS buffer for another 10 min. The signal was developed by incubating the membrane in the developer solution (33 µl of BCIP (50 mg dissolved in 1 ml of 100% (v/v) dimethyl formamide) and 66 µl of NBT (50 mg dissolved in 1 ml of 70% (v/v) dimethyl formamide) in 10 ml of buffer A (100 mM Tris-HCl pH 9.5, 5 mM $MgCl_2$, 100 mM NaCl). The membrane was then rinsed with distilled water to stop the color reaction, allowed to air-dry and kept in dark.

5.17 Synthesis of Single-stranded RNA by *In vitro* Transcription Reaction using Ribomax™ Large Scale RNA Production System-T7 RNA polymerase (Promega)

In vitro transcription reaction was applied to synthesize RNA from recombinant DNA template by using RiboMAX™ Large Scale RNA Production System-Sp6 and T7 based on the strategy according to the manufacturer's protocol. The purified DNA template should be examined by agarose gel electrophoresis prior to transcription to ensure the presence of a clean and intact DNA fragment of the expected size. The purified PCR product of GFP-sense stranded gene containing T_7 RNA polymerase promoter was used as template for the experiment. The reaction was set up at room temperature according to the components described in the reaction shown:

T7 Reaction Components of GFP sense-strand (20 µl) contained		
T7 Transcription 5X Buffer	4	µl
rNTPs (25 mM each ATP, CTP, GTP, UTP)	6	µl
Purified DNA template 500 ng in nuclease free water	8	µl
Enzyme Mix (T7)	2	µl

All components were gently pipeted and mixed in the microtube before incubation at 37°C for 6 hr. After transcription reaction was completed, the DNA template could be removed by adding 1 unit of RQ1 RNase-Free DNase (1 unit/ µl) per 1 µg of DNA template at 37°C for 15 min. The RNA was extracted with 1 volume of TE-saturated (pH 4.5) phenol:chloroform:isoamyl alcohol (25:24:1) then mixed thoroughly by vortex for 1 min. After centrifugation with 13,000 rpm at 4 °C for 2 min, the mixture was separated into 2 phases. The upper aqueous phase was transferred to a fresh microtube. In order to remove unincorporated nucleotides, 1 volume of chloroform:isoamyl alcohol (24:1) was added followed by vortex for 1 min and centrifuged with similar condition as mention in the previous step. After transferred the upper aqueous phase to fresh new micro tube, the 0.1 volume of 3 M Sodium Acetate (pH 5.2) and 1 volume of isopropanol were added. The reaction was mixed and placed on ice for 2-5 min prior to spinning at 13,000 rpm for 15 min at 4 °C. The supernatant was carefully poured off and the pellet was washed with 1 ml of

70% ethanol in DEPC water by centrifugation at 13,000 rpm for 5 min at 4 ^{o}C. The pellet was air-dried before resuspended in RNase-free water and stored at -80 ^{o}C until required.

5.18 Determination of RNA concentration and visualization by electrophoresis

After removal of the DNA template and unincorporated nucleotides, the concentration and purity of the RNA was determined by using spectrophotometer at the wavelengths 260 nm and 280 nm. One absorbance at 260 nm is equal to approximate 40 µg/ml to RNA. The RNA concentration that was calculated by the following formula:

$$\text{RNA concentration } (\mu g/\mu l) = [A_{260} \times (\text{dilution factor}) \times 40] / 1{,}000$$

The purity of RNA was determined by the absorbance ratio of A_{260}/A_{280}. The high purity of RNA should represent in the ratio range of 1.8-2.0.

5.19 Electrophoresis of RNA

5.19.1 Gel Preparation

In order to eliminate the RNase contamination in the equipment before preparing gel electrophoresis, gel apparatus, mold and comb were soak with 1% SDS containing 0.1% DEPC for at least 2-3 hr. Then rinse all the apparatus with distilled water to remove any trace of remaining reagents followed by final rinse with DEPC-treated water. To prepare gel, agarose was dissolved in 1X TBE buffer containing 0.1% DEPC for overnight before autoclave to remove DEPC. Electrophoresis was carried out in DEPC-treated 1X TBE buffer.

5.19.2 RNA Sample Preparation for Electrophoresis

Since RNA can form complicated secondary and tertiary structure that is difficult for analysis by native gel electrophoresis. In order to facilitate the characteristic of RNA, RNA is generally resolved in denaturing condition which disrupt hydrogen bonding thus prevent secondary structure. Therefore RNA loading buffer and RNA sample buffer were prepared as described following.

RNA loading buffer: - 50% glycerol
- 0.4% bromophenol blue
- 1 mM EDTA
- 1 mg/ml Ethidium bromide

RNA sample buffer: -10 ml formamide (deionized)
- 3.5 ml 37% formaldehyde
- 2 ml 10X MOPS

Both buffers were aliquoted to 500 µl and stored at -20 ^{o}C until used. Sample was prepared by mixing 1 µl of RNA sample with 3 µl of RNA sample buffer and 2 µl of RNA loading buffer before incubation at 65 ^{o}C for 5 min to denature RNA and consequently immediately cool on ice for 2-3 min. The reaction tube was subjected to short spin to collect the samples and loaded the entire reaction onto the gel. Electrophoresis was carried out with constant voltage at 90 volts until the dye front was migrated about 2/3 of the gel length. Subsequently, the gel was destained in milliQ water for 5 min before visualized under UV light and the picture was taken with Gel-Doc Documentation System.

5.20 Labeling at 5' End of Single-Stranded RNA

Single-stranded RNA was radiolabeled at 5'termini by utilizing T4 polynucleotide kinase which facilitates the transfer of γ-phosphate residue from [γ-^{32}P]ATP to the 5'-hydroxyl trmini of dephosphorylated single- or double-stranded RNA. The procedure was divided into two main steps, dephosphorylation and labeling, respectively.

5.20.1 Dephosphorylation of 5' End by Alkaline Phosphatase

A hydroxyl group at 5' end was first created by removing the unlabeled phosphate residue from the 5' end of the nucleic acid with Calf Intestinal Alkaline Phosphatase (CIAP). The dephosphorylation reaction was carried out in a 50 µl containing 500 pmole of 5' termini, 1X CIAP buffer and 1 unit of CIAP. The mixture was incubated at 37 ^{o}C for 30 min followed by adding an additional 0.5 unit of CIAP with incubation at 37 ^{o}C for another 15 min before the reaction was inactivated at 56 ^{o}C for 15 min. The RNA was extracted by phenol-chloroform extraction as described

earlier in the *in vitro* transcription before resuspended in 10 µl nuclease-free water. Morever, to precipitate the small fragment of ssRNA (21 nt), glycogen was added in the step of isopropanol precipitation to final concentration 2.5 µg/ml to improve the efficiency of precipitation.

5.20.2 Labeling of [γ-^{32}P]ATP to the 5' End of ssRNA by T4 Polynucleotide Kinase

T4 polynucleotide kinase was applied to transfer the ^{32}P from the γ position of ATP to the 5' dephosphorylated termini in the ratio of 50 pmole of 5' termini to 20 units of T4-PNK. For 50 µl of radioactive labeling reaction, 50 pmole of 5' end ssRNA was mixed with 1X T4 PNK buffer, 2 µl of T4-PNK (10 units/µl) and 1 µl of [γ-^{32}P]ATP. The reaction was carried out at 37 ^{o}C for 1 hr subsequently the enzyme was inactivated at 90 ^{o}C for 2 min. The unincorporated [γ-^{32}P]ATPs were removed by MicroSpin^{TM} G-50 column. The labeled ssRNA was then stored at -30 ^{o}C until used.

5.21 Electrophoretic Mobility Shift Assays (EMSA)

The electrophoretic mobility shift assay (EMSA) is the method for studying the DNA or RNA-binding properties of protein which based on the observation that protein-DNA or protein-RNA complexes migrate more slowly than free DNA or RNA molecules when subjected to non-denaturing polyacrylamide gel electrophoresis.

5.21.1 Non-Denaturing Polyacrylamide Gel Electrophoresis

Non-denaturing TBE-polyacrylamide gels are applied to resolved protein-RNA complexes from free RNA. The gel percentage required depends on the size of the target RNA and the size number and charge of the protein that bind to it. It is important that the protein-RNA complex enters the gel and does not remain in the bottom of the well. Polyacrylamide gels in the range of 4-8% are typically used. The electrophoresis was carried out by applying the medium set of electrophoresis set size 15x15 cm. The procedure for 5% non-denaturing polyacrylamide gels preparation is illustrated below

30% Acrylamide mix (29:1 acrylamide:bisacrylamide)	3.33	ml
10% Ammonium persulfate	150	µl
TEMED	15	µl

Total volume was adjusted into 20 ml with 0.5X TBE buffer.

The gel was allowed to polymerize at room temperature. Subsequently, the gel was pre-run for 2 hr at 10 mA to remove all traces of ammonium persulfate, to distribute/equilibrate any special stabilizing factors or ions that are added to the electrophoresis buffer and to ensure a constant gel temperature.

5.21.2 Electrophoretic Mobility Shift Assay Reaction

The RNA-protein complex was analyzed by in a 15 µl reaction composes of 20 mM HEPES (pH 7.4), 3 mM $MgCl_2$, 50 mM KCl, 2mM DTT and 5% glycerol. The amount of the recombinant proteins was varied from 0 to 750 ng. After mixing of all components, reaction tube was spun briefly to bring all fluid down to the bottom of the tube. The reaction mixtures were incubated for 45 min at room temperature then 4 µl of sample loading buffer (200 mM Tris-HCl pH 7.5, 4 mM EDTA pH 8.0, 40% glycerol, 0.1% (w/v) bromophenol blue) was added. The reactions were analyzed on 5% non-denaturing PAGE with the constant 150 volts for approximately 70 min. In order to investigate the specificity of the binding, unlabeled competitor of ssRNA, dsRNA and ssDNA were added into the binding reaction at 50 to 200 folds molar excess. Subsequently the gel was dried on Whatman paper and the protein-RNA complexes were detected by autoradiography. In addition, to prove the interaction of RNA-protein complex from the PAZ domain protein, supershift assay was performed by utilizing anti-PAZ and anti-His which recognize the PAZ domain protein as the specific binding. Anti-FMDV is the unrelated antibody which can not interact PAZ domain protein.

5.22 RISC Activity Assay

Function of the recombinant Pem-AGO was performed by determination the ability of mRNA cleavage in the present of single-stranded RNA. If the recombinant protein can cleave the target mRNA at the specific sequence, the cleavage product could be observed after analyzed on formaldehyde gel electrophoresis.

5.22.1 Formaldehyde Gel Electrophoresis

To analyze the RNA cleavage product, denaturing formaldehyde gel electrophoresis was performed. To prepare 2.5% formaldehyde agarose gel, 1.2 g agarose was dissolved in 34.8 ml DEPC-treated milliQ water then boil. When the mixture cool down to approximately 55-60 ^{o}C, add 4 ml of 10X MOPS buffer and 1.2 ml of 37 % formaldehyde to the gel solution and mix thoroughly. Pour the mixture into the assembled mold and permit the gel complete solidified. The electrophoresis was conducted in 1X MOPS in DEPC-treated milliQ water with constant voltage approximately 90-100 volts. The gel was destained in milliQ water for 5 min subsequently visualized under UV light and record by Gel-Doc Documentation.

5.22.2 mRNA Cleavage Assay Reaction

In order to permit the assembly of ssRNA into Argonaute protein, the reaction was started by incubation of the recombinant Argonaute protein with the 2 µl of 1 µM antisense-GFP siRNA (21 nt) in 10 µl reaction containing15 mM HEPES (pH 7.4), 100 mM KCl and 2 mM $MgCl_2$. The mixture was incubated at 30 ^{o}C for 30 min. Subsequently add 10 µl of reaction buffer II containing 1 mM ATP, 0.2 mM GTP, 80 units of RNasein (Promega) and 2 pmole of sense-GFP mRNA. Then further incubate at 30 ^{o}C for 2 hr. The reaction was stopped by addition 200 µl of phenol/chloroform/isoamyl alcohol and 180 µl of RNase free water. RNA was extracted according to the same strategy from *in vitro* transcription and precipitated with isopropanol in the presence of 2.5 µg/ml glycogen. The pellet was resolubilized by boiling in RNA sample buffer and RNA loading buffer before subjected to 2.5 % formaldehyde gel electrophoresis in 1X MOPS buffer.

CHAPTER VI
RESULTS PART I

6.1 Restriction Analysis of pUC19/*Pem-ago* Recombinant Plasmid

From the previous study in our laboratory (Dechkla M., M.Sc. thesis, Mahidol University, 2006), pUC19/*Pem-ago* is a recombinant plasmid harboring 2,829 bp sequences of cDNA encoding *P.monodon*'s Argonaute (Pem-AGO). This plasmid was used as a template for amplification of *Pem-ago* cDNA prior to cloning into expression vector for yeast expression system, pPICZαA. In order to verify the correct recombinant pUC19/*Pem-ago* plasmid, restriction digestion analysis was performed by using 4 restriction enzymes, *Eco*R I, *Xba* I, *Pst* I and *Bgl* II. This recombinant plasmid contained *Eco*R I and *Xba* I as cloning sites at 5' and 3'end of the gene respectively. Digestion with only *Eco*R I or *Xba* I should give rise to the linearlized recombinant plasmid with the size of 5.4 kb. Whereas digestion with both *Eco*R I and *Xba* I produced two fragments of the insert fragment of *Pem-ago* (2.8 kb) and pUC19 vector (2.7 kb). Moreover, internal restriction sites were analyzed by using *Bgl* II digestion that gave 2 fragments of 4,547 bp and 968 bp, and *Pst* I that produced 3 fragments of 248 bp, 873 bp and 4,394 bp respectively. The patterns of restriction digestion were analyzed by agarose gel electrophoresis with ethidium bromide staining as shown in figure 5.1.

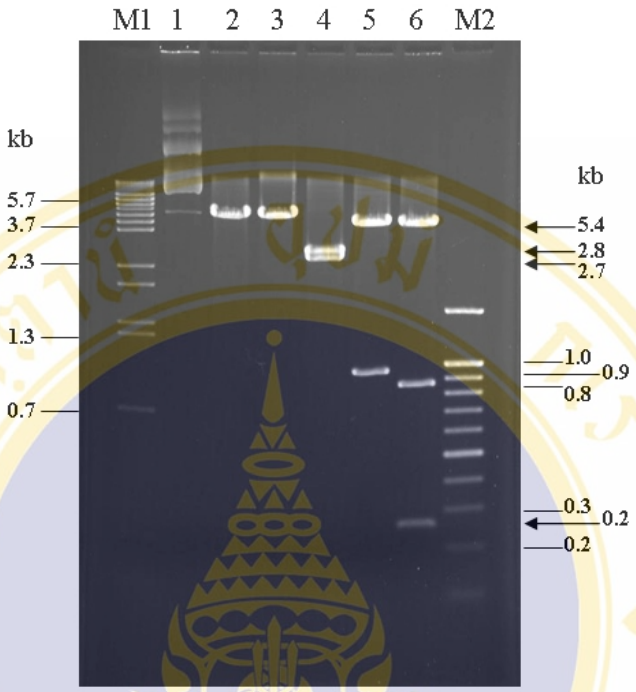

Figure 6.1 Restriction digestion analysis of pUC19/*Pem-ago* recombinant plasmid

This figure illustrates 1% agarose gel electrophoresis (ethidium bromide stained) of the restriction enzyme digestion pattern of pUC19/*Pem-ago* recombinant plasmid.

Lane M1: λ/*Bst*E II digested DNA marker

Lane 1 : Undigested pUC19/*Pem-ago*

Lane 2 : pUC19/*Pem-ago* digested with *Eco*R I

Lane 3 : pUC19/*Pem-ago* digested with *Xba* I

Lane 4 : pUC19/*Pem-ago* digested with *Eco*R I and *Xba* I

Lane 5 : pUC19/*Pem-ago* digested with *Bgl* II

Lane 6 : pUC19/*Pem-ago* digested with *Pst* I

Lane M2: 100 bp + 1.5 kb DNA ladder marker

The yeast expression system provides the advantage in secretion of the expressed recombinant protein in the native form into the culture medium which is easy for purification. In order to obtain the recombinant Argonaute protein for characterization of its biochemical function in RNA interference pathway, the first experiment was designed to express the recombinant Pem-AGO in *Pichia pastoris* strain KM71 by using pPICZαA as a cloning vector.

6.2 Construction of pPICZαA/*Pem-ago* and pPICZαA/*PAZ* Expression Recombinant Plasmid for *P. pastoris* Expression System

In order to obtain efficient secretion of the expressed recombinant protein from *P. pastoris*, the DNA fragments of either *Pem-ago* and *PAZ* domain were inserted downstream of and in-frame with the α-factor secretion signal sequence of pPICZαA vector by cloning into the *Xho* I site. The processing of the α-factor signal sequence required the preliminary cleavage of the signal sequence by the Kex2 gene product. Therefore the minimal Kex2 signal cleavage sequence, AAAAGA, was added into the forward primer in front of the insert sequence. Moreover, to generate the recombinant plasmid that express the protein as C-terminus hexahistidine tag fusion protein with minimal extra amino acid residues at the 3' end, the *Sal* I site which located upstream polyhistidine tag was employed as cloning site by adding into the reverse primer as revealed in figure 6.2.

6.2.1 Amplification of cDNA Encoding Pem-AGO and PAZ Domain for *Pichia pastoris* Expression System

The amplification of the cDNAs encoding Pem-AGO and PAZ domain protein were performed in individual PCR reactions with specific primer sets as described in method 5.4.1 by utilizing the recombinant pUC19/*Pem-ago* as a template. According to the PCR reactions, the expected band of 2,842 bp for *Pem-ago* (figure 6.3) and 442 bp of *PAZ* (figure 6.4) were generated. The negative controls were performed in the same conditions but without DNA template.

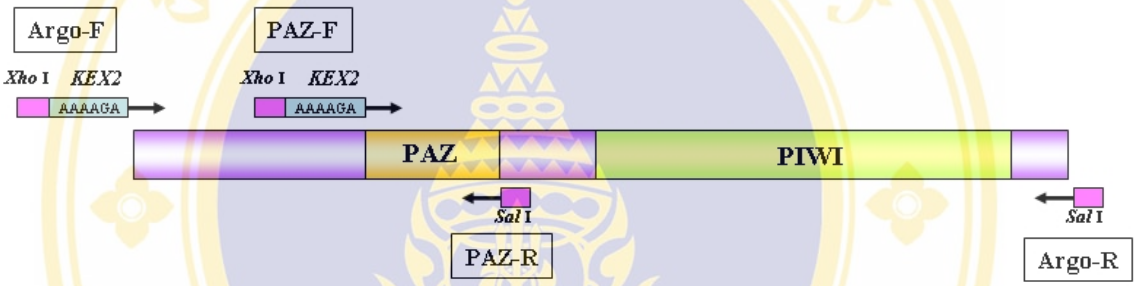

Figure 6.2 A schematic diagram represents the cDNA encoding Pem-AGO containing the regions of PAZ and PIWI domains and the binding sites of primers for cloning into pPICZαA vector

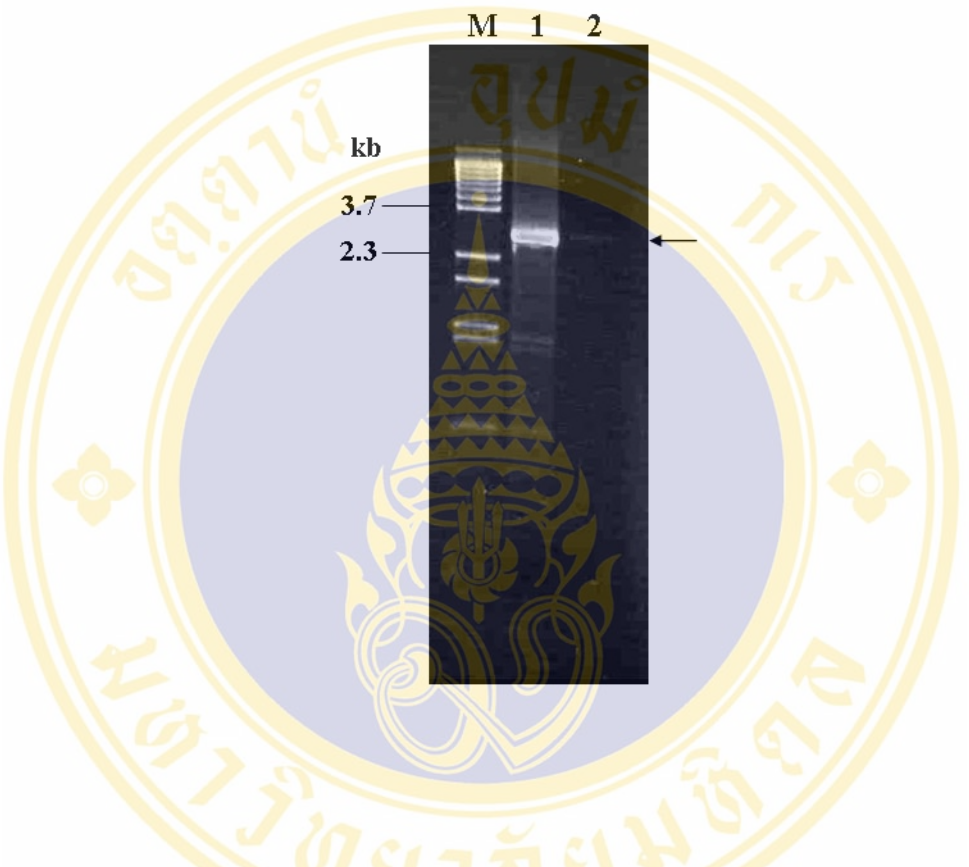

Figure 6.3 Amplification of *Pem-ago* cDNA for *P. pastoris* expression system

This figure reveals 1 % agarose gel electrophoresis (ethidium bromide stained) of the PCR product amplification of cDNA encoding Pem-AGO for cloning into pPICZαA vector by using primer Argo-F and Argo-R.

Lane M : λ/*Bst*E II digested DNA marker

Lane 1 : PCR product of cDNA encoding Pem-AGO

Lane 2 : Negative control (no template)

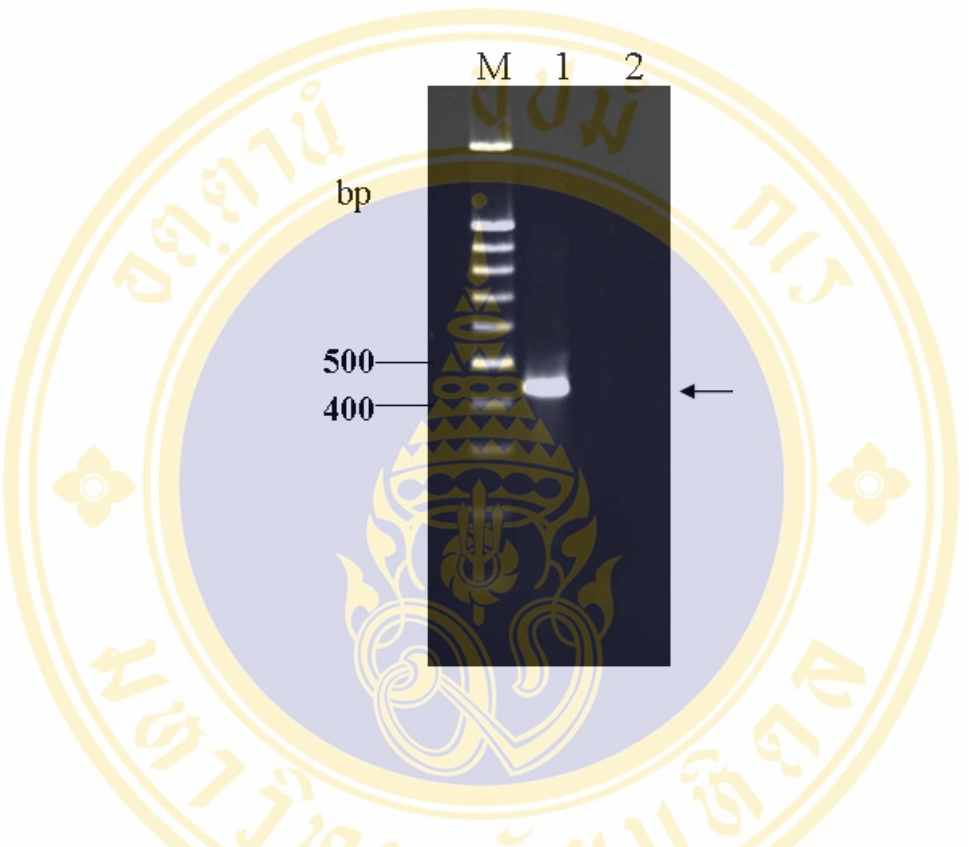

Figure 6.3 Amplification of *Pem-ago* cDNA for *P. pastoris* expression system

This figure reveals 1.5 % agarose gel electrophoresis (ethidium bromide stained) of the PCR product of the *PAZ* cDNA for cloning into pPICZαA vector by using primer PAZ-F and PAZ-R.

Lane M : 100 bp + 1.5 kb DNA ladder marker

Lane 1 : PCR product of the *PAZ* cDNA

Lane 2 : Negative control (no template)

6.2.2 Cloning of DNA Fragments into pPICZαA Vector

The PCR products of *Pem-ago* and *PAZ* cDNA at the expected size of 2,842 bp and 442 bp, respectively were excised from agarose gel and subsequently purified by QIAquick Gel Extraction Kit (QIAGEN). The purified fragments were digested with *Xho* I and *Sal* I to generate the restriction sites for cloning into pPICZαA vector. Due to the compatibility site between *Xho* I and *Sal* I, the purified *Pem-ago* fragment was further dephosphorelated by using CIAP to prevent self-ligation. The purified fragments of *Pem-ago* and *PAZ* domain gene were individually ligated with purified dephosphorylated *Xho* I and *Sal* I-digested pPICZαA using T4 DNA ligase to generate the recombinant plasmid pPICZαA/*Pem-ago* and pPICZαA/*PAZ* that were further transformed into *E. coli* strain DH5α and primarily screened based on Zeocin™ antibiotic resistance.

6.2.3 Screening of the Recombinant Clones

The transformant clones of each construct, pPICZαA/*Pem-ago* and pPICZαA/*PAZ*, were screened by rapid size screening, restriction enzyme digestion and PCR amplification reaction.

For the screening of recombinant plasmid pPICZαA/*Pem-ago* and pPICZαA/*PAZ*, the insertion of *Pem-ago* and *PAZ* cDNA in pPICZαA vector was primary checked by rapid size screening (figure 6.5 and figure 6.8, respectively). The examples of shifted clones were indicated by the asterisks. Then the plasmid from these clones were extracted by CTAB method followed by restriction digestion analysis with *Xho* I and *Sal* I, which were used as the cloning sites. The corrected clones should provide products of the insert fragment and 3.6 kb fragment of the vector (figure 6.6 and 6.9 for pPICZαA/*Pem-ago* and pPICZαA/*PAZ*, respectively). Moreover, the correct insert was also confirmed by internal digestion. The recombinant pPICZαA/*Pem-ago* was digested with *Xmn* I and *Dra* I, and the corrected clones should present the products of 4 kb and 2.3 kb (figure 6.7). Similarly, the insert fragment in pPICZαA/*PAZ* was proven by internal restriction digestion with *Dra* I and *Bgl* II that showed the products of 2,281 bp, 1,243 bp and 412 bp (figure 6.10). Finally, colony PCR-based screening using 5'*AOX1* and 3'*AOX1* primers which prime on the vector backbone were performed. The positive clone of pPICZαA/*Pem-ago*

should give the product band of 3,321 bp. However the results present non-specific products at the lower positions that could be divided into three populations of the results, whereas the PCR product from pPICZαA/*PAZ* was observed at 906 bp as expected (figure 6.11).

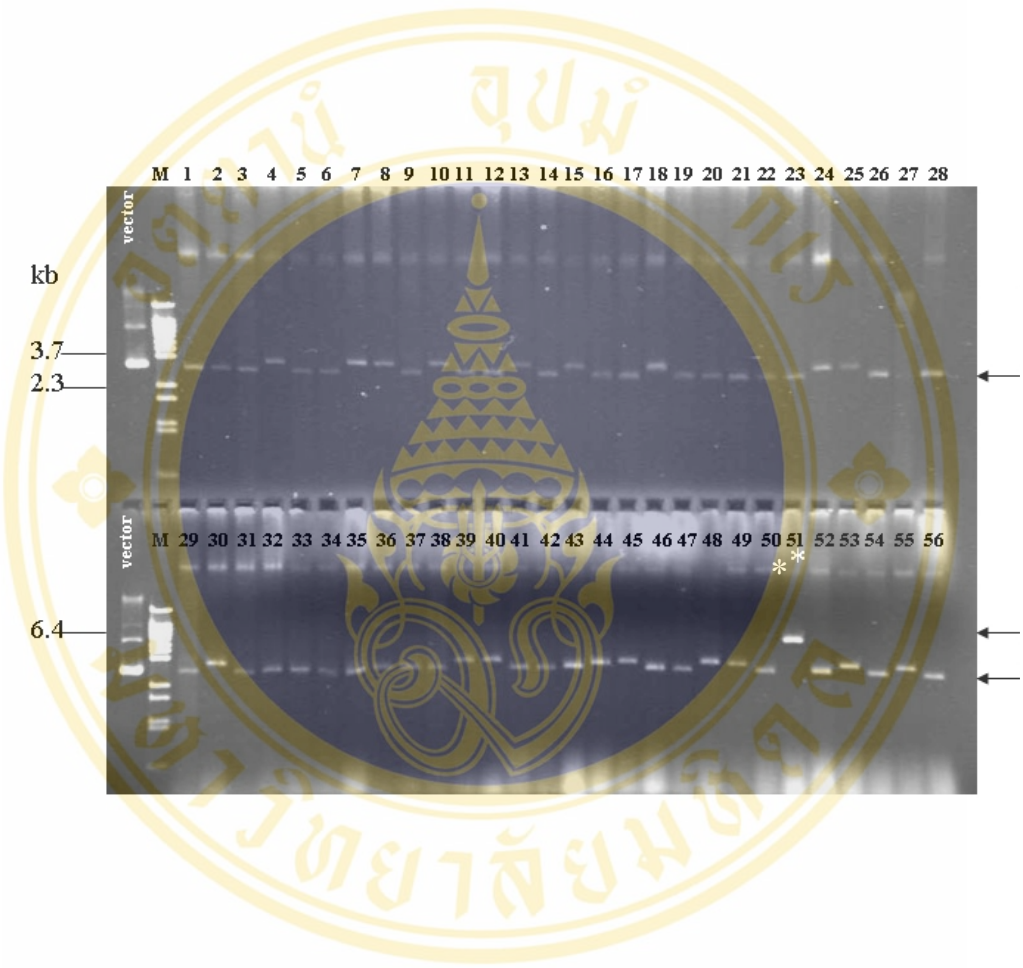

Figure 6.5 Screening of the recombinant pPICZαA/*Pem-ago* clones by rapid size screening

The figure indicates 1% agarose gel electrophoresis (ethidium bromide stained) from rapid size screening of the recombinant pPICZαA/*Pem-ago* clones.

Lane M : λ/*Bst*E II digested DNA marker

Lane vector: Plasmid pPICZαA

Lane 1-56 : Transformant clones no.1 to 56 respectively

* indicates the positive clone of the recombinant pPICZαA/*Pem-ago*

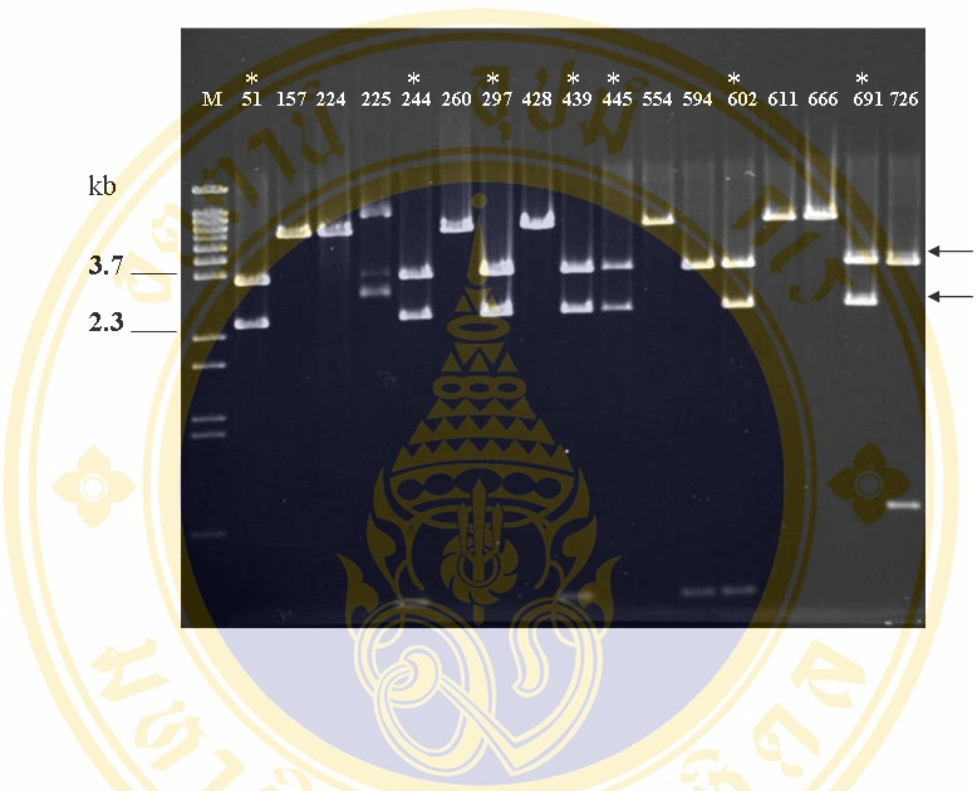

Figure 6.6 Screening of the recombinant pPICZαA/*Pem-ago* clones by restriction enzyme digestion with *Xho* I & *Sal* I (cloning sites)

The figure illustrates 1% agarose gel electrophoresis (ethidium bromide stained) of the *Xho* I & *Sal* I restriction endonuclease analysis of the recombinant pPICZαA/*Pem-ago* plasmids.

Lane M : λ/*Bst*E II digested DNA marker

The numbers in each lane indicate the number of the selected fragment clone

* indicates the positive clone of the recombinant pPICZαA/*Pem-ago*

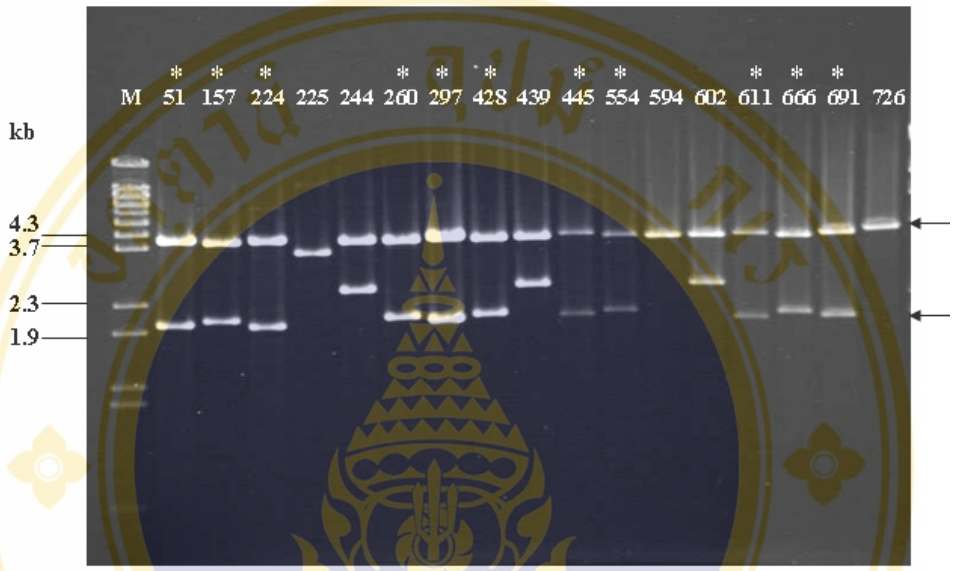

Figure 6.7 Screening of the recombinant pPICZαA/*Pem-ago* clones by internal digestion with *Xmn* I and *Dra* I

The figure indicates 1% agarose gel electrophoresis (ethidium bromide stained) of *Xmn* I and *Dra* I digestion pattern of the recombinant pPICZαA/*Pem-ago* transformants

Lane M : λ/*Bst*E II digested DNA marker

The numbers in each lane indicate the number of the selected fragment clone

* indicates the positive clone of the recombinant pPICZαA/*Pem-ago*

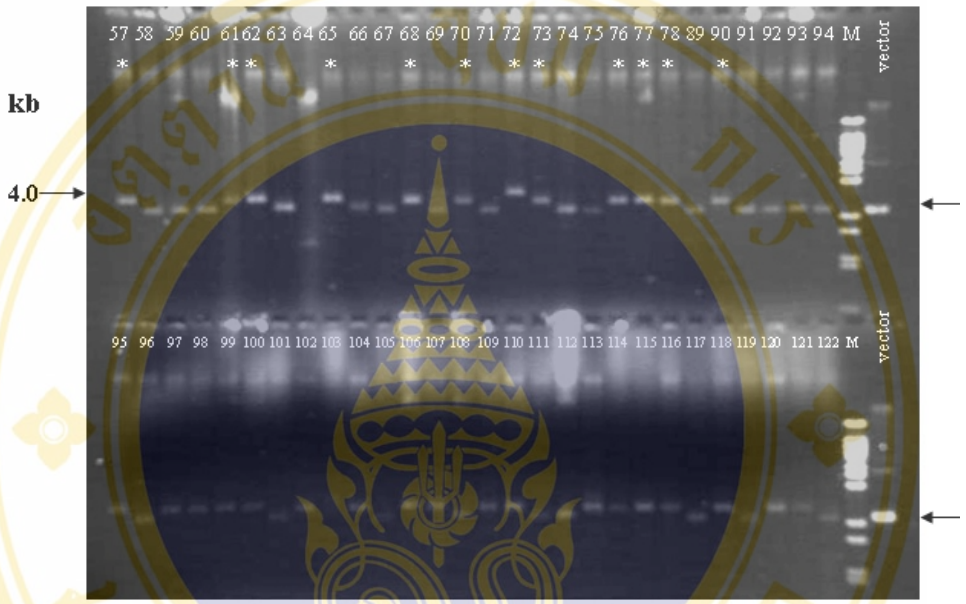

Figure 6.8 Screening of the recombinant pPICZαA/*PAZ* by rapid size screening

The figure indicates 1% agarose gel electrophoresis (ethidium bromide stained) from rapid size screening test of the recombinant pPICZαA/*PAZ*

Lane M : λ/*Bst*E II digested DNA marker

Lane vector : Plasmid pPICZαA

The numbers in each lane indicate the number of the selected fragment clone

* indicates the positive clone of the recombinant pPICZαA/*PAZ*

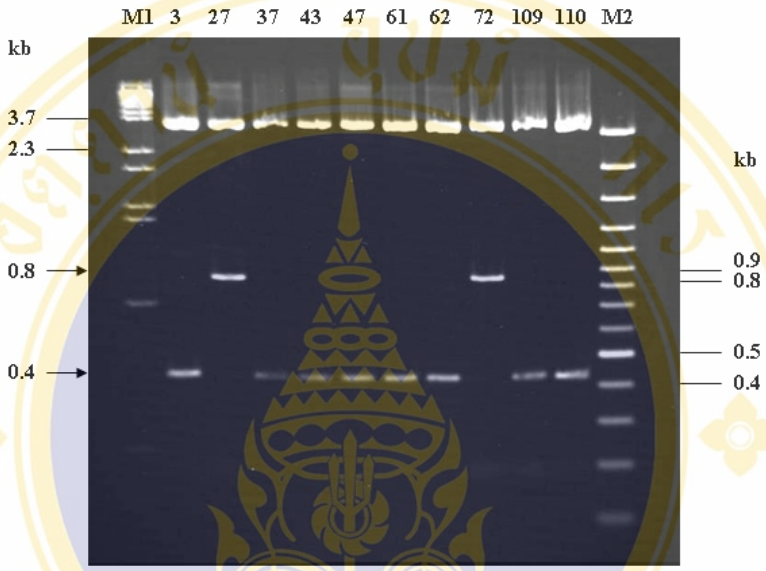

Figure 6.9 Screening of the recombinant pPICZαA/*PAZ* by restriction cloning enzyme digestion with *Xho* I & *Sal* I (cloning sites)

The figure illustrates 1% agarose gel electrophoresis (ethidium bromide stained) of the *Xho* I & *Sal* I restriction endonuclease analysis of the recombinant pPICZαA/*PAZ* plasmids

Lane M1 : λ/*Bst*E II digested DNA marker

Lane M2 : 100 bp DNA ladder marker

The numbers in each lane indicate the number of the selected fragment clone

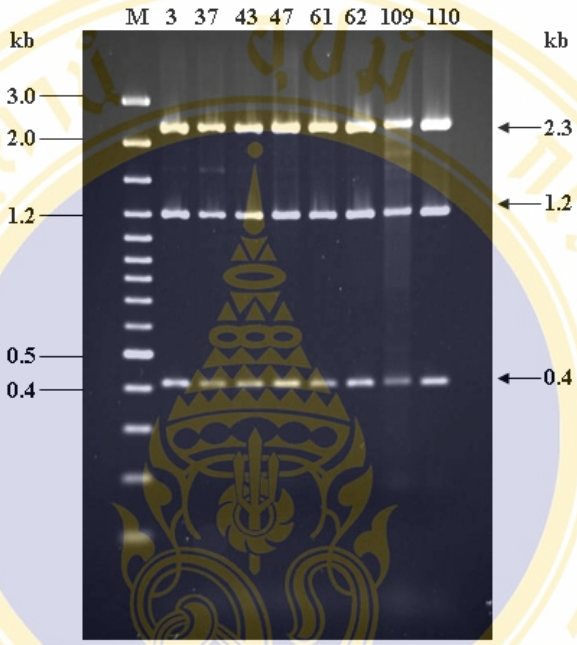

Figure 6.10 Screening of the recombinant pPICZαA/*PAZ* by internal digestion with *Dra* I & *Bgl* II

The figure indicates 1% agarose gel electrophoresis (ethidium bromide stained) of *Xmn* I and *Dra* I digestion pattern of the recombinant pPICZαA/*PAZ* transformants

Lane M : 100 bp DNA ladder marker

The numbers in each lane indicate the number of the selected fragment clone

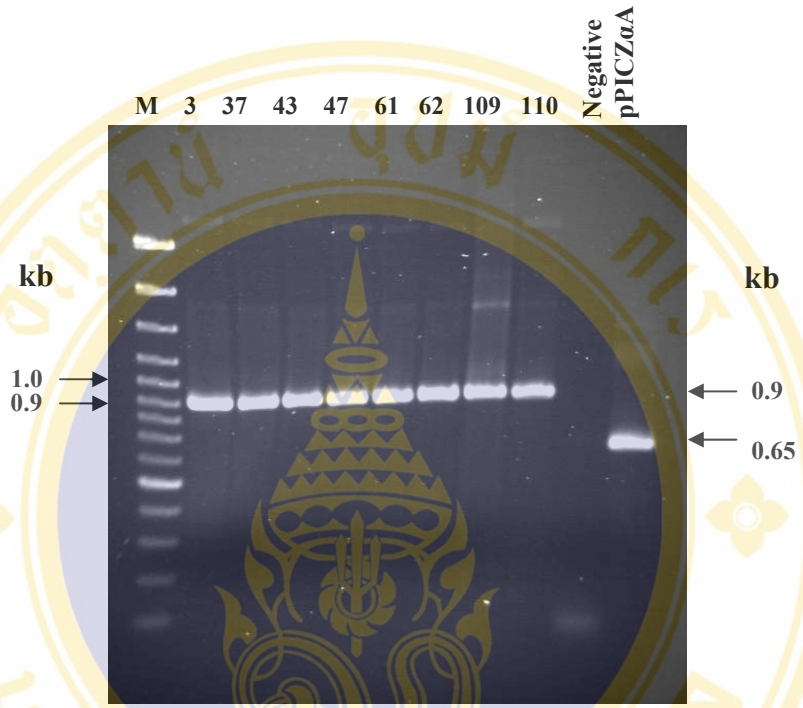

Figure 6.11 Screening of the recombinant pPICZαA/*PAZ* by PCR amplification analysis

The figure indicates 1.2 % agarose gel electrophoresis (ethidium bromide stained) from the PCR analysis with *AOX* primers for insertion of *PAZ* from Zeocin™ resistant-transformants clones

Lane M : 100 bp DNA ladder marker

Negative : PCR analysis with no template

pPICZαA : PCR analysis with pPICZαA as template

The numbers in each lane indicate the number of the selected fragment clone

6.3 Nucleotide and Deduced Amino Acid Sequence Analysis of cDNA Encoding Argonaute and PAZ domain of *Penaeus monodon*

The recombinant clones that showed the positive results from screening analysis were verified by automated DNA sequencing in both forward and reverse direction using the sequencing primers and then alignment with Vector NTI program.

Because of the large size of *Pem-ago* and non-specific results from PCR-base screening from the recombinant clones of pPICZαA/*Pem-ago*, the nucleotide sequences were preliminary verified to check the 3' and 5' end of the insert fragment by using *AOX* primers. From the results it showed that *Pem-ago* cDNA contained *Sal I* restriction sites in internal sequence near both end at the position 275 (figure 6.12) and 2,800 (figure 6.13), respectively. Therefore the *Pem-ago* cDNA obtained was about 40 nt truncated at 3' end.

In order to verify the sequences of the *PAZ* cDNA, three positive clones, numbers 3, 37 and 43, were selected. DNA sequence analysis revealed that all three clones possessed the same nucleotide sequences (figure 6.14) and their deduced amino acid residues were identical (100%) to the sequences of the original pUC19/*Pem-ago* clone.

However, as the result revealed that we could not obtain the full-length of cDNA encoding Pem-AGO, the expression in *P. pastoris* was first only employed with the construct of pPICZαA/*PAZ*.

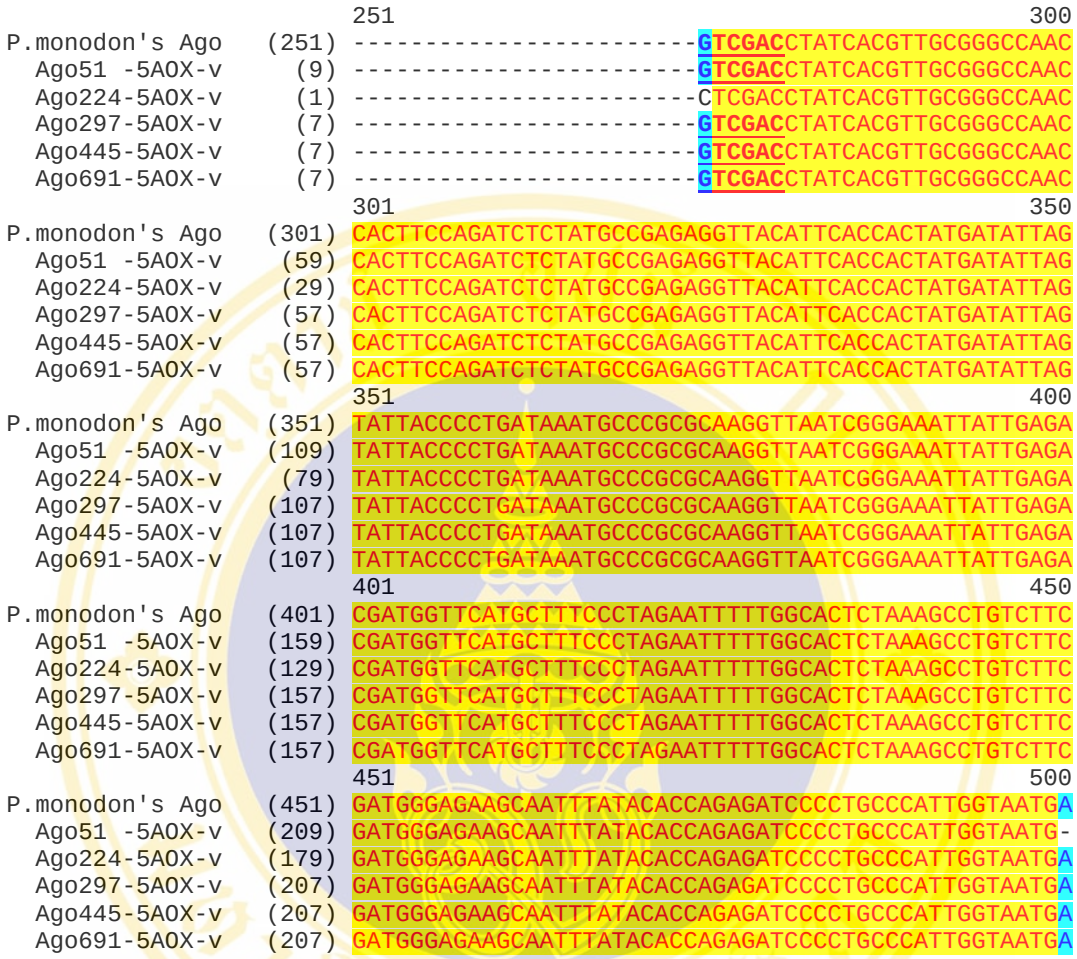

Figure 6.12 The alignment of nucleotide sequences at the 5' end of the recombinant pPICZαA/*Pem-ago* of five individual clones

The figure shows a DNA sequence alignment of 5'end region of cDNA of *P. monodon*'s Argonaute from five clones that presented the *Sal* I site at the position 275. The nucleotides that are identical in all sequences are highlight in pale gray, the dark gray highlight indicates the nucleotides that 4/5 identity. The underline letters represent *Sal* I restriction sequence.

```
                          2501                                          2550
P.monodon's Ago  (2501) GCTCTCATCAGGGTATCCAGGGCACAAGTCGTCCCAGTCACTACCACGTA
    Ago51-3AOX    (193) GCTCTCATCAGGGTATCCAGGGCACAAGTCGTCCCAGTCACTACCACGTA
   Ago224-3AOX    (211) GCTCTCATCAGGGTATCCAGGGCACAAGTCGTCCCAGTCACTACCACGTA
    Ago297-3AOX   (218) GCTCTCATCAGGGTATCCAGGGCACAAGTCGTCCCAGTCACTACCACGTA
    Ago445-3AOX   (220) GCTCTCATCAGGGTATCCAGGGCACAAGTCGTCCCAGTCACTACCACGTA
    Ago691-3AOX   (285) GCTCTCATCAGGGTATCCAGGGCACAAGTCGTCCCAGTCACTACCACGTA
                          2551                                          2600
P.monodon's Ago  (2551) CTGTGGGATGATAACCACTTTGACAGTGATGAGCTGCAGTGCCTGACTTA
    Ago51-3AOX    (243) CTGTGGGATGATAACCACTTTGACAGTGATGAGCTGCAGTGCCTGACTTA
   Ago224-3AOX    (261) CTGTGGGATGATAACCACTTTGACAGTGATGAGCTGCAGTGCCTGACTTA
    Ago297-3AOX   (268) CTGTGGGATGATAACCACTTTGACAGTGATGAGCTGCAGTGCCTGACTTA
    Ago445-3AOX   (270) CTGTGGGATGATAACCACTTTGACAGTGATGAGCTGCAGTGCCTGACTTA
    Ago691-3AOX   (335) TTGTGGGATGATAACCACTTTGACAGTGATGAGCTGCAGTGCCTGACTTA
                          2601                                          2650
P.monodon's Ago  (2601) CCAGTTGTGTCATACCTATGTAAGATGTACACGATCAGTCTCCATACCTG
    Ago51-3AOX    (293) CCAGTTGTGTCATACCTATGTAAGATGTACACGATCAGTCTCCATACCTG
   Ago224-3AOX    (311) CCAGTTGTGTCATACCTATGTAAGATGTACACGATCAGTCTCCATACCTG
    Ago297-3AOX   (318) CCAGTTGTGTCATACCTATGTAAGATGTACACGATCAGTCTCCATACCTG
    Ago445-3AOX   (320) CCAGTTGTGTCATACCTATGTAAGATGTACACGATCAGTCTCCATACCTG
    Ago691-3AOX   (385) CCAGTTGTGTCATACCTATGTAAGATGTACACGATCAGTCTCCATACCTG
                          2651                                          2700
P.monodon's Ago  (2651) CTCCAGCCTATTATGCTCACTTGGTAGCCTTCAGGGCTCGTTATCATCTC
    Ago51-3AOX    (343) CTCCAGCCTATTATGCTCACTTGGTAGCCTTCAGGGCTCGTTATCATCTC
   Ago224-3AOX    (361) CTCCAGCCTATTATGCTCACTTGGTAGCCTTCAGGGCTCGTTATCATCTC
    Ago297-3AOX   (368) CTCCAGCCTATTATGCTCACTTGGTAGCCTTCAGGGCTCGTTATCATCTC
    Ago445-3AOX   (370) CTCCAGCCTATTATGCTCACTTGGTAGCCTTCAGGGCTCGTTATCATCTC
    Ago691-3AOX   (435) CTCCAGCCTATTATGCTCACTTGGTAGCCTTCAGGGCTCGTTATCATCTC
                          2701                                          2750
P.monodon's Ago  (2701) GTCGAAAAGGAGCATGACAGTGGAGAGGGGTCACACCAATCTGGCAACAG
    Ago51-3AOX    (393) GTCGAAAAGGAGCATGACAGTGGAGAGGGGTCACACCAATCTGGCAACAG
   Ago224-3AOX    (411) GTCGAAAAGGAGCATGACAGTGGAGAGGGGTCACACCAATCTGGCAACAG
    Ago297-3AOX   (418) GTCGAAAAGGAGCATGACAGTGGAGAGGGGTCACACCAATCTGGCAACAG
    Ago445-3AOX   (420) GTCGAAAAGGAGCATGACAGTGGAGAGGGGTCACACCAATCTGGCAACAG
    Ago691-3AOX   (485) GTCGAAAAGGAGCATGACAGTGGAGAGGGGTCACACCAATCTGGCAACAG
                          2751                                          2800
P.monodon's Ago  (2751) TGAGGATCGCACACCATCTGCCATGGCAAGGGCAGTTACAGTGCATGTCG
    Ago51-3AOX    (443) TGAGGATCGCACACCATCTGCCATGGCAAGGGCAGTTACAGTGCATGTCG
   Ago224-3AOX    (461) TGAGGATCGCACACCATCTGCCATGGCAAGGGCAGTTACAGTGCATGTCG
    Ago297-3AOX   (468) TGAGGATCGCACACCATCTGCCATGGCAAGGGCAGTTACAGTGCATGTCG
    Ago445-3AOX   (470) TGAGGATCGCACACCATCTGCCATGGCAAGGGCAGTTACAGTGCATGTCG
    Ago691-3AOX   (535) TGAGGATCGCACACCATCTGCCATGGCAAGGGCAGTTACAGTGCATGTCG
                          2801
P.monodon's Ago  (2801) AC
    Ago51-3AOX    (493) AC
   Ago224-3AOX    (511) AC
    Ago297-3AOX   (518) AC
    Ago445-3AOX   (520) AC
    Ago691-3AOX   (585) AC
```

Figure 6.13 The alignment of nucleotide sequences at the 3' end of the recombinant pPICZαA/*Pem-ago* of five individual clones

The figure shows a DNA sequence alignment of 3'end region of cDNA of *P. monodon*'s Argonaute from five clones that presented the *Sal* I site at the position 2,800. The nucleotides that are identical in all sequences are highlight in pale gray, the dark gray highlight indicates the nucleotides that 4/5 identity. The underline letters represent *Sal* I restriction sequence.

```
                1                                                    50
Ref-PAZ     (1) TTTATGTGTGAAGTGTTAGATATTCGAGAAATAGGTGAGCAGAGGAAACC
   PAZ3     (1) TTTATGTGTGAAGTGTTAGATATTCGAGAAATAGGTGAGCAGAGGAAACC
  PAZ37     (1) TTTATGTGTGAAGTGTTAGATATTCGAGAAATAGGTGAGCAGAGGAAACC
  PAZ43     (1) TTTATGTGTGAAGTGTTAGATATTCGAGAAATAGGTGAGCAGAGGAAACC
                51                                                   100
Ref-PAZ    (51) TCTAACGGATTCGCAGCGTGTCAAGTTCACAAAAGAAATTAAGGGTCTGA
   PAZ3    (51) TCTAACGGATTCGCAGCGTGTCAAGTTCACAAAAGAAATTAAGGGTCTGA
  PAZ37    (51) TCTAACGGATTCGCAGCGTGTCAAGTTCACAAAAGAAATTAAGGGTCTGA
  PAZ43    (51) TCTAACGGATTCGCAGCGTGTCAAGTTCACAAAAGAAATTAAGGGTCTGA
               101                                                   150
Ref-PAZ   (101) AGATTGAGATCACACACTGTGGTGCGATGCGAAGAAAGTACAGGGTGTGT
   PAZ3   (101) AGATTGAGATCACACACTGTGGTGCGATGCGAAGAAAGTACAGGGTGTGT
  PAZ37   (101) AGATTGAGATCACACACTGTGGTGCGATGCGAAGAAAGTACAGGGTGTGT
  PAZ43   (101) AGATTGAGATCACACACTGTGGTGCGATGCGAAGAAAGTACAGGGTGTGT
               151                                                   200
Ref-PAZ   (151) AATGTCACAAGAAGGCCAGCACAGATGCAGTCGTTCCCATTGCAGCTAGA
   PAZ3   (151) AATGTCACAAGAAGGCCAGCACAGATGCAGTCGTTCCCATTGCAGCTAGA
  PAZ37   (151) AATGTCACAAGAAGGCCAGCACAGATGCAGTCGTTCCCATTGCAGCTAGA
  PAZ43   (151) AATGTCACAAGAAGGCCAGCACAGATGCAGTCGTTCCCATTGCAGCTAGA
               201                                                   250
Ref-PAZ   (201) GAATGGTCAGACTGTGGAATGTACTGTTGCAAAATATTTCCTTGACAAAT
   PAZ3   (201) GAATGGTCAGACTGTGGAATGTACTGTTGCAAAATATTTCCTTGACAAAT
  PAZ37   (201) GAATGGTCAGACTGTGGAATGTACTGTTGCAAAATATTTCCTTGACAAAT
  PAZ43   (201) GAATGGTCAGACTGTGGAATGTACTGTTGCAAAATATTTCCTTGACAAAT
               251                                                   300
Ref-PAZ   (251) ACAAAATGAAACTCAGGTTCCCCCATCTACCTTGCCTTCAGGTGGGACAA
   PAZ3   (251) ACAAAATGAAACTCAGGTTCCCCCATCTACCTTGCCTTCAGGTGGGACAA
  PAZ37   (251) ACAAAATGAAACTCAGGTTCCCCCATCTACCTTGCCTTCAGGTGGGACAA
  PAZ43   (251) ACAAAATGAAACTCAGGTTCCCCCATCTACCTTGCCTTCAGGTGGGACAA
               301                                                   350
Ref-PAZ   (301) GAACACAAACACACATACCTTCCTCTGGAAGTATGCAACATTGTACCTGG
   PAZ3   (301) GAACACAAACACACATACCTTCCTCTGGAAGTATGCAACATTGTACCTGG
  PAZ37   (301) GAACACAAACACACATACCTTCCTCTGGAAGTATGCAACATTGTACCTGG
  PAZ43   (301) GAACACAAACACACATACCTTCCTCTGGAAGTATGCAACATTGTACCTGG
               351                                                   400
Ref-PAZ   (351) ACAACGATGCATCAAGAAACTAACAGACATGCAGACATCTACCATGATCA
   PAZ3   (351) ACAACGATGCATCAAGAAACTAACAGACATGCAGACATCTACCATGATCA
  PAZ37   (351) ACAACGATGCATCAAGAAACTAACAGACATGCAGACATCTACCATGATCA
  PAZ43   (351) ACAACGATGCATCAAGAAACTAACAGACATGCAGACATCTACCATGATCA
               401       417
Ref-PAZ   (401) AGGCAACAGCTAGATCT
   PAZ3   (401) AGGCAACAGCTAGATCT
  PAZ37   (401) AGGCAACAGCTAGATCT
  PAZ43   (401) AGGCAACAGCTAGATCT
```

Figure 6.14 The alignment of nucleotide sequences of the recombinant pPICZαA/*PAZ* from three individual clones

The figure reveals a DNA sequence alignment of the *PAZ* of *P. monodon* from three clones. Ref-PAZ indicates the sequence of *PAZ* region from the original pUC19/ *Pem-ago* clone. The results illustrated that the nucleotide sequences are identical in all clones with the reference. The gray shade represents identical nucleotides.

6.4 Transformation and Integration of *PAZ* fragment into *P. pastoris* genome

6.4.1 Transformation of *PAZ* fragment into *P. pastoris* genome

In order to allow integration of *PAZ* cDNA into the genome of *P. pastoris* host strain KM71 for expression the recombinant protein, the recombinant plasmid of pPICZαA/*PAZ* was linearlized with *Dra* I, which is the restriction site located in the 5'*AOX1* promoter region. This digestion provides the integration region for *PAZ* cDNA fragment into *P. pastoris* genome by electrophoration. The *P. pastoris* transformants were preliminary screened on rich medium (YEPD) agar containing 100 µg/ml Zeocin^{TM} culture. The transformants clones that harbored the recombinant plasmid pPICZαA/*PAZ* containing Zeocin^{TM}-resistance gene could grow on this selective medium.

6.4.2 Determination of *PAZ* cDNA in *P. pastoris* genome

The integration of *PAZ* DNA into *P. pastoris* genome was identified by colony PCR method using 5'*AOX1* and 3'*AOX1* primers. The positive clones should provide the PCR product with the size of 0.9 kb. The negative control for expression was the *P. pastoris* clone that contained pPICZαA integration in its genome that gave the PCR product of 0.6 kb. The clone KM71/pPICZαA/Der p3.1 containing Der p3.1 fragment integration into *P. pastoris* genome which was kindly provided by Miss Nipawan Nuemket from Asst. Prof. Surapon Piboonphokanun's laboratory was used as a positive control for expression and would show the PCR product at 1.2 kb after PCR reaction. The results that reveal the expected PCR products in all transformants indicated that the linearlized plasmids harboring *PAZ* fragment were successfully integrated into the *P. pastoris* genome (figure 6.15).

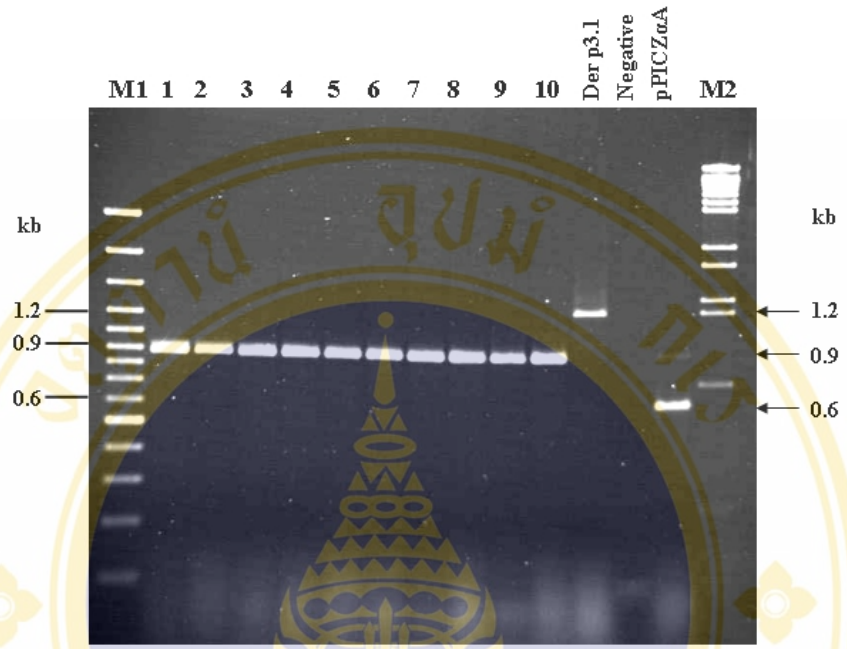

Figure 6.15 Colony PCR screening for integration of pPICZαA/*PAZ* recombinant plasmid into the genome of *P. pastoris* transformants.

The figure shows 1.2 % agarose gel electrophoresis (ethidium bromide stained) from the colony PCR analysis with 5'*AOX1* and 3'*AOX1* primers from Zeocin™ resistant-transformants clones to confirm the integration of the *PAZ* cDNA into *P. pastoris* genome.

Lane M1 : 100 bp DNA ladder marker

Lane 1-10 : colony-PCR analysis from clone 1 to 10, respectively

Der p3.1 : colony-PCR analysis from KM71/pPICZαA/Der p3.1 clone

Negative : colony-PCR analysis with no template

pPICZαA : colony-PCR analysis with KM71/pPICZαA clone

Lane M2 : λ/*Bst*E II digested DNA marker

6.5 Expression of the Recombinant PAZ domain in *P. pastoris*

6.5.1 Expression of secreted recombinant PAZ protein in culture medium

According to the construction of pPICZαA/*PAZ*, the recombinant protein should be expressed and secreted into the culture medium as the native form containing hexahistidine tag (6XHis) at C-terminus. Clones 1 and 2 were randomly selected for small-scale expression with 1% (v/v) methanol induction for 5 days. After the clones were first grown in BMGY medium until OD_{600} reached 5-6 which is the mid log phase of *P. pastoris* culture, the cells were harvested by centrifugation and resuspended in BMMY medium in the final concentration approximately 30 OD_{600} cells to 1 ml of BMMY medium. In order to induce the expression, methanol was added to a final concentration 1% (v/v) into the culture every 24 hr to maintain the induction under the control of *AOX1* promoter. After 5 days of the induction, the cell pellet and supernatant culture were separated by centrifugation. An aliquot of 20 µl of the supernatant medium from clones 1 and 2 was analyzed on 15% SDS-PAGE with Coomassie blue staining with the negative control of KM71/pPICZαA expression. The results revealed that no recombinant protein of PAZ domain was observed in the culture medium at the expected size about 17 kDa (figure 6.16). In order to prove whether the recombinant PAZ domain protein was expressed but could not be secreted, and existed as intracellular protein, the cell pellet lysate from clones 1 and 2 were analyzed by Western Blot using anti-His antibody as primary antibody and anti-mouse conjugated with alkaline phosphatase as secondary antibody. However, the signal could not be observed on the membrane in both clones whereas the positive control of the Western Blot which is Cathecolamine Acetyl Transferase (CAT) protein that contained histidine tag at N-terminus, provided by Miss Pornwarat Niyomrattanakit from Asst. Prof. Gerd Katzenmeier's laboratory, was presented at the expected size 37 kDa (figure 6.17).

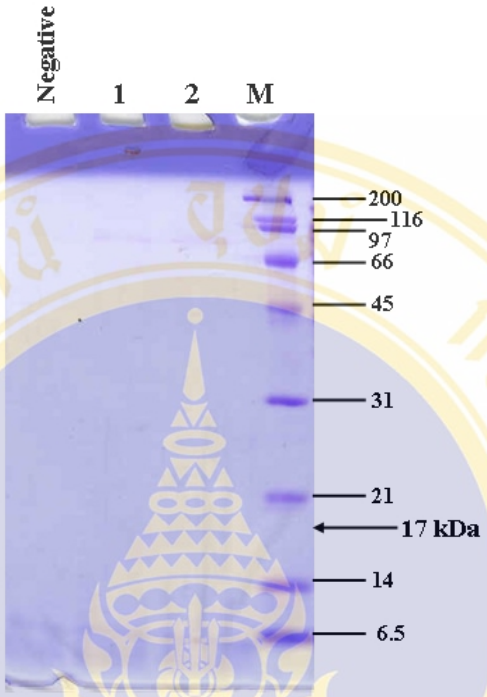

Figure 6.16 SDS-PAGE analysis of the recombinant PAZ protein expression in the culture medium under 1% (v/v) methanol induction for 5 days

The figure shows 15% SDS-PAGE with Coomassie blue staining of the 20 µl culture medium after 5 days-induction with 1% (v/v) methanol from clones 1 and 2.

Lane M : Standard broadrange protein marker

Lane 1 : Culture supernatant of recombinant KM71/pPICZαA/*PAZ* clone 1

Lane 2 : Culture supernatant of recombinant KM71/pPICZαA/*PAZ* clone 2

Negative : Negative control of culture supernatant from KM71/pPICZ

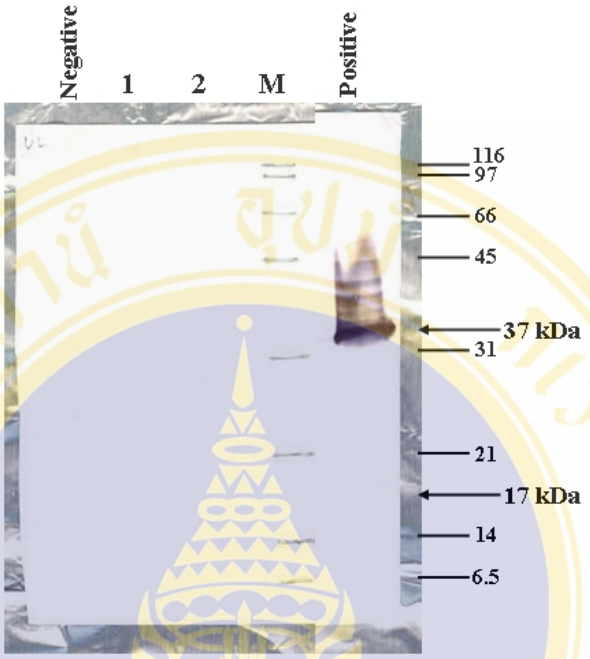

Figure 6.17 Western Blot analysis of expressed intracellular recombinant PAZ domain protein from crude cell lysate under 1% (v/v) methanol induction for 5 days

The figure reveals the Western Blot with anti-His antibody as primary antibody and anti-mouse conjugated with alkaline phosophatase as secondary antibody.

Lane M : Standard broadrange protein marker

Lane 1 : Culture supernatant of recombinant KM71/pPICZαA/*PAZ* clone 1

Lane 2 : Culture supernatant of recombinant KM71/pPICZαA/*PAZ* clone 2

Negative : Negative control of culture supernatant from KM71/pPICZ

Positive : Positive control of Western Blot from CAT protein (37 kDa)

6.5.2 Optimization of the Expression Conditions for the Recombinant PAZ domain Protein in *P. pastoris* Expression System

Because the expected recombinant PAZ domain protein could not be observed in both intracellular (in crude cell lysate) and extracellular (in supernatant medium) when expressed with the condition in 6.5.1. The expression conditions were firstly optimized by varying the period of expression from 0 to 5 day with 3 % (v/v) methanol induction. Five clones of KM71/pPICZαA/*PAZ* were selected. After the induction, the supernatant was concentrated 100 folds with 100 % TCA precipitation before analyzed on 15% SDS-PAGE. The results from the 5 clones revealed similar protein pattern to that from the negative control with an extra faint band of approximately 17 kDa in all clones. However, the confirmation of this results band after Western Blot analysis with anti-His antibody could not detect any signal on the membrane. It indicated that this faint band was also the background of the expression from *P. pasotris* host cell. Moreover, these results showed that the amounts of expressed proteins were decreased after 3 days of expression period, especially in positive control that illustrated the large amount of degraded product in day 4 and 5. Therefore the appropriate period of expression should not be longer than 3 days (figure 6.18).

The expression conditions were also optimized by varying the percentage of methanol induction between 0 to 5 %. However, the expression could not be observed in both supernatant medium and crude cell lysate at any concentration of methanol tested (figure 6.19).

In order to ensure that the expression of KM71/pPICZαA/*PAZ* clones was not successful, twenty five clones of the recombinant KM71/pPICZαA/*PAZ* were subjected for expression in *P. pasotris* with the conditions of 5 % methanol induction for 2 days. However, the expression of the recombinant PAZ domain protein could not be observed in both intracellular and extracellular (data not shown).

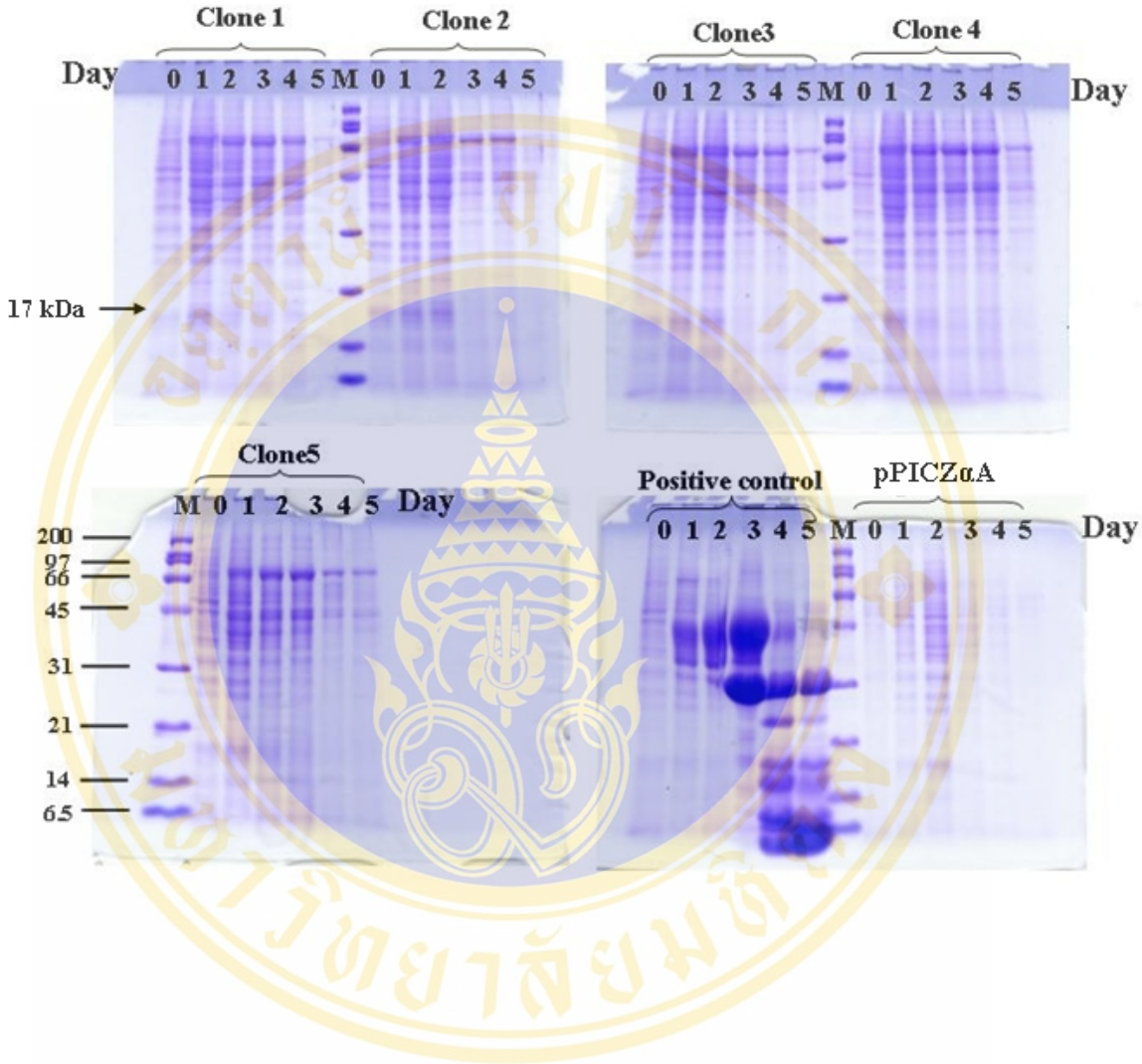

Figure 6.18 SDS-PAGE analysis of the recombinant PAZ protein expression that was induced with 3% (v/v) methanol for 0 to 5 days

The figures show 15% SDS-PAGE with Coomassie blue staining of the 1 ml TCA precipitated culture medium after induction with 3 % (v/v) methanol for 0-5 days in clones 1 to 5. The recombinant DerP3.1 protein and KM71/pPICZαA were used as positive and negative control, respectively.

Lane M : Standard broad range protein marker

Lane 0-5 : Protein expression for 0 to 5 days, respectively

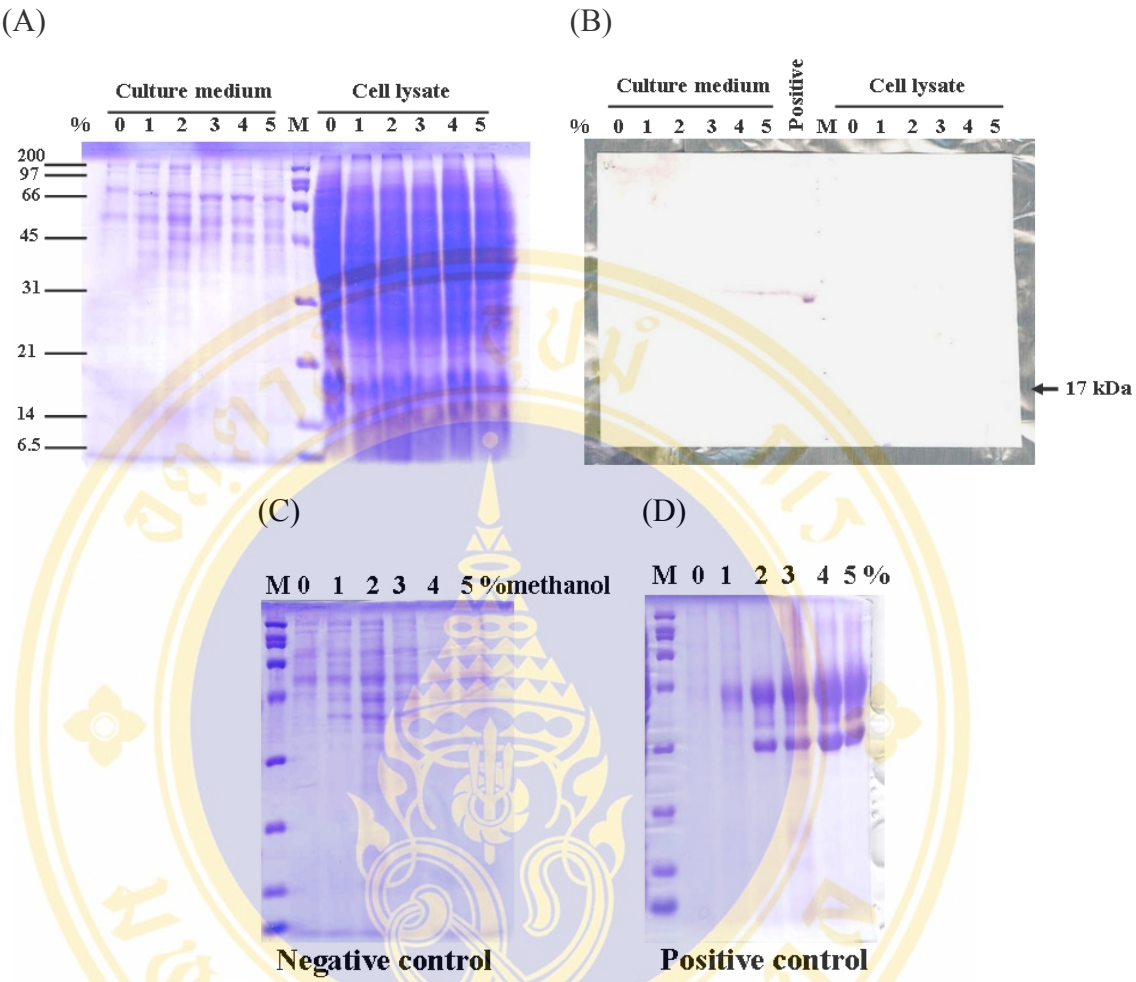

Figure 6.19 SDS-PAGE and Western Blot analysis of the recombinant PAZ protein expression from supernatant and crude cell lysate under 0 to 5% (v/v) methanol induction for 2 days

(A) The figure shows 15% SDS-PAGE with Coomassie blue staining of the 1 ml TCA precipitated culture medium and 6 OD_{600} cell lysate from the recombinant PAZ after induction with methanol for 2 days.

(B) Western Blot analysis of extracellular and intracellular expression with the same samples from figure (A). Positive control for Blotting was loaded in the lane labeled “positive”.

(C) SDS-PAGE shows the expression of Negative control

(D) SDS-PAGE shows the expression of Positive control

Lane M : Standard broadrange protein marker

Lane 0-5 : Protein expression induced by 0 to 5% methanol, respectively

CHAPTER VII
RESULTS PART II

The results from *P. pastoris* expression system that utilized pPICZαA as vector illustrated that expression of the recombinant PAZ domain protein could not be observed in both extracellular (in culture medium) and intracellular (crude cell lysate) fractions in various conditions. Recently, there are a few publications demonstrating that Argonaute and PAZ domain proteins could be expressed in *Eschericia coli* expression system and the recombinant proteins retained biochemical activities that are involved in RNA interference pathway. Therefore, the expression system was altered into *Escherichia coli* system by applying *E. coli* strain BL21(DE3)pLysS as a host for expression with pET-15b as a vector to express *P. monodon*'s PAZ domain and Argonaute recombinant proteins as N-terminus hexahistidine tag which provides the detection of recombinant proteins by Western Blot analysis with anti-His antibody and the advantage for purification step with Ni^{2+} column affinity chromatography. The expression was conducted by induction with IPTG under the control of T7 promoter.

7.1 Construction of pET-15b/*Pem-ago* and pET-15b/*PAZ* Expression Recombinant Plasmids for *E. coli* Expression System

In order to acquire the recombinant plasmids for expression of *P. monodon*'s Argonaute (Pem-AGO) and PAZ domain (PAZ) proteins as N-terminus hexahistidine fusion tag, the constructs were engineered by utilizing *Nde* I and *BamH* I that was added to the forward and reverse primers, respectively as cloning sites (figure 7.1).

7.1.1 Amplification of cDNA Encoding *P.monodon*'s Pem-AGO and PAZ Domain for *E. coli* Expression System

The cDNAs encoding Pem-AGO and PAZ domain regions were amplified in individual PCR reactions with specific primer sets as described in method 5.4.2 by employing the recombinant pUC19/*Pem-ago* as a template. According to the PCR reactions, the expected band of 2.8 kb for *Pem-ago* (figure 7.2) and 438 bp of PAZ domain (figure 7.3) were generated. The negative controls were performed in the same conditions but without DNA template.

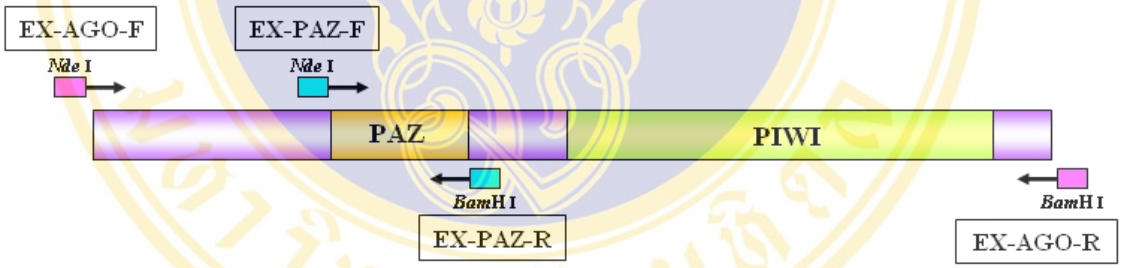

Figure 7.1 A schematic diagram represents the binding sites of primers on *Pem-ago* cDNA template for amplification of *Pem-ago* (EX-AGO-F and EX-AGO-R) and PAZ domain (EX-PAZ-F and EX-PAZ-R).

The arrows represent the primers and the attached square boxes represent the recognition sequence of restriction enzymes for cloning into pET-15b vector.

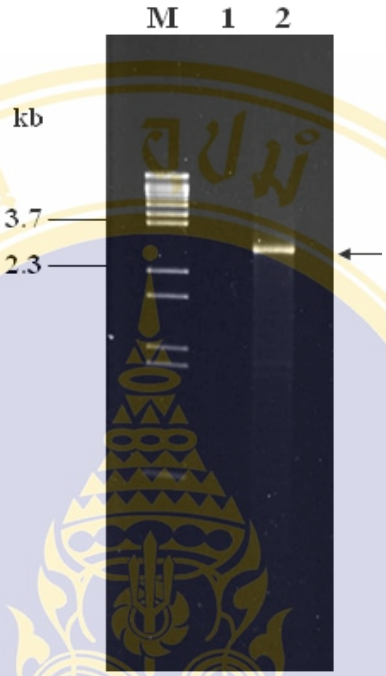

Figure 7.2 Amplification of *Pem-ago* cDNA for construction in *E. coli* expression system

This figure shows 1% agarose gel electrophoresis (ethidium bromide stained) of the PCR product of the cDNA encoding Pem-AGO for cloning into pET-15b vector by using EX-AGO-F and EX-AGO-R primers.

Lane M : λ/*Bst*E II digested DNA marker

Lane 1 : Negative control (no template)

Lane 2 : PCR product of the cDNA encoding Pem-AGO

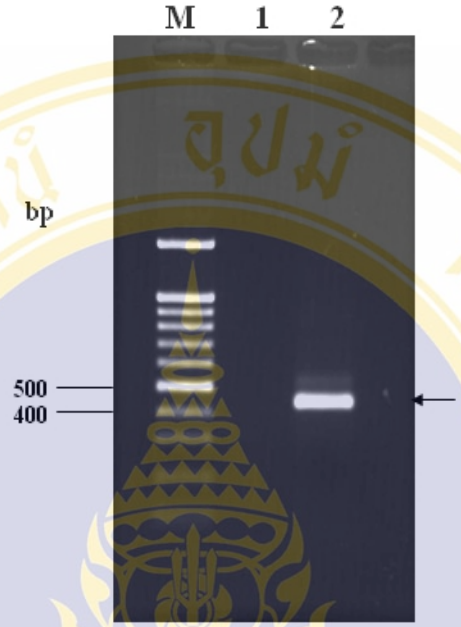

Figure 7.3 Amplification of *P.monodon*'s *PAZ* for construction in *E. coli* expression system

This figure reveals 1.5% agarose gel electrophoresis (ethidium bromide stained) of the PCR product of the *PAZ* for cloning into pET-15b vector by utilizing EX-PAZ-F and EX-PAZ-R primers.

Lane M : 100 bp + 1.5 kb DNA ladder marker

Lane 1 : Negative control (no template)

Lane 2 : PCR product of the PAZ domain

7.1.2 Cloning of DNA Fragments into pET-15b Vector

The PCR products at the expected sizes of 2.8 kb and 438 bp corresponding to the *Pem-ago* and *PAZ* regions, respectively were excised from agarose gel and subsequently purified by QIAquick Gel Extraction Kit (QIAGEN). The purified fragments were digested with *Nde* I and *Bam*H I to generate the restriction sites for cloning into pET-15b vector. The purified fragments of *Pem-ago* and *PAZ* gene were individually ligated with purified dephosphorylated *Nde* I and *Bam*H I-digested pET-15b using T4 DNA ligase to generate the recombinant plasmids pET-15b/*Pem-ago* and pET-15b/*PAZ* that were further transformed into *E. coli* strain DH5α and primarily screened based on ampicillin antibiotic resistance after grown on LB agar containing 100 μg/ml ampicillin.

7.1.3 Screening of the Recombinant Clones

The transformant clones of each construct were screened by rapid size screening and restriction enzyme digestion.

For the screening of recombinant plasmid pET-15b/*Pem-ago* and pET-15b/*PAZ*, the insertion of *Pem-ago* and *PAZ* in pET-15b vector was primary checked by rapid size screening. Then the plasmids from these clones were extracted by CTAB method followed by restriction digestion analysis with *Nde* I and *Bam*H I which were used as the cloning sites. The corrected clones should provide products of the insert fragment (2.8 kb for *Pem-ago* and 417 bp for *PAZ* domain fragment) and 5.7 kb fragment of the pET-15b vector. Figure 7.4 represents incomplete digestion of pET-15b/*Pem-ago* clone number 114 and 116 which were observed at 8.5 kb. The 5.7 kb and 2.8 kb were the fragments of pET-15b and *Pem-ago*, respectively (figure 7.4). The restriction digestion analysis of the pET-15b/*PAZ* was showed in figure 7.5 which generated the insert fragment product from all 5 selected clones at 417 bp after digestion reaction.

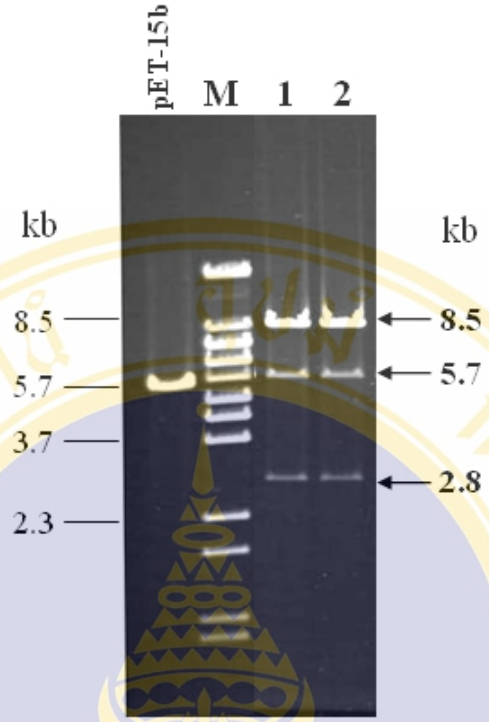

Figure 7.4 Screening of the recombinant pET-15b/*Pem-ago* clones by restriction enzyme digestion with *Nde* I and *Bam*H I (cloning sites)

The figure illustrates 0.8% agarose gel electrophoresis (ethidium bromide stained) of the *Nde* I and *Bam*H I restriction endonuclease analysis of the recombinant pET-15b/*Pem-ago* plasmids

Lane M : λ/*Bst*E II digested DNA marker

Lane 1 : *Nde* I and *Bam*H I digested pET-15b/*Pem-ago* clone no.114

Lane 2 : *Nde* I and *Bam*H I digested pET-15b/*Pem-ago* clone no.116

pET-15b indicates the *Nde* I and *Bam*H I-digested pET-15b vector

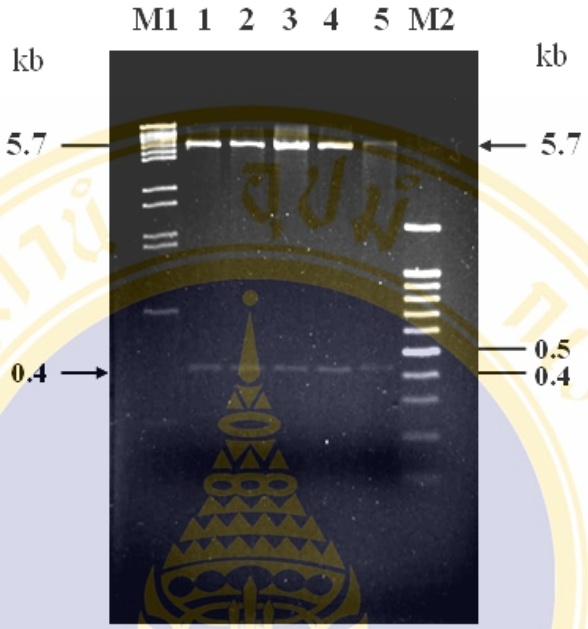

Figure 7.5 Screening of the recombinant pET-15b/*PAZ* by restriction cloning enzyme digestion with *Nde* I and *Bam*H I (cloning sites)

The figure reveals 1.5% agarose gel electrophoresis (ethidium bromide stained) of the *Nde* I and *Bam*H I restriction endonuclease analysis of the recombinant pET-15b/*PAZ* plasmids

Lane M 1 : λ/*Bst*E II digested DNA marker

Lane M2 : 100 bp + 1.5 kb DNA ladder marker

Lanes 1-5 : pET-15b/*PAZ* recombinant clones no. 1-5, respectively

7.2 Nucleotide and Deduced Amino Acid Sequence Analysis of the cDNA Encoding Argonaute and PAZ domain of *Penaeus monodon*

The sequence of the recombinant clones that showed the positive results from screening analysis were verified by automated DNA sequencing in both forward and reverse directions using the sequencing primers and followed by alignment with Vector NTI program.

The sequences result in figure 7.6 showed that pET-15b/*Pem-ago* clone 116 contained the correct insert sequence comparing to the original pUC19/*Pem-ago* (figure 7.6). Likewise, the sequencing result of pET-15b/*PAZ* clones with T7 promoter and T7 terminator primers that bind on the vector backbone represented 100% identity with the original PAZ domain in pUC19/*Pem-ago* (figure 7.7)

```
                1                                                                  70
Pem-ago     (1) ATGTACCCTGTTGGGCAGCCACCTGGTCCTCCTGGCCCACCCGGTCCCTCGGGTCCGGGTGGACCCCCAG
Ago-116     (1) ATGTACCCTGTTGGGCAGCCACCTGGTCCTCCTGGCCCACCCGGTCCCTCGGGTCCGGGTGGACCCCCAG
               71                                                                 140
Pem-ago    (71) GACCAGCTGGCCCCCCAGTGCCCCGACCCTTGACCTTGCCGCCGGGACCCACGCCGGTCCCTGGCCCAAT
Ago-116    (71) GACCAGCTGGCCCCCCAGTGCCCCGACCCTTGACCTTGCCGCCGGGACCCACGCCGGTCCCTGGCCCAAT
              141                                                                 210
Pem-ago   (141) CACTACCATTGTACCGCAGGCCCCTGGTACGCCGGCTGTGGCAACGGGGACAGGCATGACTGCCCTCTTA
Ago-116   (141) CACTACCATTGTACCGCAGGCCCCTGGTACGCCGGCTGTGGCAACGGGGACAGGCATGACTGCCCTCTTA
              211                                                                 280
Pem-ago   (211) CCGCCAGAACTACCTAACACACCAGCTTTTGTAGCACCAAGAAGACCGAATCTCGGGCGAGAAGGTCGAC
Ago-116   (211) CCGCCAGAACTACCTAACACACCAGCTTTTGTAGCACCAAGAAGACCGAATCTCGGGCGAGAAGGTCGAC
              281                                                                 350
Pem-ago   (281) CTATCACGTTGCGGGCCAACCACTTCCAGATCTCTATGCCGAGAGGTTACATTCACCACTATGATATTAG
Ago-116   (281) CTATCACGTTGCGGGCCAACCACTTCCAGATCTCTATGCCGAGAGGTTACATTCACCACTATGATATTAG
              351                                                                 420
Pem-ago   (351) TATTACCCCTGATAAATGCCCGCGCAAGGTTAATCGGGAAATTATTGAGACGATGGTTCATGCTTTCCCT
Ago-116   (351) TATTACCCCTGATAAATGCCCGCGCAAGGTTAATCGGGAAATTATTGAGACGATGGTTCATGCTTTCCCT
              421                                                                 490
Pem-ago   (421) AGAATTTTTGGCACTCTAAAGCCTGTCTTCGATGGGAGAAGCAATTTATACACCAGAGATCCCCTGCCCA
Ago-116   (421) AGAATTTTTGGCACTCTAAAGCCTGTCTTCGATGGGAGAAGCAATTTATACACCAGAGATCCCCTGCCCA
              491                                                                 560
Pem-ago   (491) TTGGTAATGAAAAAATGGAGCTTGAGGTAACGTTACCAGGGGAAGGACGTGACAGGGTGTTCAAGGTAGC
Ago-116   (491) TTGGTAATGAAAAAATGGAGCTTGAGGTAACGTTACCAGGGGAAGGACGTGACAGGGTGTTCAAGGTAGC
              561                                                                 630
Pem-ago   (561) GATGAAATGGTTAGCACAAGTAAATCTATATACGTTAGAAGAAGCATTGGAGGGACGGACGAGAACCATT
Ago-116   (561) GATGAAATGGTTAGCACAAGTAAATCTATATACGTTAGAAGAAGCATTGGAGGGACGGACGAGAACCATT
              631                                                                 700
Pem-ago   (631) CCTTATGATGCAATACAGGCACTAGATGTCGTTATGCGTCACCTGCCATCCATGACTTACACACCAGTGG
Ago-116   (631) CCTTATGATGCAATACAGGCACTAGATGTCGTTATGCGTCACCTGCCATCCATGACTTACACACCAGTGG
              701                                                                 770
Pem-ago   (701) GCAGGTCCTTTTTCTCCGCTCCAGATGGCTATTATCACCCCTTGGGAGGTGGAAGGGAAGTGTGGTTTGG
Ago-116   (701) GCAGGTCCTTTTTCTCCGCTCCAGATGGCTATTATCACCCCTTGGGAGGTGGAAGGGAAGTGTGGTTTGG
              771                                                                 840
Pem-ago   (771) CTTCCATCAAAGTGTAAGACCTTCACAGTGGAAGATGATGCTTAACATTGACGTGTCAGCTACAGCATTC
Ago-116   (771) CTTCCATCAAAGTGTAAGACCTTCACAGTGGAAGATGATGCTTAACATTGACGTGTCAGCTACAGCATTC
              841                                                                 910
Pem-ago   (841) TACAAGGCCCAGGCAGTAATAGAGTTTATGTGTGAAGTGTTAGATATTCGAGAAATAGGTGAGCAGAGGA
Ago-116   (841) TACAAGGCCCAGGCAGTAATAGAGTTTATGTGTGAAGTGTTAGATATTCGAGAAATAGGTGAGCAGAGGA
              911                                                                 980
Pem-ago   (911) AACCTCTAACGGATTCGCAGCGTGTCAAGTTCACAAAAGAAATTAAGGGTCTGAAGATTGAGATCACACA
Ago-116   (911) AACCTCTAACGGATTCGCAGCGTGTCAAGTTCACAAAAGAAATTAAGGGTCTGAAGATTGAGATCACACA
              981                                                                1050
Pem-ago   (981) CTGTGGTGCGATGCGAAGAAAGTACAGGGTGTGTAATGTCACAAGAAGGCCAGCACAGATGCAGTCGTTC
Ago-116   (981) CTGTGGTGCGATGCGAAGAAAGTACAGGGTGTGTAATGTCACAAGAAGGCCAGCACAGATGCAGTCGTTC
             1051                                                                1120
Pem-ago  (1051) CCATTGCAGCTAGAGAATGGTCAGACTGTGGAATGTACTGTTGCAAAATATTTCCTTGACAAATACAAAA
Ago-116  (1051) CCATTGCAGCTAGAGAATGGTCAGACTGTGGAATGTACTGTTGCAAAATATTTCCTTGACAAATACAAAA
             1121                                                                1190
Pem-ago  (1121) TGAAACTCAGGTTCCCCCATCTACCTTGCCTTCAGGTGGGACAAGAACACAAACACACATACCTTCCTCT
Ago-116  (1121) TGAAACTCAGGTTCCCCCATCTACCTTGCCTTCAGGTGGGACAAGAACACAAACACACATACCTTCCTCT
             1191                                                                1260
Pem-ago  (1191) GGAAGTATGCAACATTGTACCTGGACAACGATGCATCAAGAAACTAACAGACATGCAGACATCTACCATG
Ago-116  (1191) GGAAGTATGCAACATTGTACCTGGACAACGATGCATCAAGAAACTAACAGACATGCAGACATCTACCATG
             1261                                                                1330
Pem-ago  (1261) ATCAAGGCAACAGCTAGATCTGCACCTGATAGGGAGAGAGAGATCAACAATCTGGTCCGAAAGGCGGACT
Ago-116  (1261) ATCAAGGCAACAGCTAGATCTGCACCTGATAGGGAGAGAGAGATCAACAATCTGGTCCGAAAGGCGGACT
             1331                                                                1400
Pem-ago  (1331) TTAACAATGACCCGTACATGCAAGAATTTGGTCTGACGATCAGTACAGCTATGATGGAGGTCCGAGGTCG
Ago-116  (1331) TTAACAATGACCCGTACATGCAAGAATTTGGTCTGACGATCAGTACAGCTATGATGGAGGTCCGAGGTCG
             1401                                                                1470
Pem-ago  (1401) CGTACTCCCACCCCCAAAGCTCCAATATGGAGGGCGAACAAAGCAGCAAGCTCTGCCCAACCAGGGGGTG
Ago-116  (1401) CGTACTCCCACCCCCAAAGCTCCAATATGGAGGGCGAACAAAGCAGCAAGCTCTGCCCAACCAGGGGGTG
             1471                                                                1540
Pem-ago  (1471) TGGGACATGAGGGGGAAACAGTTCTTCACAGGGGTAGAAATCCGCGTGTGGGCCGTTGCGTGCTTCGCCC
Ago-116  (1471) TGGGACATGAGGGGGAAACAGTTCTTCACAGGGGTAGAAATCCGCGTGTGGGCCGTTGCGTGCTTCGCCC
             1541                                                                1610
Pem-ago  (1541) CACAGCGCACAGTGAGAGAAGATGCGCTGCGCAATTTTACACAGCAACTACAAAAGATTAGTAATGATGC
Ago-116  (1541) CACAGCGCACAGTGAGAGAAGATGCGCTGCGCAATTTTACACAGCAACTACAAAAGATTAGTAATGATGC
             1611                                                                1680
Pem-ago  (1611) TGGCATGCCCATCATTGGCCAGCCGTGCTTCTGCAAGTATGCCAACGGTCCTGACCAGGTAGAGCCCATG
Ago-116  (1611) TGGCATGCCCATCATTGGCCAGCCGTGCTTCTGCAAGTATGCCAACGGTCCTGACCAGGTAGAGCCCATG
             1681                                                                1750
Pem-ago  (1681) TTCCGTTACCTGAAGAGCACATTCACCGGTCTGCAGCTTGTATGTGTTGTTCTACCAGGCAAAACTCCTG
Ago-116  (1681) TTCCGTTACCTGAAGAGCACATTCACCGGTCTGCAGCTTGTATGTGTTGTTCTACCAGGCAAAACTCCTG
             1751                                                                1820
Pem-ago  (1751) TCTATGCTGAAGTGAAGCGTGTGGGTGACACTGTCTTAGGAATGGCTACCCAATGTGTCCAGGCCAAGAA
Ago-116  (1751) TCTATGCTGAAGTGAAGCGTGTGGGTGACACTGTCTTAGGAATGGCTACCCAATGTGTCCAGGCCAAGAA
             1821                                                                1890
Pem-ago  (1821) TGTGAACAAAACCTCACCTCAAACACTGTCCAACCTCTGTCTCAAAATAAATGTGAAGTTGGGAGGCATC
Ago-116  (1821) TGTGAACAAAACCTCACCTCAAACACTGTCCAACCTCTGTCTCAAAATAAATGTGAAGTTGGGAGGCATC
```

```
                1891                                                    1960
Pem-ago  (1891) AACTCCATTCTTGTTCCAGGCATCAGACCAAAAGTGTTCAATGAGCCTGTGATCTTCCTGGGTGCTGATG
Ago-116  (1891) AACTCCATTCTTGTTCCAGGCATCAGACCAAAAGTGTTCAATGAGCCTGTGATCTTCCTGGGTGCTGATG
                1961                                                    2030
Pem-ago  (1961) TAACTCATCCACCAGCGGGTGATAATAAGAAGCCGTCCATTGCAGCCGTAGTAGGATCTATGGATGCTCA
Ago-116  (1961) TAACTCATCCACCAGCGGGTGATAATAAGAAGCCGTCCATTGCAGCCGTAGTAGGATCTATGGATGCTCA
                2031                                                    2100
Pem-ago  (2031) TCCATCACGCTATGCTGCAACTGTCCGGGTCCAGCAGCACAGACAGAATGGATCAACAACACAAGGCCAA
Ago-116  (2031) TCCATCACGCTATGCTGCAACTGTCCGGGTCCAGCAGCACAGACAGAATGGATCAACAACACAAGGCCAA
                2101                                                    2170
Pem-ago  (2101) AGTGCCAGTGACGGCTCGCGACCCAGACAACTGACTTTCGCGAGGACGGCACATGACGAGGTGATCCAGG
Ago-116  (2101) AGTGCCAGTGACGGCTCGCGACCCAGACAACTGACTTTCGCGAGGACGGCACATGACGAGGTGATCCAGG
                2171                                                    2240
Pem-ago  (2171) AGCTCTCTTCTATGGTGAAGGAGCTGCTCATCCAATTCTACAAGTCTACGCGGTTCAAGCCCAACAGGAT
Ago-116  (2171) AGCTCTCTTCTATGGTGAAGGAGCTGCTCATCCAATTCTACAAGTCTACGCGGTTCAAGCCCAACAGGAT
                2241                                                    2310
Pem-ago  (2241) CATCCTTTATCGGGATGGTGTGAGCGAGGGACAATTCCAAACCGTGCTCCAGCATGAGCTGACTGCCATG
Ago-116  (2241) CATCCTTTATCGGGATGGTGTGAGCGAGGGACAATTCCAAACCGTGCTCCAGCATGAGCTGACTGCCATG
                2311                                                    2380
Pem-ago  (2311) AGAGAGGCTTGCATAAAGTTGGAAGCGGACTACAAGCCTGGCATCACGTACATTGCTGTGCAGAAGAGAC
Ago-116  (2311) AGAGAGGCTTGCATAAAGTTGGAAGCGGACTACAAGCCTGGCATCACGTACATTGCTGTGCAGAAGAGAC
                2381                                                    2450
Pem-ago  (2381) ATCATACAAGATTGTTCTGTTCTGACAAGAAAGAACAGAGTGGCAAGAGTGGTAATATTCCTGCTGGTAC
Ago-116  (2381) ATCATACAAGATTGTTCTGTTCTGACAAGAAAGAACAGAGTGGCAAGAGTGGTAATATTCCTGCTGGTAC
                2451                                                    2520
Pem-ago  (2451) AACTGTTGATGTGGGCATCACGCATCCAACTGAGTTTGACTTCTACCTCTGCTCTCATCAGGGTATCCAG
Ago-116  (2451) AACTGTTGATGTGGGCATCACGCATCCAACTGAGTTTGACTTCTACCTCTGCTCTCATCAGGGTATCCAG
                2521                                                    2590
Pem-ago  (2521) GGCACAAGTCGTCCCAGTCACTACCACGTACTGTGGGATGATAACCACTTTGACAGTGATGAGCTGCAGT
Ago-116  (2521) GGCACAAGTCGTCCCAGTCACTACCACGTACTGTGGGATGATAACCACTTTGACAGTGATGAGCTGCAGT
                2591                                                    2660
Pem-ago  (2591) GCCTGACTTACCAGTTGTGTCATACCTATGTAAGATGTACACGATCAGTCTCCATACCTGCTCCAGCCTA
Ago-116  (2591) GCCTGACTTACCAGTTGTGTCATACCTATGTAAGATGTACACGATCAGTCTCCATACCTGCTCCAGCCTA
                2661                                                    2730
Pem-ago  (2661) TTATGCTCACTTGGTAGCCTTCAGGGCTCGTTATCATCTCGTCGAAAAGGAGCATGACAGTGGAGAGGGG
Ago-116  (2661) TTATGCTCACTTGGTAGCCTTCAGGGCTCGTTATCATCTCGTCGAAAAGGAGCATGACAGTGGAGAGGGG
                2731                                                    2800
Pem-ago  (2731) TCACACCAATCTGGCAACAGTGAGGATCGCACACCATCTGCCATGGCAAGGGCAGTTACAGTGCATGTCG
Ago-116  (2731) TCACACCAATCTGGCAACAGTGAGGATCGCACACCATCTGCCATGGCAAGGGCAGTTACAGTGCATGTCG
                2801                2829
Pem-ago  (2801) ACACAAACAGAGTCATGTACTTTGCTTAA
Ago-116  (2801) ACACAAACAGAGTCATGTACTTTGCTTAA
```

Figure 7.6 The alignment of nucleotide sequences of pET-15b/*Pem-ago* from clone no. 116

The figure reveals a nucleotide sequence alignment of pET-15b/*Pem-ago* from clone no. 116 with the original sequence from pUC19/*Pem-ago* as indicated by Pem-ago. The nucleotides that are identical in all sequences are highlight in gray.

Figure 7.7 The alignment of nucleotide sequences of pET-15b/*PAZ* from clone no. 1 and 2 respectively

The figure represents a nucleotide sequence alignment of pET-15b/*PAZ* from clone no. 1 and 2 to the original sequence from pUC19/*Pem-ago* as indicated by Pem-PAZ. The nucleotides that are identical in all sequences are highlight in gray.

7.3 Expression of the Recombinant Pem-AGO Protein in *E. coli* Strain BL21(DE3)pLysS

The recombinant plasmid of pET-15b/*Pem-ago* was transformed into expression host, *E. coli* strain BL21(DE3)pLysS. The selected clones were subjected to small-scale expression upon induction with IPTG in LB medium containing 100 μg/ml of ampicillin to optimize the conditions which provided the highest yield of soluble recombinant N-terminus hexahistidine tagged Pem-AGO protein. Cells corresponding to 1 OD_{600} were collected and the sample was prepared for SDS-PAGE and Western Blot analysis. The level of total protein expression was determined by Western Blot analysis with anti-His antibody which recognizes the hexahistidine tag at the N-terminus of the recombinant protein.

7.3.1 Pem-AGO Protein Expression of the Positive Clone No. 1 to 6

In order to obtain the positive clones that produced the highest yield of Pem-AGO expression, six recombinant clones were selected for expression at 25 ^{o}C with 1 mM IPTG induction for overnight. The results of Western Blot analysis in figure 7.8 revealed different expression levels of the protein band at the expected size of 108 kDa (Pem-AGO). The highest expression level was observed in clone no. 3 and 4. Moreover, anti-His antibody could also detect the additional protein bands of lower molecular weight with the similar pattern in all expressed clones (figure 7.8). Positive control for the expression was BL21(DE3)pLysS/pET-15b/T-CyaA that express the recombinant T-cyaA protein as an N-terminal hexahistidine tag fusion protein. Negative control was the expression of BL21(DE3)pLysS that contained pET-15b expression vector alone.

(A) SDS-PAGE (B) Western Blot

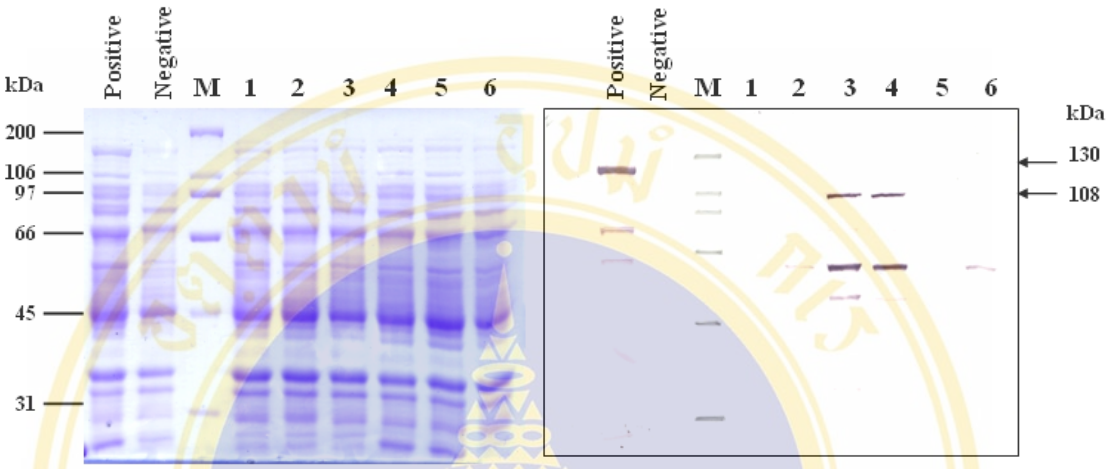

Figure 7.8 SDS-PAGE and Western blot analysis of the Pem-AGO from BL21(DE3)pLysS/pET-15b/*Pem-ago* expression clones

The figures show SDS-PAGE (A) and Western Blot (B) of the expression from the recombinant pET-15b/*Pem-ago* clones after induction with 1 mM IPTG at 25 ^{o}C for overnight.

(A) 10% SDS-PAGE (Coomassie staining) analysis

(B) Western Blot analysis of 10% SDS-PAGE with the same loading as (A) using anti-His antibody

Lane M : Standard broad range protein marker

Lane 1-6 : Crude cell lysate from BL21(DE3)pLysS/pET-15b/ *Pem-ago* clones No.1 to 6, respectively

Positive : Crude cell lysate from BL21(DE3)pLysS/pET-15b/T-CyaA

Negative : Crude cell lysate from BL21(DE3)pLysS/pET-15b

7.3.2 Optimization of Recombinant Pem-AGO Expression from pET-15b/*Pem-ago* Recombinant Plasmid in *E. coli* Strain BL21(DE3)pLysS

The results from 7.3.1 showed that clone no.3 represented the highest yield of Pem-AGO protein expression. In order to attain the maximum level of target protein, the period of expression was varied from 0 to 20 hr at 25^{o}C with 1 mM IPTG induction. From Western Blot analysis, the expression level of recombinant Pem-AGO at 108 kDa reached the highest level at 2 hr of IPTG induction and the amount of the recombinant protein decreased after longer period of incubation (figure 7.9).

7.3.3 Optimization of the Expression Temperature and IPTG Concentration Induction of the Pem-AGO Protein in *E. coli* Strain BL21(DE3)pLysS

In order to acquire the condition which yielded satisfactory amounts of protein expression from the recombinant Pem-AGO protein clone no.3, comparative analysis was performed at various expression temperatures between 25^{o}C and 30^{o}C and IPTG concentration from 0.1, 0.4 and 1.0 mM. The cultures were induced for 2 hr and subsequently analyzed by Western Blot detected with anti-His antibody. The expression pattern illustrated that the expression level at 25^{o}C provided higher amount of Pem-AGO protein than at 30^{o}C. However, the expression level was not significantly different among the IPTG concentration of 0.1, 0.4 and 1.0 mM (figure 7.10). Therefore, the suitable conditions for the recombinant Pem-AGO expression was executed at 25^{o}C and 0.1 mM IPTG induction for 2 hr.

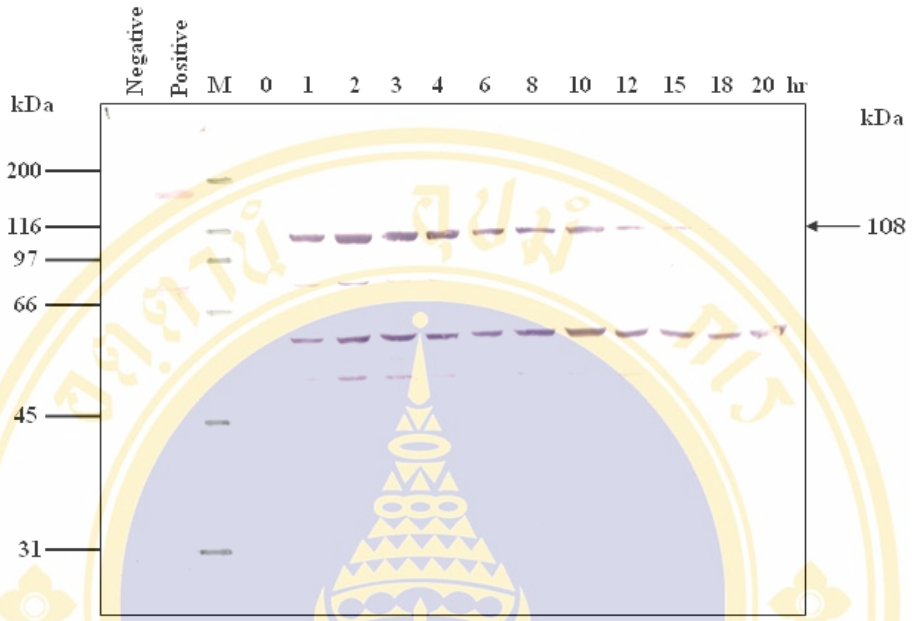

Figure 7.9 Western Blot analysis of recombinant Pem-AGO expression from clone no.3 at various periods of induction

The figure illustrates the Western Blot profile (10% SDS-PAGE with anti-His antibody) of the crude cell lysate from BL21(DE3)pLysS/pET-15b/*Pem-ago* clone no.3 at 25^{o}C with 1 mM IPTG induction by vary the period of expression from 0 to 20 hr.

Lane M : Standard broad range protein marker

Positive : Crude cell lysate from BL21(DE3)pLysS/pET-15b/T-CyaA

Negative : Crude cell lysate from from BL21(DE3)pLysS/pET-15b

The numbers in each lane indicates the period of induction (hr)

(A) SDS-PAGE

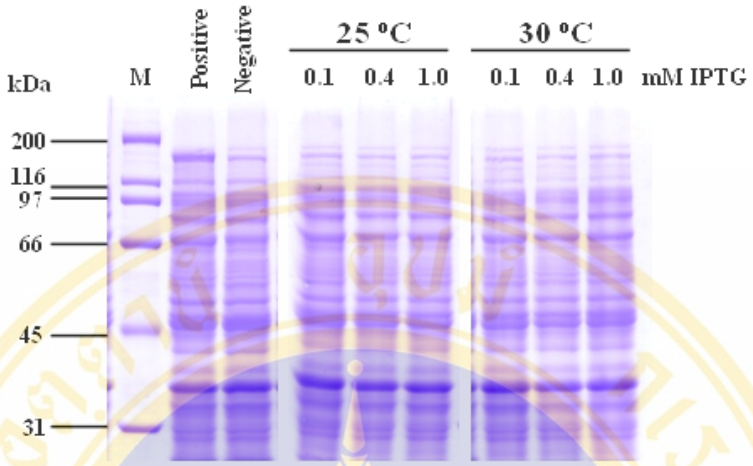

(B) Western Blot

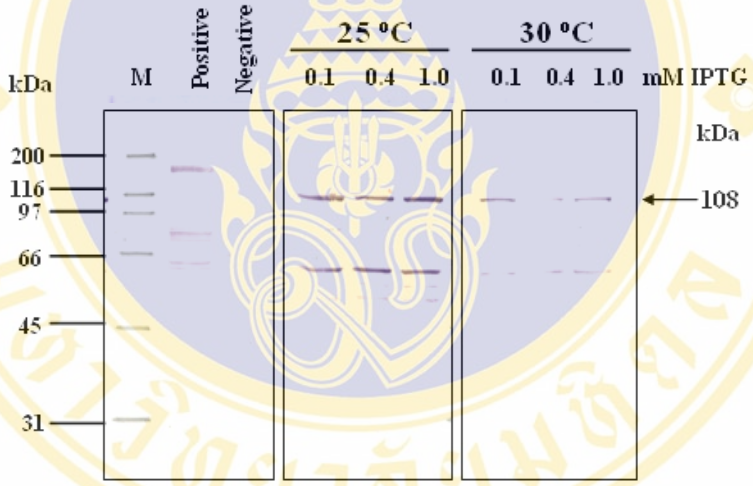

Figure 7.10 SDS-PAGE and Western Blot analysis of Pem-AGO expession from clone no.3 expression at various temperatures and IPTG concentrations

The figures illustrate SDS-PAGE (A) and Western Blot analysis (B) of the crude lysate from BL21(DE3)pLysS/pET-15b/*Pem-ago* clone no.3 at different temperature between 25°C and 30°C and various IPTG concentrations from 0.1, 0.4 and 1.0 mM, respectively

Lane M : Standard broad range protein marker

Positive : Crude cell lysate from BL21(DE3)pLysS/pET-15b/T-CyaA (Positive control of T-cyaA protein expression)

Negative : Crude cell lysate from from BL21(DE3)pLysS/pET-15b (Negative control of protein expression)

7.3.4 Determination of The Recombinant Pem-AGO Protein in Inclusion and Soluble fractions

For further functional characterization of the recombinant Pem-AGO fusion protein with mRNA cleavage assay, the recombinant proteins was preferable to be expressed in the soluble form. After small scale expression of the BL21(DE3)pLysS/pET-15b/*Pem-ago* clone at 25^{o}C with 0.1 mM IPTG for 2 hr, 0.25 OD_{600} cells were harvested and lysed by sonication or French Pressure. Three fractions inducing whole cells, inclusion pellet and supernatant were first analyzed by SDS-PAGE followed by Western Blot analysis. The results indicated that the recombinant Pem-AGO proteins predominantly existed in the inclusion fraction but were not detectable in the soluble fraction (figure 7.11). This is probably due to the low amount of the recombinant protein. However, this experiment was confirmed by Dot Blot analysis. The result revealed the recombinant Pem-AGO fusion protein was presented in the soluble fraction (figure 7.12), though at lower level comparing with the protein in the inclusion.

(A) SDS-PAGE (B) Western Blot

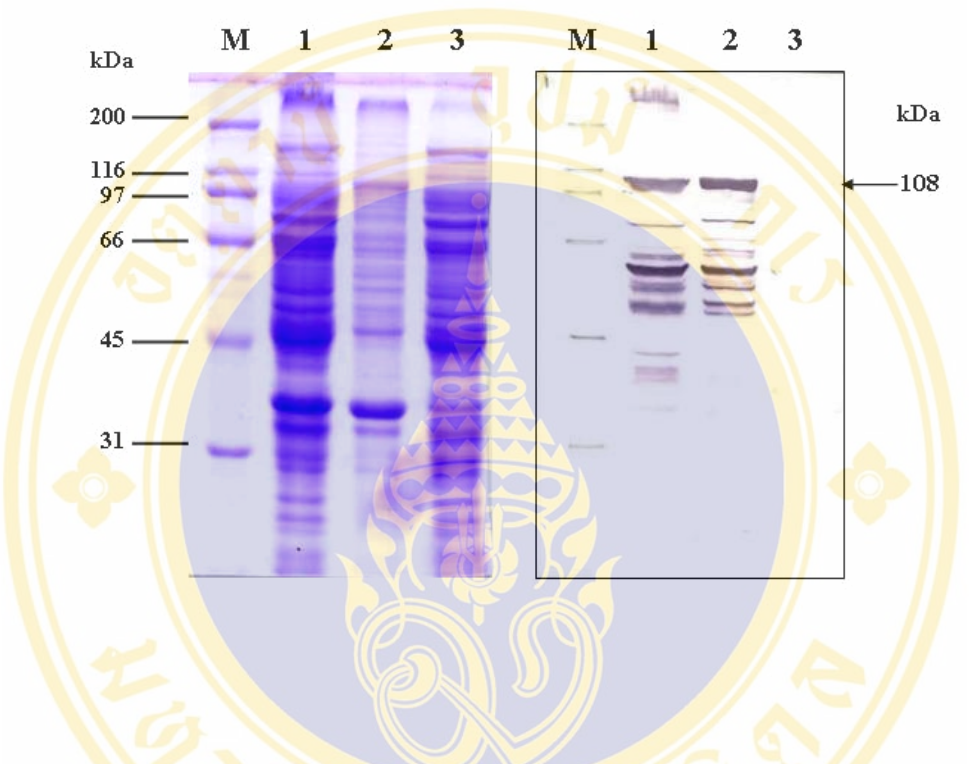

Figure 7.11 SDS-PAGE and Western Blot analysis of Pem-AGO fusion protein in inclusion and soluble fractions

The figures indicate SDS-PAGE (A) and Western Blot analysis (B) of BL21(DE3)pLysS/pET-15b/*Pem-ago* expression in three different fractions; whole cells, inclusion and supernatant at 25^{o}C with 0.1 mM IPTG for 2 hr.

Lane M : Standard broad range protein marker

Lane 1 : Crude cell lysate (whole cell fraction)

Lane 2 : Inclusion pellet fraction

Lane 3 : Supernatant fraction

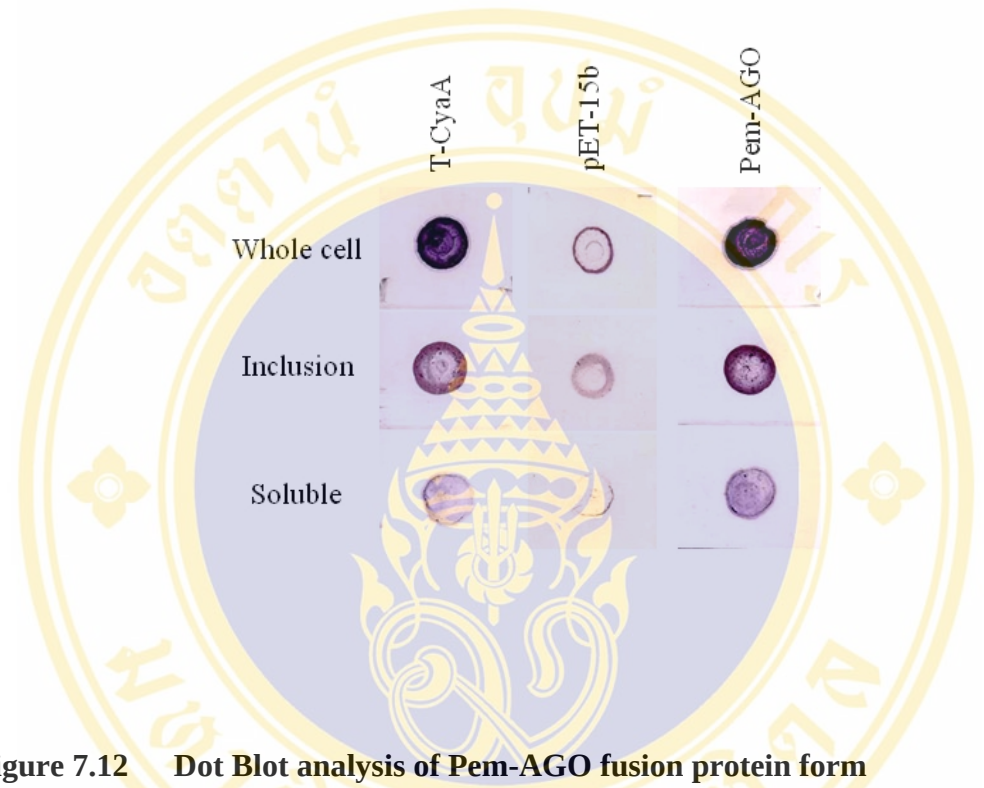

Figure 7.12 Dot Blot analysis of Pem-AGO fusion protein form

The figures represent Dot Blot analysis of BL21(DE3)pLysS/pET-15b/*Pem-ago* expression from, whole cells, inclusion and supernatant at 25^{o}C with 0.1 mM IPTG for 2 hr

T-CyaA indicates protein fraction from BL21(DE3)pLysS/pET-15b/T-CyaA

pET-15b indicates protein fraction from BL21(DE3)pLysS/pET-15b

Pem-AGO indicates protein fraction from BL21(DE3)pLysS/pET-15b/*Pem-ago*

7.4 Expression of the Recombinant PAZ Domain in *E. coli* Strain BL21(DE3)pLysS

The recombinant PAZ domain was also designed to be expressed in *E. coli* strain BL21(DE3)pLysS as N-terminal hexahistidine tagged in soluble form. The expression was performed with the same strategies as the experiment of recombinant Pem-AGO.

7.4.1 Optimization of the Expression Period of the PAZ Domain Protein from pET-15b Recombinant Plasmid in *E. coli* Strain BL21(DE3)pLysS

In order to obtain the satisfactory amounts of recombinant PAZ domain protein, three positive clones of BL21(DE3)pLysS/pET-15b/*PAZ* were selected to optimize the expression condition by comparing the amount of expressed protein at the period of expression between 7 hr and overnight at 30 ^{o}C with 1 mM IPTG induction. The results in figure 7.13 illustrated that the expression level of the target protein from all three clones were presented at the expected size of 19 kDa with no difference in the yield. However, at the 7 hr incubation time, the culture provided higher purity of the expected recombinant protein than overnight culture due to the presence of another extra band at higher molecular weight at overnight expression condition in all three clones as detected by Western Blot analysis.

7.4.2 Optimization of the Expression Temperature and IPTG Concentration of the PAZ Domain in *E. coli* Strain BL21(DE3)pLysS

The result from figure 7.13 indicates that expression of the recombinant PAZ domain for 7 hr gave a major band of His-fusion proteins and the expression level was not different among the three positive clones. Then one clone, clone no. 1 was selected for further optimization to obtain suitable expression condition by comparing the expression level between 25^{o}C and 30^{o}C and IPTG concentration from 0.1, 0.4 and 1.0 mM. The expression level was detected by performing Western Blot analysis with anti-His antibody. After 7 hr of induction, the results illustrated that the expression levels of PAZ domain protein that were induced with 0.1, 0.4 and 1 mM IPTG were not significant different at both 25^{o}C and 30^{o}C (figure 7.14). Therefore, the expression

condition at 25°C with 0.1 mM IPTG for 7 hr induction was employed for expression of the recombinant PAZ domain protein.

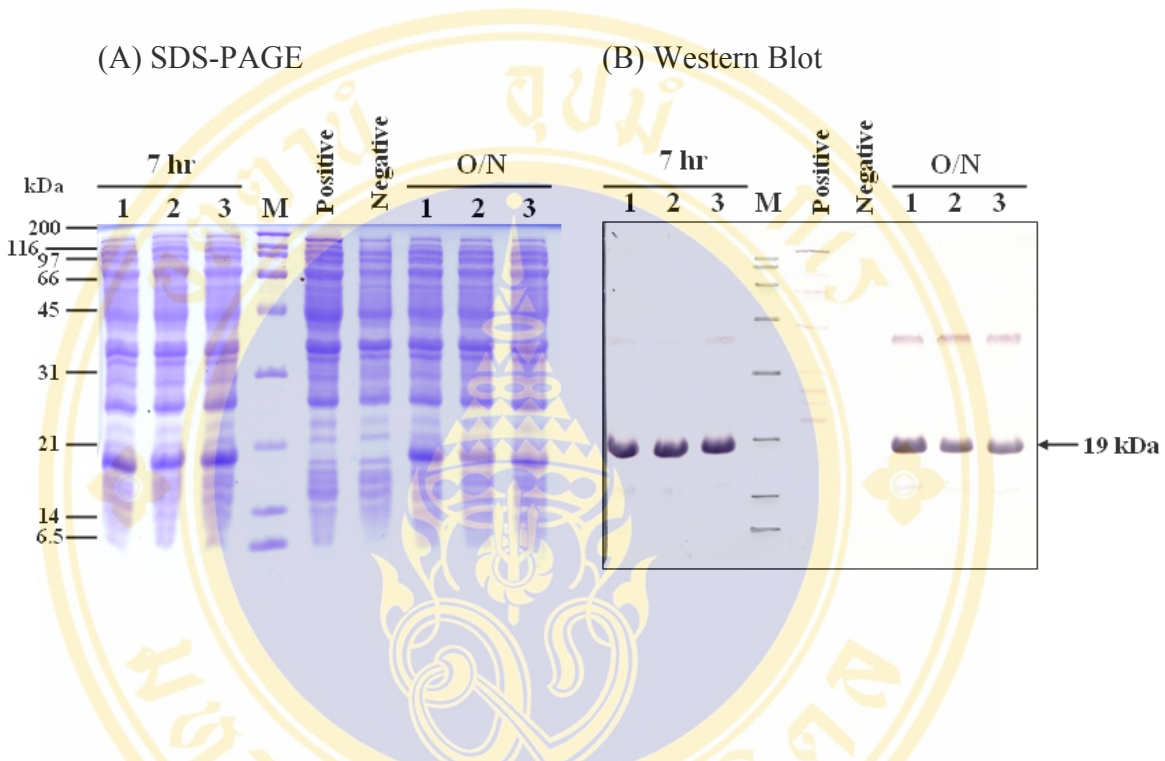

Figure 7.13 SDS-PAGE and Western Blot analysis of recombinant PAZ domain expression at different period of incubation time

The figures show the SDS-PAGE (A) and Western Blot (B) (15% SDS-PAGE with anti-His antibody) of the crude cell lysate from BL21(DE3)pLysS/pET-15b/*PAZ* clone no.1 to 3 at 25°C with 1 mM IPTG induction by compare the expression level at the different period of expression between 7 hr and overnight (O/N).

Lane M : Standard broad range protein marker

Positive : Crude cell lysate from BL21(DE3)pLysS/pET-15b/T-CyaA (Positive control of T-cyaA protein expression)

Negative : Crude cell lysate from from BL21(DE3)pLysS/pET-15b (Negative control of protein expression)

The numbers in each lane indicates the selected positive clone number.

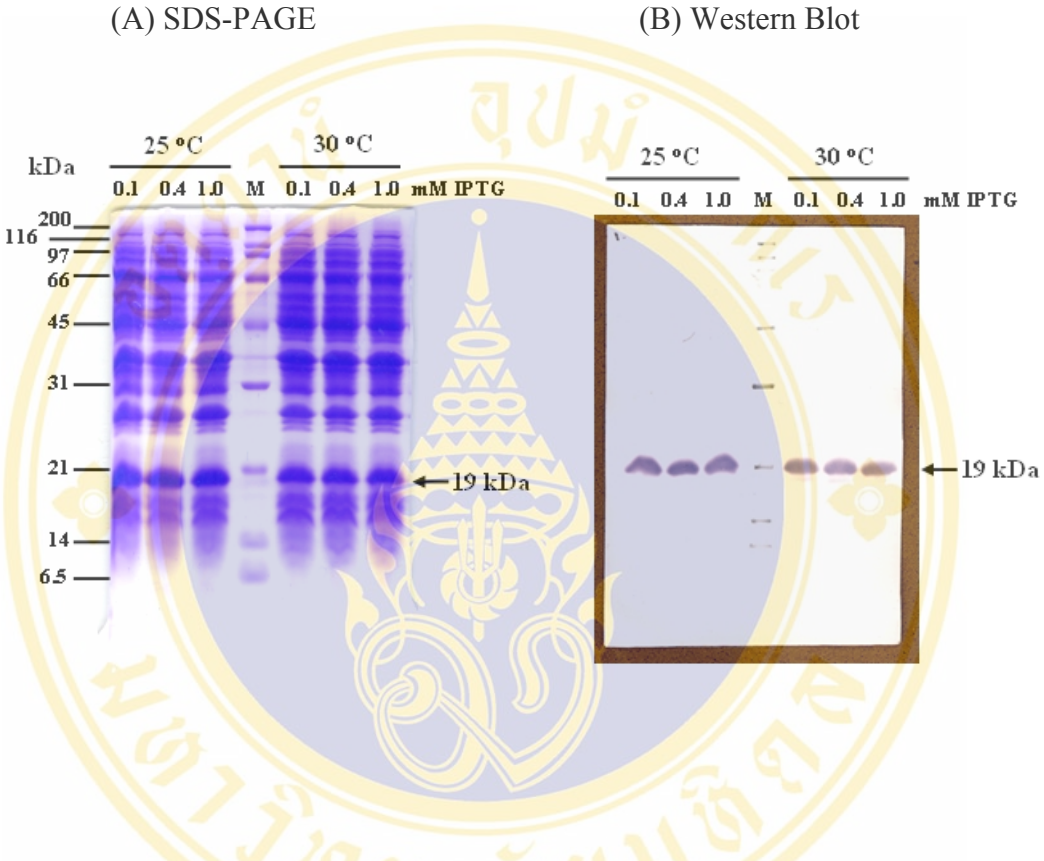

Figure 7.14 SDS-PAGE and Western Blot analysis of recombinant PAZ domain expression at the various temperature and IPTG concentration

The figures illustrate SDS-PAGE (A) and Western Blot (B) analysis (15% SDS-PAGE with anti-His antibody) of the crude lysate from BL21(DE3)pLysS/pET-15b/*PAZ* at 25°C and 30°C with various IPTG concentration from 0.1, 0.4 and 1.0 mM

Lane M : Standard broad range protein marker

7.4.3 Determination of the Recombinant PAZ Domain Protein in Inclusion and Soluble Fractions

In order to determine the recombinant PAZ expression form, BL21(DE3)pLysS/pET-15b/*PAZ* clone was culture in LB broth containing 100 μg/ml before induction with 0.1 mM IPTG at 25^{o}C for 7 hr. Subsequently, the cells were subjected to lysis by sonication or French Pressure as described for the recombinant Pem-AGO. Then, whole cells, inclusion pellet and supernatant were analyzed by Western Blot and Dot Blot analysis. The Western Blot analysis showed that the recombinant PAZ was obviously presented in inclusion pellet fraction and could not be observed in supernatant fraction (figure 7.15). However, the result of Dot Blot analysis revealed that a small amount of the recombinant PAZ domain fusion protein was presented in the soluble fraction (figure 7.16).

(A) SDS-PAGE (B) Western Blot

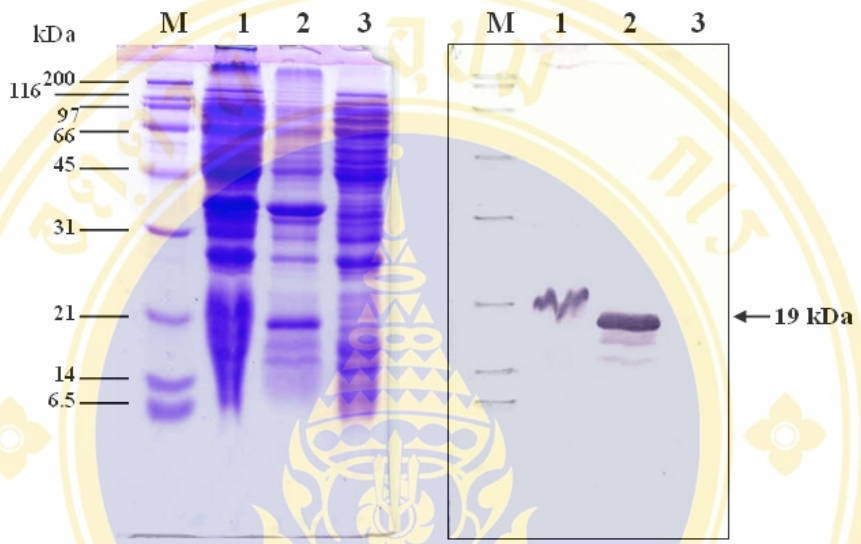

Figure 7.15 SDS-PAGE and Western Blot analysis of recombinant PAZ domain fusion protein in inclusion and soluble fractions

The figures represent 15% SDS-PAGE (A) and Western Blot analysis (B) of BL21(DE3)pLysS/pET-15b/*PAZ* expression from whole cell, inclusion and supernatant at 25^{o}C with 0.1 mM IPTG for 7 hr.

Lane M : Standard broad range protein marker

Lane 1 : Crude cell lysate (whole cell fraction)

Lane 2 : Inclusion pellet fraction

Lane 3 : Supernatant fraction

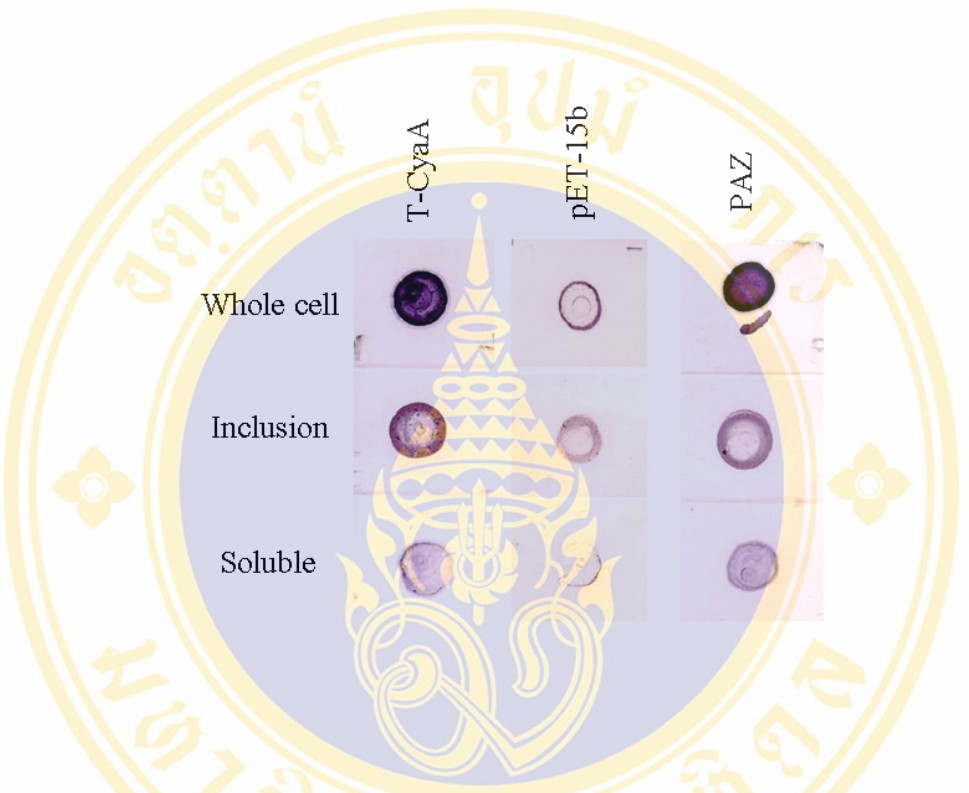

Figure 7.16 Dot Blot analysis of recombinant PAZ domain fusion protein

The figure reveals Dot Blot analysis of BL21(DE3)pLysS/pET-15b/*PAZ* expression from, whole cell, inclusion and supernatant at 25^{o}C with 0.1 mM IPTG for 7 hr.

T-CyaA indicates protein fraction from BL21(DE3)pLysS/pET-15b/T-CyaA

pET-15b indicates protein fraction from BL21(DE3)pLysS/pET-15b

PAZ indicates protein fraction from BL21(DE3)pLysS/pET-15b/*PAZ*

7.5 Purification of the Recombinant Pem-AGO and Recombinant PAZ Domain Proteins

The overnight culture of the recombinant clones of *E. coli* BL21(DE3)pLysS containing pET-15b/*Pem-ago* (clone no. 3)or pET-15b/*PAZ* (clone no. 1) plasmids was transferred to a new 750 ml of LB broth containing 100 μg/ml ampicillin to yield the final dilution of 1:100 followed by incubation at 37°C for an additional time until cell density of the culture reached the mid log phase (OD_{600} approximately 0.5-0.6). Recombinant protein expression was induced by adding IPTG into final concentration of 0.1 mM and further incubated at 25°C with shaking for 2 hr (Pem-AGO) or 7 hr (PAZ). After harvested the cells by centrifugation, the cell pellet was disrupted twice by French Pressure. Subsequently, the soluble and insoluble fractions were separated by centrifugation.

7.5.1 Purification of Recombinant AGO Fusion Protein Under Native Condition by Immobilized Affinity Column (IMAC)

The soluble Pem-AGO recombinant protein harboring the hexahistidine tag fused to the N-terminus was purified under native conditions by Ni^{2+} affinity chromatography, employing the HisTrap™ FF crude column (Amersham) (method 5.13). The supernatant fraction was loaded onto the equilibrated column. Then, non-specific binding proteins were subsequently removed by washing the column with buffer H containing 30 mM imidazole. The fusion protein was eluted by applying buffer H containing the gradient of imidazole from 100, 200, 300, 400 and 500 mM, respectively. The fractions were collected and subsequently analyzed by SDS-PAGE with Coomassie staining. The expected protein band of Pem-AGO could be observed at 108 kDa in the 5th to 10th elution fractions with the highest yield of target protein in fraction 7. However, additional protein bands at the lower molecular weight were also co-eluted in these fractions (figure 7.17). From Western Blot analysis, many bands could be detected by anti-PAZ antibody (lane 2) and anti-His antibody (lane 3) (figure 7.18). The smaller bands might be the truncated products at the C-terminus of the recombinant Pem-AGO.

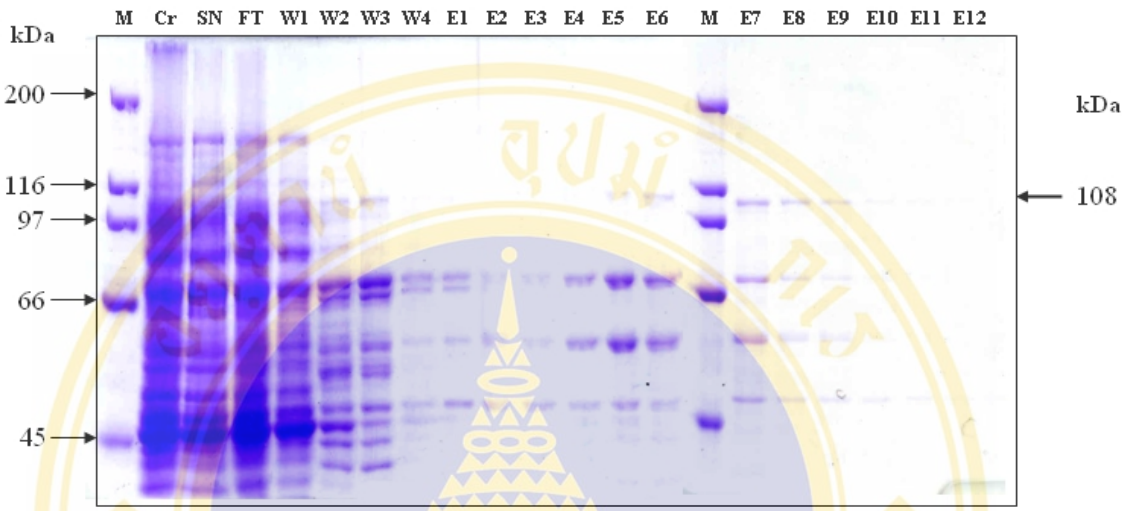

Figure 7.17 SDS-PAGE analysis of purification profile of the recombinant Pem-AGO under native condition by Ni^{2+} affinity chromatography

The figure illustrates the SDS-PAGE profile (Coomassie staining from 8% SDS-PAGE) of the purification of recombinant BL21(DE3)pLysS containing pET-15b/*Pem-ago* under native condition by affinity chromatography utilizing imidazole gradient step elution.

Lane M : Standard broad range protein marker

Lane Cr : Crude cell lysate from BL21(DE3)pLysS/pET-15b/*Pem-ago*

Lane SN : Supernatant fraction before loading onto the column

Lane FT : Flow-through fraction containing unbound protein

Lane W1-W4: Wash fractions 1 to 4 (buffer H + 30 mM imidazole)

Lane E1-E12 : Elution fractions 1 to 12 (buffer H + 100-500 mM imidazole)

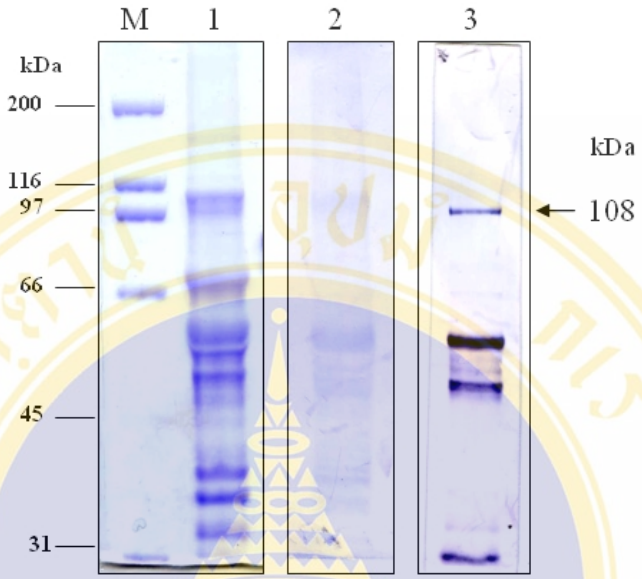

Figure 7.18 Western Blot analysis of the Ni^{2+} affinity chromatography purified recombinant Pem-AGO

The figures show the 10% SDS-PAGE (lane 1) and Western Blot analysis with anti-PAZ (lane 2) and anti-Histidine (lane3) of the eluted recombinant Pem-AGO from Ni^{2+} affinity chromatography.

Lane M : Standard broad range protein marker

Lane 1 : Eluted recombinant Pem-AGO after purification by Ni^{2+} affinity chromatography detected by Coomassie blue staining

Lane 2 : Eluted recombinant Pem-AGO after purification by Ni^{2+} affinity chromatography detected with anti-PAZ antibody

Lane 3 : Eluted recombinant Pem-AGO after purification by Ni^{2+} affinity chromatography detected with anti-His antibody

7.5.2 Purification of Recombinant PAZ domain Under Native Condition by Immobilized Affinity Column (IMAC)

The soluble recombinant PAZ domain protein harboring the hexahistidine tag fused to the N-terminus was purified under native conditions by Ni^{2+} affinity chromatography with the same strategies as the recombinant Pem-AGO as described previously. The fractions were collected and subsequently analyzed by SDS-PAGE with Coomassie staining. The expected protein band of PAZ fusion protein could be observed at 19 kDa in the 4^{th} to 16^{th} elution fractions. However, it was co-eluted with other proteins of both high and lower molecular weight (figure 7.19). The Western Blot analysis with anti-PAZ (lane 2) and anti-His antibody (lane 4) was performed to confirm the recombinant PAZ domain protein and the results implied that only the expected band around 19 kDa could be detected by anti-PAZ antibody. However, this experiment also produced signal in the negative control at the same position of the recombinant protein. For result that using anti-His antibody, not only signal at the 19 kDa could be detected, it also represented the signal at about 38 kDa while the signal from other protein bands was not detectable (figure 7.20).

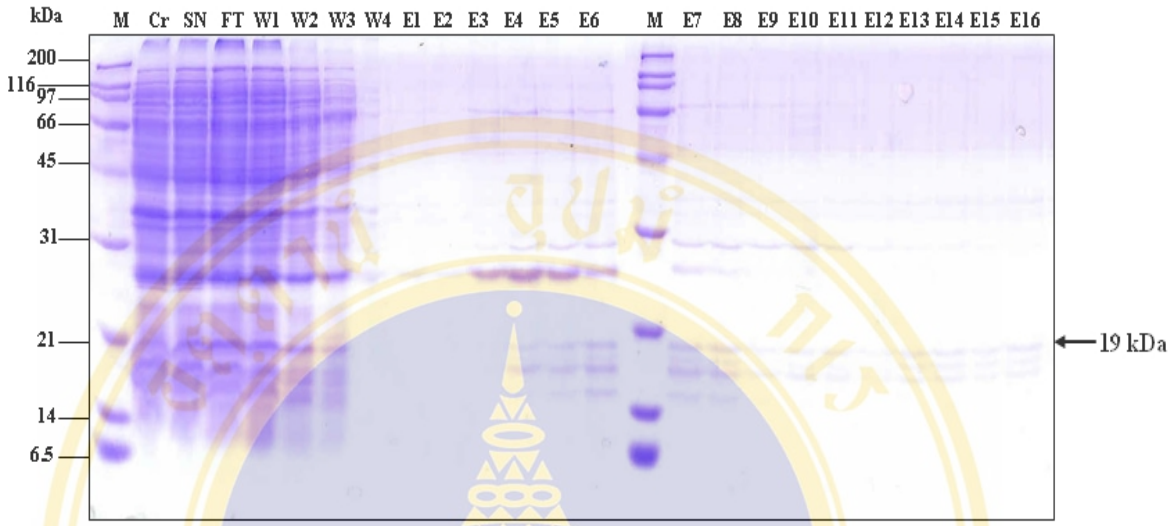

Figure 7.19 SDS-PAGE analysis of purification profile of the recombinant PAZ under native condition by Ni^{2+} affinity chromatography

The figure reveals the SDS-PAGE profile (Coomassie staining from 15% SDS-PAGE) of the purification of recombinant BL21(DE3)pLysS containing pET-15b/ PAZ under native condition by affinity chromatography utilizing imidazole gradient step elution.

Lane M : Standard broad range protein marker

Lane Cr : Crude cell lysate from BL21(DE3)pLysS/pET-15b/ PAZ

Lane SN : Supernatant fraction before loading onto the column

Lane FT : Flow-through fraction containing unbound protein

Lane W1-W4: Wash fractions 1 to 4 (buffer H + 30 mM imidazole)

Lane E1-E16 : Elution fractions 1 to 16 (buffer H + 100-500 mM imidazole)

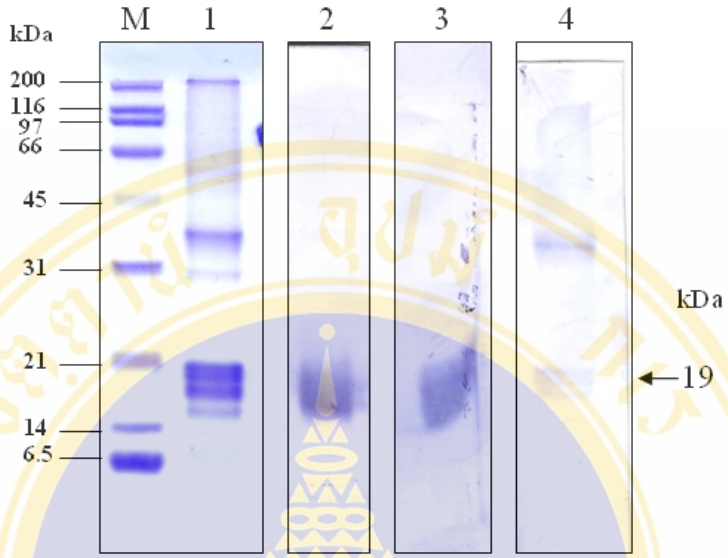

Figure 7.20 Western Blot analysis of the Ni^{2+} affinity chromatography purified recombinant PAZ

The figures illustrate the 15% SDS-PAGE (lane 1) and Western Blot analysis with anti-PAZ (lane 2) and anti-Histidine (lane 4) of the elution fraction after purification of recombinant BL21(DE3)pLysS containing pET-15b/*PAZ* under native condition by affinity chromatography.

Lane M : Standard broad range protein marker

Lane 1 : Eluted recombinant PAZ after purification by Ni^{2+} affinity Chromatography detected by Coomassie blue staining

Lane 2 : Eluted recombinant PAZ after purification by Ni^{2+} affinity Chromatography detected with anti-PAZ antibody

Lane 3 : Negative control detected with anti-PAZ antibody

Lane 4 : Eluted recombinant PAZ after purification by Ni^{2+} affinity Chromatography detected with anti-His antibody

7.6 Stability of the Recombinant Proteins When Exposed to Different Temperatures

The stability of the recombinant protein was tested at different temperatures. The purified recombinant proteins were incubated at several temperatures, -20°C, 4 °C, 25°C and 37°C for 4 hr. Subsequently, the recombinant proteins was visualized by Western Blot. The results showed that after 4 hr incubation time at the mentioned temperatures the amount of recombinant proteins were not significantly different for both recombinant Pem-AGO (figure 7.21) and PAZ domain (figure 7.22)

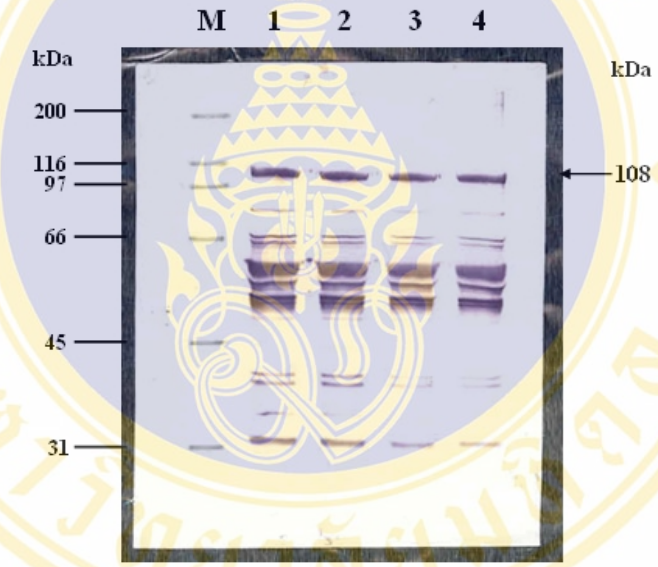

Figure 7.21 Western Blot analysis with anti-His antibody of the recombinant Pem-AGO after incubating at various temperatures for 4 hr.

Lane M : Standard broad range protein marker

Lane 1 : Purified Pem-AGO protein after incubated at -20°C

Lane 2 : Purified Pem-AGO protein after incubated at 4°C

Lane 3 : Purified Pem-AGO protein after incubated at 25°C

Lane 4 : Purified Pem-AGO protein after incubated at 37°C

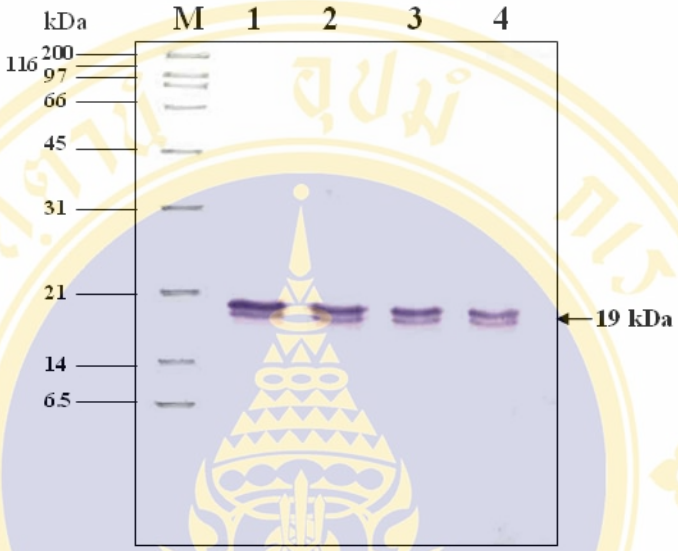

Figure 7.22 Western Blot analysis of the recombinant PAZ with anti-His antibody after incubating at various temperatures for 4 hr.

Lane M : Standard broad range protein marker

Lane 1 : Purified PAZ protein after incubated at -20^{o}C

Lane 2 : Purified PAZ protein after incubated at 4^{o}C

Lane 3 : Purified PAZ protein after incubated at 25^{o}C

Lane 4 : Purified PAZ protein after incubated at 37^{o}C

7.7 Electrophoretic Mobity Shift Assay (EMSA)

The RNA-binding function of the *P. monodon*'s PAZ domain protein was investigated by incubation of the purified recombinant PAZ protein with ^{32}P-labeled siRNA which was 21 nt sense-strand GFP. Subsequently, the shift band of RNA-protein interaction complex was analyzed by Electrophoretic Mobity Shift Assay (EMSA) on native polyacrylamide gel before visualized by autoradiography.

7.7.1 Optimization of the Amount of PAZ Protein in the Reaction

The amount of purified recombinant PAZ domain protein for the reaction was adjusted from 100 to 500 ng with 1 pmole of ^{32}P-labeled GFP-siRNA. The reaction was analyzed by TBE-native polyacrylamide gel before visualized by autoradiography. After 7 days exposure time, the shifted band of PAZ-RNA complex compared to the free probe could be observed. The intensity of the shifted band was increased according to the amount of purified recombinant PAZ domain protein in the reaction. The shifted band could not be observed in the absence of recombinant PAZ domain protein (figure 7.23).

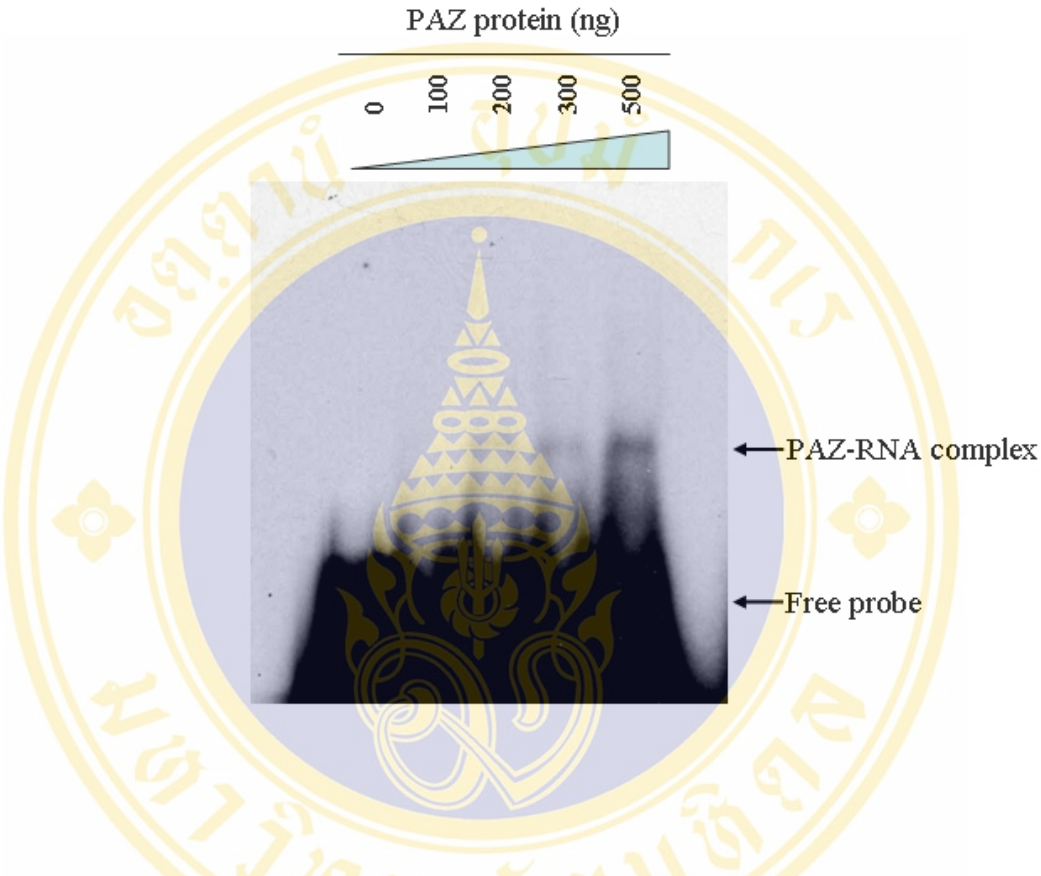

Figure 7.23 RNA Electrophoretic Mobility Shift Assay of *P. monodon*'s PAZ domain protein.

The figure illustrates RNA electrophoretic mobility shift assay of *P. monodon*'s PAZ domain protein. Approximately 1 pmole of ^{32}P-labeled GFP siRNA was incubated with various amount of recombinant *P. monodon*'s PAZ domain protein. The Protein-RNA complex was analyzed on 5% naitve polyacrylamide gel and visualized by autoradiography. The amount of recombinant PAZ domain protein is indicated above each lane.

7.7.2 Determination of specific RNA-Binding Activity of the Recombinant PAZ domain Protein

In order to investigate the characteristic of binding function of the PAZ domain, substrate specificity was performed by adding the excess amount of unlabeled competitors, which are ssRNA, dsRNA and ssDNA, into the reactions. The interaction between competitor and PAZ domain protein will compete for the binding of ^{32}P-labeled GFP-siRNA-PAZ complex. Therefore, the intensity of the shifted band should decrease proportional to the amount of competitor-PAZ formed in the reaction. However, if the competitor could not bind to PAZ protein, the intensity of shifted band would not be different when compared to the reaction not containing competitor. Competitors in the reaction composed of, ssRNA which was the unlabeled 21 nt GFP-sense-stranded RNA, dsRNA was unlabeled duplex of 21 nt GFP which was similar in the sequences to ^{32}P-labeled GFP-siRNA and ssDNA was 21 nt oligonucleotides containing unrelated sequence. The amount of competitor was varied from 50 to 200 folds excess comparing to the ^{32}P-labeled GFP-siRNA. The results in figure 7.24 indicated that the recombinant PAZ domain preferentially bind to RNA than DNA as the the intensity of the shifted band reduced gradually when higher amount of RNA competitor, both single and double-stranded, was added to the reaction, whereas the signal of the shifted band in the reaction containing DNA competitor was not different from the reaction without competitor. In addition, comparing between ssRNA and dsRNA, the ssRNA seemed to be more efficient in competing the binding reaction than dsRNA.

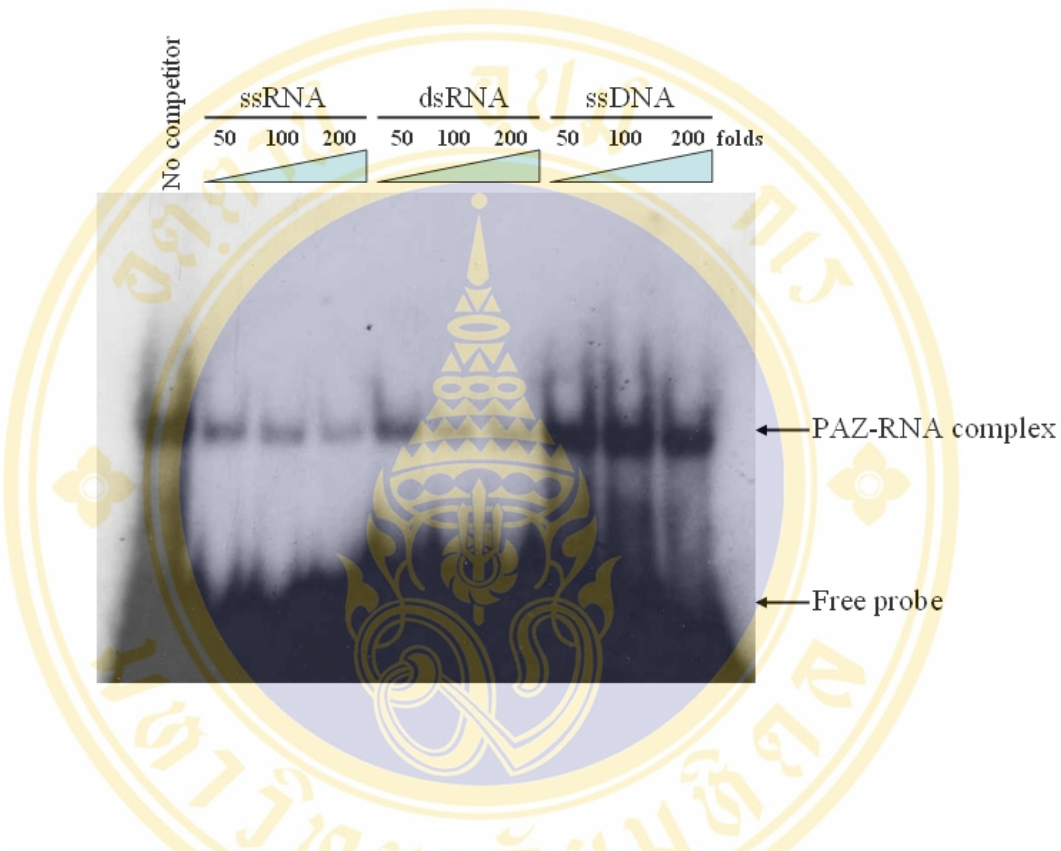

Figure 7.24 RNA electrophoretic mobility shift assay assessing RNA binding of *P. monodon's* PAZ domain in the presence of competitors

The figure illustrates RNA electrophoretic mobility shift assay of *P. monodon*'s PAZ domain protein in the presence of competitor. The number indicated the molar excess of each competitor, which are ssRNA, dsRNA and dsRNA, in the reactions.

7.7.3 Determination of the Protein that Binds to RNA by Supershift EMSA

To characterize the specific protein that binds target ssRNA, the antibody was added into the reaction to identify the protein in the RNA-protein complex. The antibody will bind to the specific protein in the complex and retards the mobility of this complex, causing the effect called “supershift”. On the other hand, binding of antibody to the protein may disrupt the protein:RNA interaction resulting in loss of the shift characteristic.

In this study, the recombinant PAZ domain protein was expressed as hexahistidine fusion protein that can be recognized by either anti-His antibody or anti-PAZ antibody. Anti-FMDV is the unrelated antibody to the PAZ domain that was used to prove specificity of the reaction. The results in the presence of anti-PAZ and anti-His antibody at the final dilution of 1:500 and 1:1,000 showed the loss in the shifted band of RNA-protein complex, whereas the lower titers of antibody did not significantly disrupted the complex. By contrast, the anti-FMDV did not seem to have effect on the protein-RNA complex.

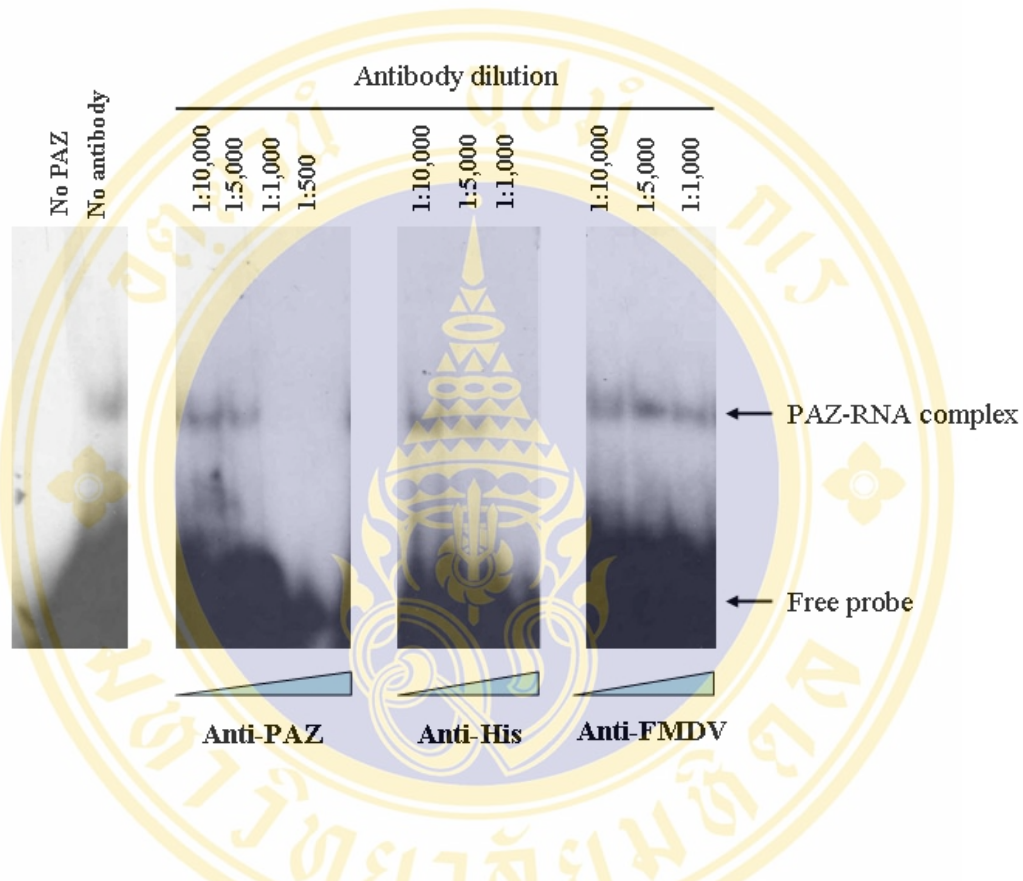

Figure 7.25 Supershift of RNA electrophoretic mobility shift assay assessing RNA binding of *P. monodon's* PAZ domain in the presence of antibodies.

The figure illustrates supershift RNA electrophoretic mobility shift assay of *P. monodon*'s PAZ domain protein in the presence of anti-PAZ, anti-His and anti-FMDV. The number indicated the final dilution of antibody in the reaction.

7.8 Determination of RISC Activity of Recombinant Pem-AGO by mRNA Cleavage Assay

RISC is responsible for the function of siRNA-speccific mRNA cleavage. The reaction was conducted in the presence of siRNA harboring complementary sequence to the target mRNA. The sense-stranded GFP RNA of 251 nt that was derived from *in vitro* transcription was employed as cleavage substrate. An antisense-stranded GFP (21 nt that harboring dTdT at 3' end) siRNA was incubated with Pem-AGO protein in order to allow the association between siRNA and Argonaute protein prior to incubation with *in viro*-transcribed sense-stranded GFP RNA (251 nt) in the presence of ATP, GTP and RNase inhibitor. The siRNA recognized GFP transcript at the position where the cleavage by Argonaute would produce the cleavage products of 116 and 135 nt, respectively. The cleavage products were analyzed by RNA formaldehyde gel electrophoresis compared to the standard RNA marker and visualized under UV light.

The reactions were set by utilizing shrimp's lymphoid extract protein instead of Pem-AGO as a positive control (lane 2) of the reaction. Additionally, negative control was performed in various conditions: using purified fraction of the expressed product form pET-15b vector alone (lane 3); no addition of protein (lane 4); no addition of antisense-siRNA (lane 5); and the presence of sense-GFP siRNA instead of antisense-GFP siRNA (lane 6) as illustrated in figure 7.27.

The result in figure 7.27 revealed that the smaller product of approximately 111 nt was observed as a faint band in the reaction (lane 1). However, this pattern was also present in negative controls employing purified pET-15b protein instead of Pem-AGO (lane 3) and in other reactions that also contained Pem-AGO protein (lanes 5 and 6) but the pattern could not observed in the reaction into which Pem-AGO was not added (lane 4). Moreover, the positive control in this experiment using crude protein extract of lymphoid organ did not produce the cleavage products at the expected size. The result therefore indicated that the cleavage reaction was not successful and the smaller band observed in the reactions containing recombinant Pem-AGO was probably due to the nucleic acid of *E. coli* that contaminated in the expression and purification steps.

Figure 7.26 ***in vitro*** **Transcription of sense-GFP**

This figure reveals 1.8% agarose gel electrophoresis of *in vitro* transcription of sense-stranded GFP RNA (lane 1) compared to the 100 bp + 1.5 kb DNA ladder marker (M).

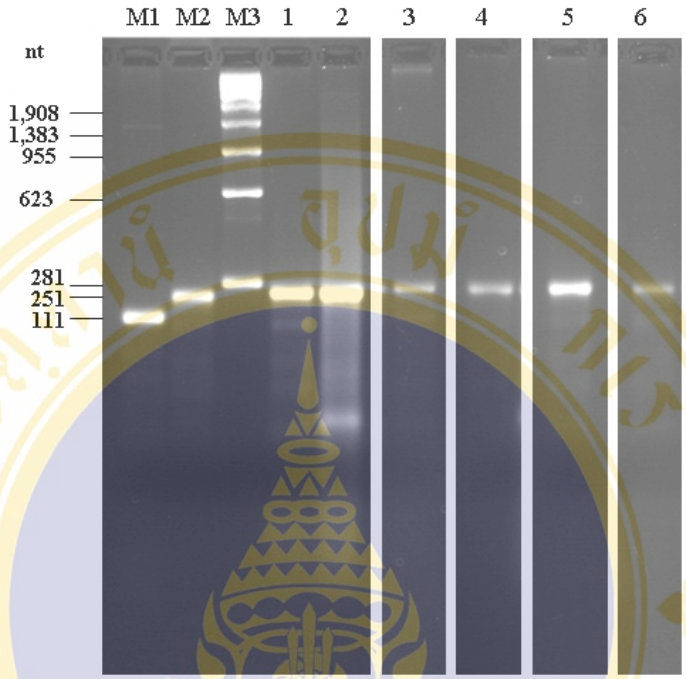

Figure 7.27 mRNA cleavage assay of the Pem-AGO

This figure reveals 2.5% RNA formaldehyde agarose gel electrophoresis of mRNA cleavage assay.

Lane M1 : single-stranded RNA 111 nt

Lane M2 : single-stranded RNA 251 nt

Lane M3 : RNA marker

Lane 1 : mRNA cleavage reaction with recombinant Pem-AGO and GFP antisene siRNA

Lane 2 : reaction with lymphoid's crude extract instead of Pem-AGO

Lane 3 : reaction with purified pET-15 expressed protein instead of Pem-AGO

Lane 4 : reaction in the absence of Pem-AGO

Lane 5 : Negative control (absence of antisense-siRNA)

Lane 6 : Negative control (presence sense-siRNA instead of antisense-siRNA)

CHAPTER VIII
DISCUSSION

Argonaute is the key component of RISC, the effector complex in RNAi pathway. Argonaute family proteins are multidomain molecules composed of two conserved regions, PAZ and PIWI domains. Argonaute plays an important role in several pathways including siRNA and miRNA pathways to regulate gene expression and involved in development, respectively. One biological function of RNAi pathway is to act as an adaptive immune system against viral infection. Black tiger shrimp or *Penaeus monodon* is the economically important marine animal which is also affected by viral infection as a major problem. The understanding of RNAi in shrimp will be the crucial knowledge for employing this mechanism as a strategy for viral prevention in this economic animal (Tirasophon *et al*., 2005).

P. monodon's Argonaute gene (*Pem-ago*) is 2,829 nucleotides in length that encodes 942 amino acid residues of Pem-AGO protein with the molecular weight approximately 105 kDa and pI of 9.36. The PAZ domain of *Pem-ago* is 417 nucleotides encoding 139 amino acid residues PAZ protein with approximately 16 kDa and pI of 9.62 (Calculated from http://us.expasy.org).

1. Expression in *Pichia pastoris* System

Preliminary studies of Argonaute protein function in *Drosophila* have been performed by utilizing eukaryotic system (Hammond *et al*., 2001; Williams *et al*., 2002), especially in insect cell culture which is rather complicated and expensive. In order to obtain the recombinant protein for biochemical function study of the recombinant Pem-AGO and its PAZ domain in this project, the experiment was first designed to express the recombinant proteins in yeast expression system by employing *Pichia pastoris* strain KM71, which is the higher eukaryotic expression system that provides protein processing, protein folding and posttranslational modification (Gurkan *et al.,* 2005; Invitrogen Pichia Expression Kit Manual Version E). In

addition, yeast has rapid growth rate, can facilitate to scale-up without loss of yield, is easy to manipulate and is less expensive to use than other eukaryotic expression system. Moreover, *P. pastoris* provides high level of secreted protein expression into culture medium as biologically active form that is useful for purification step (Invitrogen Pichia Expression Kit Manual Version E). Therefore, *Pichia* was firstly selected for expression of Argonaute protein and PAZ domain protein.

1.1 Construction of *P. monodon*'s Argonaute (*Pem-ago*) and *PAZ* Domain Protein Expression in Plasmid pPICZαA Vector

The minimal *KEX2* cleavage sequence (excluded Glu-Ala repeats) that showed efficient secreted expression of *P. monodon*'s recombinant peptide hormones (Eurwilaichitr *et al*., 2002; Yodmuang ,2003) was added into forward primers next to the *Xho* I site to provide the cleavage site in order to remove the signal sequence and secrete the recombinant protein into the culture medium. In addition, to minimize the extra amino acid in the recombinant protein as well as to eliminate c-myc epitope from the C-terminal hexahistidine tag fusion protein, *Sal* I was added in reverse primers.

The restriction digestion patterns of some recombinant pPICZαA/*Pem-ago* clones with the cloning enzymes (*Xho* I and *Sal* I; figure 6.6) and internal enzymes (*Xmn* I and *Dra* I; figure 6.7) were not correlated. For instance, clone 224 did not release the insert fragment when digested with cloning enzymes but gave correct pattern of internal digested products as well as correct sequence of the insert *Pem-ago* cDNA (figure 6.12 and 6.13). This is probably because of the compatible sequence between *Xho* I and *Sal* I that were used in the cloning step. The clone 224 might result from the ligation of *Xho* I and *Sal* I between the vector and the insert fragment in inverted orientation that can joined together but the ligated site cannot be digested with either of the enzymes.

In the screening results of recombinant pPICZαA/*PAZ* with *Xho* I and *Sal* I digestion, the positive clones should provide the digested products of insert fragment at 417 bp and pPICZαA vector at 3.6 kb. However, clones no. 27 and 72 gave the digested products of the insert fragment at approximately 800 bp. This might occur from self-ligation between two insert fragments by the compatible sequence of *Xho* I and *Sal* I before insertion into the vector. Subsequently, the sequences of five and

three positive clones of pPICZαA/*Pem-ago* and pPICZαA/*PAZ* were verified by DNA sequencing analysis and illustrated the 100 % identity to the original template.

1.2 Expression of the recombinant *PAZ* in *P. pastoris* system

The expression in *P. pastoris* was induced by methanol under the control of *AOX1* promoter. The expression conditions were optimized in small scale 1 ml culture medium at general expression condition under 1 % (v/v) methanol induction at 30°C for 5 days. The expression of recombinant PAZ protein (approximately 17 kDa) could not be observed by SDS-PAGE analysis from supernatant culture medium. This could be explained by several possibilities as follows: the PAZ protein was expressed at low level; the condition of expression was not suitable; the secretion of the protein may not be successful. The detail of each possibility was discussed below.

First, the expression level of the recombinant PAZ protein was so low that could not be detected by SDS-PAGE with Coomassie staining. From the results in figure 6.16, only 20 µl of supernatant were analyzed by SDS-PAGE. To solve this problem, 1 ml of the culture medium after induction was concentrated by TCA prior to SDS-PAGE analysis. However, no clear recombinant protein band was observed.

Second, the period of expression was not suitable. The time of induction also influence the expression level as demonstrated in protein Der p3.1 which was used as positive control for *Pichia* expression in this experiment. To determine the time suitable for high expression level, the recombinant protein was expressed at different period of induction. At the condition of 3 % (v/v) methanol induction at 30°C, the amount of the expressed Der p3.1 protein was highest on day 3. The degradation of protein could be observed when expressed longer than 3 days. In addition, the protein expressed for longer period was also contaminated with more host secreted proteins. However, in case of the expression from five recombinant clones containing KM71/pPICZαA/*PAZ* expression cassette, the pale band at 17 kDa were observed in every clone, especially in clone 2 and 3, on day 1and 2 before disappearing on day 3 to 5. Similar pattern of the reduction in the amount of proteins at longer period of expression was also observed in the negative control. However, the high expression level was still not achieved.

Third, the concentration of methanol for induction also affects expression level (Invitrogen Pichia Expression Kit Manual Version E). This occurrence was displayed in positive control, protein Der p3.1. The level of expressed Der p 3.1 increased with the higher concentration of methanol. After optimization of the percentage of methanol induction from 0 to 5 %, however, the PAZ protein could not be observed in both supernatant and crude cell lysate at every methanol concentration.

Finally, the disruption of secretion step of the recombinant protein may result in the presence of the expressed protein in the intracellular compartment. The construct in this study was engineered by adding only the minimal *KEX2* cleavage sequence (excluding the double Glu-Ala repeats) in the forward primer to facilitate the secretion of recombinant protein. The double Glu-Ala repeats enhance the removal of α-factor secretion signal by Kex2 protease, and it is further cleaved by Ste13 enzyme (Romanos *et al.,* 1995; Cereghinno and Cregg, 2000). Although secretion of the recombinant protein in the absence of the double Glu-Ala repeats could be successful (Treerattrakool *et al.,* 2002), the possibility that double Glu-Ala repeats may be necessary for cleavage by Kex2 enzyme in certain cases may not be excluded. In addition, the tertiary structure of the recombinant protein may protect the cleavage site from the cleavage by KEX2 (Cereghinno and Cregg, 2000). In order to prove whether the recombinant PAZ, existed as intracellular protein, Western Blot analysis with anti-His antibody that recognized hexahistidine tag at the C-terminus of the recombinant protein was performed in crude cell lysate. However, the signal could not be observed whereas positive control for Western blot (Cathecolamine Acetyl Transferase (CAT) protein containing histidine tag at N-terminus) was detected at the expected size (figure 6.17) suggesting that no recombinant PAZ protein was present in the intracellular compartment. This implies that the PAZ recombinant protein could not be expressed or expressed at undetectable low level in *P. pastoris*. The explanation could be as follows:

1) Intracellular expression occurs in the cytoplasmic compartment which also contains many host proteases (Li Z *et al.*, 2001) and PAZ protein might be susceptible to degradation by host proteases.

2) Codon usage difference between organisms. It has been suggested that using yeast codon usage may enhance the expression of foreign gene in *P. pastoris*

(Eurwilaichitr L *et al*., 2002; Yadava A and Ockenhouse CF, 2003; Jean-Marc D *et al*., 2005). Whether or not this is the case for unsuccessful expression of the PAZ domain of Pem-AGO, the presence of PAZ transcript should be investigated in recombinant *P. pastoris.*

3) The premature termination in yeast that occur due to the AT-rich region (Henikoff and Cohen, 1984; Scorer *et al*., 1993) that is also present in *P. monodon*'s Argonaute gene.

In order to verify these possibilities, RT-PCR or Northern Blot analysis should be performed to check the transcript.

Recently, there is the study demonstrating that recombinant human Argonaute2 protein could be expressed in *Escherichia coli* system and provided the recombinant soluble protein that possessed the activity of RISC (Rivas FV *et al*., 2005). From this reason, the expression system for Pem-AGO and its PAZ domain was altered from *P. pastoris* to *E. coli* system by applying pET-15b as expression vector in order to construct the recombinant protein as hexahistidine fusion protein at N-terminus. *E. coli* strain BL21(DE)pLysS was selected as expression host, this strain is deficient in the *lon* protease and lack *ompT* protease that can degrade proteins during purification. Additionally, it also contains pLysS plasmid containing chloramphenicol antibiotic resistance marker and low lysozyme accumulation in the host that is useful for the stability of the expressed protein (Baneyx F, 1999, Novagen Corporation. pET system manual).

2. Expression in *Escherichia coli* System

2.1 Expression of the Recombinant Pem-AGO Protein in *E. coli* Strain BL21(DE3)pLysS

According to the expression conditions from Rivas FV *et al*., 2005 that provided the substantial recombinant human Argonaute 2 protein in soluble form, six recombinant BL21(DE)pLysS/pET-15b/*Pem-ago* clones were expressed with 1 mM IPTG overnight at 25^{o}C. This recombinant Pem-AGO was expressed as the N-terminal hexahistidine tag fusion protein with the molecular weight 107.5 kDa and pI of 9.39 (Calculated from http://us.expasy.org). The expression level of Pem-AGO from crude

lysate could not be detected from SDS-PAGE analysis. However, in the analysis by Western Blot with anti-His antibody the expression of the protein at the expected size 108 kDa, for the recombinant Pem-AGO protein was observed. The expression level varied among different clones with the highest level in clone 3 and 4. Additionally, anti-His antibody could detect other protein bands at lower molecular weight in every clone. The presence of these smaller protein bands was probably due to the primary structure of Argonaute protein that might contain the cleavage sites which can be recognized by host proteases. Therefore, these smaller bands might be the C-terminal truncated products from proteolysis by endogenous bacterial proteases. Another possibility that it might be the products form premature translation termination at the rarely used codons as could be examined form http://gcua.schoedl.de/sequential.html. From the result, Pem-AGO represented 79 positions of significant number of codons rarely used in *E. coli* (less than 10 %). It is possible that ribosomal slippage may occur at these rarely used codes, resulting in frame-shifts and premature termination of translation when out-of-frame termination codons are encountered (Arakaki *et al*., 2002). An attempt to identify all impurities via N- or C-terminal amino acid sequencing was not conducted in this study. The recombinant human Argonaute2 that expressed in *E. coli* system was also co-purified with some other low molecular weight proteins (Rivas *et al*., 2005). The experiment in which Pem-AGO was expressed for different period of time indicated that the amount of the expected product at 108 kDa was decreased in longer period of induction. It is possible that Pem-AGO protein was sensitive to host proteases, therefore it could be degraded at longer incubation time (Gottesman, 1996).

2.2 Expression of the Recombinant PAZ Domain in *E. coli* Strain BL21(DE3)pLysS

The functional study of PAZ domain has been reported in *Drosophil*a. The *Drosophil*a's PAZ recombinant protein was also expressed in *E. coli* expression system with N-terminal His10-tagged protein that was subsequently cleaved away and the recombinant protein still possessed the activity of RNA-binding domain (Yan, 2003). In this study, the recombinant PAZ domain was constructed and engineered similarly to the recombinant Pem-AGO. The recombinant PAZ domain was expressed

as the N-terminal hexahistidine tag fusion protein with the molecular weight 18.8 kDa and pI of 9.64 (Calculated from http://us.expasy.org). The results suggested that optimal condition for *P. monodon*'s PAZ domain protein expression is 25 ^{o}C for 7 hr with 0.1 mM IPTG, which exhibited the highest yield of the expected 19 kDa protein band with the lowest amount of other proteins.

2.3 Purification of the Recombinant Pem-AGO and Recombinant PAZ Domain Proteins

Although the recombinant Pem-AGO and PAZ domain proteins were expressed predominantly in inclusion fractions, the inclusion proteins need more complicated steps of solubilization and renaturation to convert the protein folding into a biochemically active form. To avoid these problems in the re-folding step, the recombinant protein in soluble fraction was used instead of the inclusion in further steps, although the yield of soluble recombinant proteins was much lower than the inclusion. The proteins in the soluble fraction were further purified by Ni^{2+} column chromatography that specifically binds to metal ion including histidine tagged protein. Then, the trapped protein can be eluted by imidazole which acts as competitor of the binding protein.

In order to improve the purity of the purified protein and to minimize binding of host cell proteins, low concentration of imidazole was also added into the binding buffers. In addition, the purity of the eluted protein can be improved by performing stepwise imidazole elution (Biswas *et al.,* 1995) by gradually increase the imidazole concentration from 100 mM to 500 mM in the elution step since the one step elution with 500 mM imidazole provided high amount of impurity proteins due to non-specific binding (data not shown).

For Pem-AGO, the soluble fraction was used for Ni^{2+} column chromatography purification, yielding about 0.2 mg/L of the purified protein. The pattern of the purification displayed the protein bands corresponding to molecular weights of 108, 70, 60 and 50 kDa in the elution fractions 5 to 10 (Figure 7.17). The Pem-AGO protein at 108 kDa represented the highest yield in elution fraction 7. This fraction is therefore selected for further biochemically characterization by mRNA cleavage assay. The recombinant Pem-AGO in the purified fraction was confirmed by Western Blot

analysis with anti-PAZ antibody and anti-His antibody. The results indicated the signal at the expected size at of 108 kDa. However, both antibodies also recognized the other lower molecular weight proteins at the lower molecular weight. This result indicated that all four bands in the purified fraction contain the PAZ domain and thus suggested that the purified Histidine-tagged Pem-AGO was probably subjected to protease cleavage (figure 7.18). Additionally, anti-His antibody produced stronger signal than the anti-PAZ antibody.

For the PAZ domain protein, the yield of the purified protein was approximately 1.5 mg/L. The expected PAZ protein was detected in elution fractions 4 to 16 (figure 7.19). The highest yield and more purity fraction (elution fraction 15) was subjected to further experiment on siRNA-binding property. In addition, the other protein products were also co-eluted into the purified fraction. However, only the expected size of 19 kDa was specifically detected by anti-PAZ antibody. Unexpectedly, the negative control (the proteins from the clone containing pET15-b vector alone) also showed the signal at similar size. The explanation is probably because anti-PAZ antibody was induced in mouse by using the protein band which was excised from SDS-polyacrylamid gel at expected size of the PAZ domain, 19 kDa. This band might contain other proteins expressed from the vector that located at similar position. The signal from anti-His antibody, however, revealed the faint bands at both 19 kDa and 40 kDa, which may indicated that the 40 kDa protein was not related to PAZ.

Although the Ni^{2+} column purified proteins displayed some impurity, the recombinant proteins were not subjected to further purification steps in order to prevent further loss of the proteins due to the low yield of the target protein in the eluted fractions.

2.4 Functional Characterization of the Recombinant *P. monodon*'s PAZ Domain by Electrophoretic Mobility Shift Assay

PAZ domain is an evolutionarily conserved region found in both Dicer and Argonaute family protein which are the essential components of RNAi pathway (Yan *et al*., 2003). Previous studies on biochemical function assay as well as elucidation of the crystal structure have exhibited that this domain is responsible for RNA-binding in

a sequence-independent manner (Song *et al*., 2003; Yan *et al*., 2003; Lingel A *et al*., 2003; Collin *et al.,* 2005; Carmell *et al.,* 2004; Cerutti *et al.,* 2000). In this study, to investigate the biochemical function of *P. monodon*'s PAZ domain, Electrophoretic Mobility Shift Assay (EMSA) (www.nature.com/nmeth/journal/v2/n7/full/nmeth0705-557.html), one of the most sensitive methods for studying the DNA- or RNA-binding properties of a protein, was applied by utilizing siRNA corresponding to GFP sequence that was labeled at 5' end with [γ-^{32}P]ATP. The result in figure 7.23 demonstrated that recombinant PAZ domain was able to bind the 21 nt sense-stranded GFP RNA as presented by the retarded labeled-RNA band. The protein-RNA complex formation was dependent on the amount of recombinant PAZ protein in the reaction. This result may imply that the recombinant PAZ domain protein from soluble fraction was expressed and folded in the correct conformation providing the oligo-binding (OB) fold which is consisted of a six-stranded β-barrel capped by two a-helices and an αβ module on the N- and C terminus (Ma *et al*., 2004) to retain the RNA-binding activity.

The substrate binding specificity of the PAZ domain could be elucidated by competitor mobility shift assay (Singh H *et al*., 1986; Burafowski S and Chodosh LA, 1996) by adding unlabeled RNA or DNA competitors into the reactions. The binding efficiency of the recombinant PAZ domain protein to ssRNA (21nt containing dTdT at 3' end corresponding to sense stranded-GFP sequence) was analyzed by adding three types of competitors in the reactions, unlabeled ssRNA which possess the similar sense stranded-GFP sequence, unlabeled dsRNA which was the similar GFP sequence harboring dTdT overhang at 3' end and unlabeled ssDNA which containing unrelated sequence to sense stranded-GFP. At 50 molar excess comparing to the labeled GFP RNA, the unlabeled RNA competitors, both single- and double-stranded, could compete the binding between the PAZ domain protein and the labeled GFP RNA as shown by the reduction in the signal of protein-RNA complex comparing with the complex formed in the absence of competitor. The formation of the complex between PAZ domain and the labeled RNA was inversely proportional to the amount of unlabeled competitors added. This result indicated that recombinant PAZ domain of Pem-AGO possessed the activity to bind 21 nt siRNA. In addition, unlabeled ssRNA competitor seemed to compete with the complex formation between the PAZ domain

and GFP RNA probe more efficiently than the dsRNA competitor. However, this result was not obviously observed, therefore in order to compare the binding efficiency between ssRNA and dsRNA, the amount of competitors in the reactions should be varied until cover the range that will show the clear result. The binding of ssRNA compared to dsRNA has reported in PAZ domain from *Drosophila* Ago 1 that also exhibited more efficient binding to ssRNA than dsRNA (Yan *et al*., 2003). However, the PAZ domain of *Drosophila* Ago 2 displayed equal binding between ssRNA and dsRNA (Song *et al*., 2003). Moreover, unlabeled DNA competitor failed to compete with the binding of the recombinant PAZ domain from *P. monodon* to ssRNA even at the amount of 200 molar excess. Theses results were consistent to the previous reports in PAZ domain of *Drosophila* Ago 1 and human Piwi-like 1 PAZ domain (Yan *et al.,* 2003; Carmell *et al.,* 2004). However, this result was not in concurrence with the PAZ domain of *Drosophila* Ago 2 that exhibited similar relative affinity to both ssRNA and dsDNA (Lingel *et al*., 2003). Moreover, the *Drosophila* Ago 2 PAZ could also bind either single-stranded or double-stranded DNA which may suggested its function in regulation gene expression by binding RNA or DNA (Lingel *et al*., 2003).

To address whether the recombinant PAZ domain was really participated in the protein-RNA complex formation, antibody supershift assays (Kristie TM and Roizman B., 1986, Burafowski S and Chodosh LA, 1996) with specific and non-related antibodies to the recombinant PAZ domain protein were applied. The disappearance of the shifted band was observed when either anti-His antibody or anti-PAZ antibody were added to the reaction. Although the addition of the antibody did not result in further retardation of the complex, or supershfit, as expected, it is possible that the specific binding of antibody to the protein may disrupt the protein:RNA interaction resulting in the loss of the characteristic shift (Buratowski S and Chodosh LA., 1996). However, the amount of free RNA probe was reduced in the reaction upon the addition of anti-His or anti-PAZ antibodies indicating that the protein-RNA complex was formed. Similar evidence of the undetectable ribonucleoprotein complex from EMSA has been mentioned and discussed on *Drosophila* Ago 1 PAZ domain (Yan *et al*., 2003) that was due to the high isoelectric point of the PAZ protein (approximately 9.5) which is too positively charged to migrate towards the positive electrode in

EMSA. However, this occurrence also depends upon the buffer applied in the reaction (Yan *et al.,* 2003). It is therefore possible that the antibody-protein-RNA complex formed in this study may possess high positive charge and thus did not migrate toward the positive electrode but rather migrate to opposite direction. However, from Western Blot analysis, anti-PAZ and anti-His antibodies also could recognize other proteins in the purified PAZ protein as shown in figure 7.20. So, the possibility that other *E. coli* proteins that were co-purified with recombinant PAZ may contribute to the RNA-binding activity could not be excluded. However, the specificity of PAZ domain binding was supported by employing unrelated antibody, anti-FMDV antibody, which was also raised by using the recombinant protein expressed in *E. coli* as the antigen, instead of specific antibody. It demonstrated that anti-FMDV did not affect the binding of PAZ-RNA complex indicating that the protein in the complex should be the recombinant PAZ domain. These results imply that the histidine-tagged recombinant PAZ domain protein from Pem-AGO function as RNA-binding domain, which is the important step for the function of RNAi pathway.

2.5 Functional Characterization of Recombinant *P. monodon*'s Argonaute Protein

Argonaute protein family is the core component of RISC that plays an important role in RNAi and leads to the cleavage of homologous mRNA, which is the characteristic of siRNA pathway to regulate gene expression or by translation inhibition that is involved in the developmental control in miRNA pathway (Rivas *et al*., 2005; Rand *et al*., 2004; Liu *et al*., 2004; Traci M and Tanaka H, 2005).

The slicer activity of the recombinant human Argonaute 2 protein that was derived from *E. coli* expression system has been reported and demonstrated. Only Argonaute protein and siRNA could form minimal RISC that accurately cleaves cognate RNAs (Rivas *et al.*, 2005). To investigate the slicer activity of Pem-AGO in the cleavage of the target mRNA in the presence of specific-siRNA, mRNA cleavage assay was applied by utilizing the purified recombinant histidine-tag Pem-AGO and 251 nt RNA sequence corresponding to the sense-stranded GFP obtained from *in vitro* transcription as a substrate in the reaction. The reaction contained antisense GFP siRNA that will complementarily binds to the GFP transcript substrate. In the presence

of the Argonaute protein, it should trigger the cleavage of the substrate to give specific cleavage products.

Crude protein extract from shrimp lymphoid organ, the source from which the cDNA encoding Pem-AGO was cloned (Dechkla M., M.Sc. thesis, Mahidol University, 2006), was used as positive control reaction. The reaction was expected to produce the cleavage products of 116 and 135 nt from the 251 nt substrate. Although we can observed the faint band located near the expected size of the cleavage products when compare to the 111 nt standard RNA in the reaction containing purified fraction of the recombinant Pem-AGO and antisense GFP siRNA, this pattern also occured in the negative control reactions that contained the purified pET-15b protein instead of the Pem-AGO, or in the absence of the siRNA as well as when the sense-siRNA was used instead of the antisense-siRNA. However, this pattern could not be observed in the negative control reaction into which no protein was added. This data suggested that the band at approximately 111 nt was not the specific cleavage product from the siRNA-triggered Argonaute's endonuclease activity, and was probably the nucleic acid from the *E. coli* host for the recombinant protein expression.

The unsuccessful mRNA cleavage assay could be explained by the following possibilities. The reaction setting may not be appropriate for the cleavage activity. Since mRNA cleavage assay to determine the activity of Argonaute protein from different sources also used different conditions (Rivas *et al.,* 2005; Andersson MG *et al.,* 2005; Liu *et al*., 2004). It is possible that the Pem-AGO may require specific condition for its cleavage activity: for example, the salt concentration, the requirement of ATP, or it may require more factors or components for cleavage activity.

However, the crude protein extract from lymphoid organ, which was used as a positive control of this experiment also did not produce the cleavage products at the expected size. Since there is no information on the amount of the Argonaute in the cells, it is possible that there is not enough Argonaute protein in the lymphoid extract to provide the detectable activity. This was supported by the Western Blot result with anti-PAZ antibody in which the expected Argonaute could not be observed in the lymphoid protein extract. However, the SDS-PAGE analysis of shrimp's lymphoid extract illustrated two major protein bands located at approximately 70 to 80 kDa (Appendix 1). These might be the two subunits of hemocyanin that plays an important

role in shrimp innate immune response against viruses (Zhang *et al*., 2004). To address this problem, the suitable control should be prepared. As the previous study showed that Argonaute protein was associated with ribosomal protein (Ishizuka A *et al.*, 2002), to acquire the Argonaute protein, the sample might be purified from the ribosomal fraction. Soluble RISC from the ribosome-bound protein in the lysate could be recovered by concentrating the ribosome pellet via high speed centrifugation prior to extraction with high concentration of salts (Hammond *et al.,* 2001).

Another possibility that still needs conclusive proof is that Pem-AGO may not be involved in siRNA pathway but functions in miRNA pathway that affects the target mRNA by inhibition of translation, not the cleavage of specific mRNA. The major function of Argonaute in miRNA pathway is responsible for the developmental control. In *Drosophila*, only Argonaute 2 has been shown biochemically to be involved in siRNA pathway that can function as slicer. The *Drosophila* Ago2 contains aspartate-aspartate-histidine catalytic site that is essential for the cleavage of the target mRNA that harbor complementary sequence to siRNA (Liu J *et al.*, 2004; Hammond SM *et al.,* 2001; Rand TA *et al.,* 2004; Rivas *et al*., 2005; Rand TA *et al.*, 2005). By contrast, Argonaute 1 which did not exhibit the endonuclease activity and represent incomplete aspartate-aspartate-histidine catalytic site is responsible for developmental control and plays an important role in microRNA pathway (Williams RW and Rubin GM, 2002; Rivas *et al*., 2005). In order to enhance this evidence, the amino acid sequence from *Drosophila* Ago 1 and Ago 2 were aligned with Pem-AGO. The alignment results demonstrated that *Drosophila* Ago 1 and Pem-AGO shared 77.2 % identity (Appendix 2) whereas alignment of *Drosophila* Ago 2 and Pem-AGO exhibited only 21.8 % identity (Appendix 3). In addition, the complete catalytic motif aspartate-aspartate-histidine could not be found in Pem-AGO (Appendix 2). Therefore, it is possible that this Pem-AGO may involve in microRNA pathway. However, the appropriate positive control in the mRNA cleavage assay is necessary to demonstrate the clear result prior to interpretation of this hypothesis.

Although the biochemical activity of *Penaeus monodon*'s Argonaute protein cannot be summarized in this study whether it can function as a slicer or not, the Electrophoretic Mobility Shift Assay (EMSA) of the PAZ domain illustrated that the Pem-AGO contains the function of RNA-binding protein which is the distinct

characteristic of RISC in RNAi pathway. To determine whether Pem-AGO functions in siRNA or miRNA pathway, both the transcript and the protein levels of particular gene product that is subjected to silencing by corresponding dsRNA should be investigated in the cells that are depleted for Pem-AGO.

CHAPTER IX
CONCLUSION

1. The expression cassettes for recombinant protein expression of *P. monodon*'s Argonaute protein (Pem-AGO) and PAZ domain protein (pPICZαA/*Pem-ago* and pPICZαA/*PAZ*, respectively) in *Pichia pastoris* were constructed in pPICZαA vector.

2. pPICZαA/*PAZ* was transformed into *P. pastoris* strain KM71. The colony PCR analysis of the transformed clones indicated stable integration of the recombinant plasmid in the *Pichia* genome.

3. The expression of the recombinant PAZ domain could not be detected in both intracellular and extracellular compartment by Western Blot analysis with anti-His antibody under various expression conditions with the induction with 0-5 % methanol for the period of 0-5 days.

4. The recombinant Pem-Ago and PAZ domain was successfully expressed as N-terminal hexahistidine fusion tagged protein under the control of IPTG induction from pET-15b vector in *E. coli* strain BL21(DE3)pLysS. The majority of the recombinant proteins were expressed as inclusion.

5. Expression of recombinant Pem-AGO could be detected in Western Blot analysis utilizing anti-His antibody with the optimum conditions at 25 ^{o}C with 0.1 mM IPTG induction for 2 hours and the recombinant protein could be obtained from soluble fraction.

6. Expression of recombinant PAZ domain protein of *Peaneus monodon* could be detected in both SDS-PAGE and Western Blot analysis utilizing anti-His antibody

with the optimum conditions at 25 ^{o}C with 0.1 mM IPTG induction for 7 hours and the recombinant protein was present in soluble fraction.

7. The soluble fractions of both recombinant Pem-AGO and PAZ domain protein were purified by Ni^{2+} affinity chromatography with stepwise imidazole elution yielding the amounts of Pem-AGO and PAZ domain protein approximately 0.2 and 1.5 mg/L, respectively.

8. Biochemical function of the recombinant PAZ domain was accomplished by Electrophoretic Mobility Shift Assay (EMSA) that revealed the function of RNA-binding domain. Moreover, the presence of competitors of unlabeled ssRNA, dsRNA, and ssDNA, suggested that PAZ domain of Pem-AGO preferentially binds to RNA over DNA, and may bind to ssRNA more efficiently than to dsRNA.

9. Biochemical function of Pem-AGO in siRNA pathway was elucidated by mRNA cleavage assay. The assay did not show the RNA cleavage activity of the recombinant Pem-AGO. However, the positive control also did not give cleavage products, which is probably due to the small amount of Pem-AGO in the lymphoid crude protein extract that was used as the positive control or the condition of the reaction was not appropriate. Therefore, it could not be summarized whether Pem-AGO can function as a slicer or not.

10. The amino acid sequence of PemAGO exhibits higher level of similarity to *Drosophila* Ago 1 which plays the role in microRNA pathway than to *Drosophila* Ago 2 that involve in siRNA pathway. In addition, the complete aspartate-aspartate-histidine catalytic motif for endonuclease activity was not found in Pem-AGO. Therefore, this evidence may support the function of Pem-AGO in miRNA pathway.

11. The results in this study demonstrated that the PAZ domain of Pem-AGO exhibits the function of RNA-binding protein that is one crucial characteristic of RISC in RNAi pathway. Therefore, it suggested that Pem-AGO may involve in RNAi

pathway. However, the function of Pem-AGO in which siRNA or miRNA pathway needs to be elucidated.

REFERENCES

Agami R. RNAi and related mechanisms and their potential use for therapy. Curr Opin Chem Biol 2002; 6: 829-834.

Agrawal N, Dasaradhi PVN, Mohmmed A, Malhotra P, Bhatnagar RK, Mukherjee SK. RNA Interference: Biology, Mechanism, and Applications. Microbiol Mol Biol Rev 2003; 67: 657-685.

Almeida R, Allshire RC. RNA silencing and genome regulation. Trends Cell Biol 2005; 15: 251-258.

Ambros V. MicroRNA pathway in flies and worms: growth, death, fat, stress, and timing. Cell 2003; 113: 673-676.

Andersson MG, Haasnoot PCJ, XU N, Berenfian S, Berkhout B, Akusjarvi G. Suppression of RNA interference by Adenovirus Virus-associated RNAi. J Virol 2005; 79: 9556-9565.

Arakaki TL, Fang NX. Fairlie DP, Young PR, Martin JL. Catalytically active dengue virus NS3 protease forms aggregates that are separable by size exclusion chromatography. Protein Expr Purif 2002; 25: 241-247.

Aravin A, Tuschl T. Identification and characterization of small RNAs involved in RNA silencing. FEBS 2005; 579: 5830-5840.

Assavalapsakul W. Characterization of yellow head virus infection on lymphoid (Oka) organ primary cell culture of *Penaeus monodon*: Identification of a receptor protein. [P.hD. Thesis in Molecular Genetic-Genetic Engineering]. Bangkok: Faculty of Graduate Studies, Mahidol University; 2004

Aza-Blanc P, Cooper CL, Wagner K, Batalov S, Deveraux QL, Coke MP. Identification of modulators of TRAIL-induced apoptosis via RNAi-based phenotypic screening. Mol Cell 2003; 12: 627-637.

Bachere E. Introduction shrimp immunity and disease control. Aquaculture. 2000; 191: 3-11.

Baneyx F. Recombinant protein expression in *Escherichia coli*. Curr Opin Biotechnol 1999; 10: 411-421.

Bartel DP, Chen CZ. Micromanagers of gene expression: the potentially widespread influence of metazoan microRNAs. Nature 2004; 5: 396-400.

Bartel DP. MicroRNAs: genomics, biogenesis, mechanism, and function. Cell 2004; 116: 281-297.

Basyuk E, Suavet F, Doglio A, Bordonne R, Bertrand E. Human let-7 stem-loop precursors harbor features of RNase III cleavage products. Nucleic Acids Res 2003; 31: 6593-6597.

Baulcombe D. RNA silencing in plants. Nature 2004; 431: 356-363.

Bernstein E, Caudy AA, Hammond SM, Hannon GJ. Role for a bidentate ribonuclease in the initiation step of RNA interference. Nature 2001; 409: 295-296.

Blaszczyk J, Tropea JE, Bubunenko M, Routzahn KM, Waugh DS, Court DL, Ji X. Crystallographic and Modeling studies of RNase III suggest a mechanism for double-stranded RNA cleavage. Structure 2001; 9: 1225-1236.

Boonyaratpalin S, Kasornchandra J. Yellow-head disease in *Penaeus monodon*. National Institute of Coastal Aquaculture, Kaoseng, A.Muang, Songkhla.

Buratowski S, Chodosh LA. Mobility Shift DNA-Binding Assay Using Gel Electrophoresis. Curr Protocols in Molecularbiol 1996; 2: 12.2.1-12.2.11.

Carmell MA, Hannon GJ. RNase III enzymes and the initiation of gene silencing. Nat Struct Mol Biol 2004; 11: 214-218.

Cereghinno J, Cregg J. Heterologous protein expression in the methylotrophic yeast *Pichia pastoris*. FEMS Microbiol Rev 2000; 24: 45-66.

Cerutti HJ, Mollano AC. On the origin and functions of RNA-mediated silencing: from protists to man. Curr Gene 2006; 50: 81-99.

Cerutti L, Mian N, Bateman A. Domains in gene silencing and cell differentiation proteins: the novel PAZ domain and redefinition of the Piwi domain. Trends Biochem Sci 2000; 25: 481-482.

Chalfie M, Horvitz HR, Sulston JE. Mutations that lead to reiterations in the cell lineages of *C. elegans*. Cell 1981; 24: 59-69.

Chen CZ, Li L, Lodish HF, Bartel DP. MicroRNAs modulate hematopoietic lineage differentiation. Science 2004; 303: 83-86.

Chicas A, Macino G. Characteristics of post-transcriptional gene silencing. EMBO 2001; 2: 992-996.

Chiu YL, Rana TM. RNAi in human cells: basic structural and functional features of small interfering RNA. Mol. Cell 2002; 10: 549-561.

Cogoni C, Macino G. Post-transcriptional gene silencing across kingdoms. Curr Opin Gene Dev 2000; 10: 638-643.

Cold Spring Harbor Laboratory Press. Electrophoretic mobility shift assays. Nature methods 2005; 2: 557-558.

Cowley JA, Cadogan LC, Wongteerasupaya C, Hodgson RAJ, Boonsaeng V, Walker PJ. Multiplex RT-nested PCR differentiation of gill-associated virus (Australia) from yellow head virus (Thailand) of *Penaeus monodon*. J Virol Meth 2004; 117: 49-59.

Denli AM, Hannon GJ. RNAi: An ever-growing puzzle. Trends Biochem Sci 2003; 28: 196-201.

Destoumieux-Garzon D, Saulnier D, Garnier J, Jouffrey C, Bulet P, Bachere E. Crustacean immunity: antifungal peptides are generated from C terminus of shrimp hemocyanin in response to microbial challenge. J Biol Chem 2001; 276: 47070-47077.

Doench JG, Petersen CP, Sharp PA. siRNAs can function as miRNAs. Genes Dev 2003; 17: 438-442.

Dudley NR, Labbe JC, Goldstein B. Using RNA interference to identify genes required for RNA interference. Proc Natl Acad Sci USA 2002; 99: 4191-4196.

Elbashir SM, Lendeckel W, Tuschl T. RNA interference is mediated by 21- and 22-nucleotide intervals. Gene Dev 2001; 15: 188-200.

Englemann P, Cooper EL, Nemeth P. Anticipating innate immunity without a Toll. Mol. Immunol. 2005; 42: 931-942.

Eurwilaichitr L, Roytrakul S, Suprasongsin C, Manitchotpisit P and Panyim S. Glutamic acid and alanine spacer is not necessary for removal of MFα-1 signal sequence fused to the human growth hormone produced from Pichia pastoris. World Journal of Microbiology and Biotechnology 2002; 18: 493-498.

Fire A, Xu S, Montgomery MK, Kostas SA, Driver SE, Mello CC. Potent and specific genetic interference by double-stranded RNA in *Caenorhabditis elegans*. Nature 1998; 391: 806-811.

Flegel TW. Special topic review: major viral disease of the black tiger prawn (*Penaeus monodon*) in Thailand. World J. Microbiol Biotechnol 1997; 13: 433-442.

Geley S, Muller C. RNAi: ancient mechanism with a promising future. Experi Gerontol 2004; 39: 985-998.

Gottesman S. Protease and their targets in *Escherichia coli*. Ann Rev Genet. 1996; 30: 465-506.

Grewal SIS, Rice JC. Regulation of heterochromatin by histone methylation and small RNAs. Curr Opin Cell Biol 2004; 16: 230-238.

Grishok A, Pasquinelli AE, Conte D, Li N, Parrish S, Ha I, Baillie DL, Fire A, Ruvkun G, Mello CC. Gene and mechanisms related to RNA interference regulate expression of the small temporal RNAs that control *C. elegans* development timing. Cell 2001; 106: 23-34.

Gurkan C, Ellar DJ. Recombinant production of bacterial toxins and their derivatives in the methylotrophic yeast *Pichia pastoris*. Microbial Cell Fractories 2005; 4: 1-8.

Hall IM, Noma K, Grewal SI. RNA interference machinery regulates chromosome dynamics during mitosis and meiosis in fission yeast. Proc Natl Acad Sci USA 2003; 100: 193-198.

Hall TMT. Structure and function of Argonaute proteins. Structure 2005; 14: 87-96.

Hamilton A, Voinnet O, Chappell L, Baulcombe D. Two classes of short interfering RNA in RNA silencing. EMBO J 2002; 21: 4671-4679.

Hammond SM, Bernstein E, Beach D, Hannon GJ. An RNA-directed nuclease mediates post-transcriptional gene silencing in *Drosophila*. Nature 2000; 404: 293-296.

Hammond SM, Boettcher S, Caudy AA, Kobayashi R, Hannon GJ. Argonaute 2, a link between genetic and biochemical analyses of RNAi. Science 2001; 293 : 1146-1150.

Hammond SM. Dicing and Slicing The core machinery of the RNA interference pathway. FEBS 2005; 579: 5822-5829.

Han J, Lee Y, Yeom KH, Kim YK, Jin H, Kim VN. The Drosha-DGCR8 complex in primary microRNA processing. Genes Dev 2004; 18: 3016-3027.

Hannon GJ. RNA interference. Nature 2002; 418: 244-251.

He L, Hannon GJ. MicroRNAs: Small RNAs with a big role in gene regulation. Nature review 2004; 5: 522-531.

Holmquist GP, Ashley T. Chromosome organization and chromatin modification: influence on genome function and evolution. *Cytogenet Genome Res* 2006; 114(2): 96-125.

Hutvagner G, McLanchlan J, Pasquinelli AE, Balint E, Tuschl T, Zamore PD. A cellular function for the RNA-interference enzyme Dicer in the maturation of the let-7 small temporal RNA. Science 2001; 293: 834-838.

Invitrogen Corporation. *Pichia* Expression Kit Protein Expression: A Manual of methods for Expression of Recombinant Proteins in *Pichia pastoris* Catalog no. K1710-01. Version E: 1.

Invitrogen Corporation. pPICZαA, B and C: *Pichia* expression vectors for selection on Zeocin™ and purification of secreted, recombinant proteins Catalog no. v195-20. Version A.

Ishizuka A, Siomi MC, Siomi H. A *Drosophila* fragile X protein interacts with components of RNAi and ribosomal protein. Gene Dev 2002; 16: 2497-2508.

Ito M, Kawano K, Miyagishi M, Taira K. Genome-wide application of RNAi to the discovery of potential drug targets. FEBS 2005; 579: 5988-5995.

Jantama K. Cloning and characterization of the NS3 serine protease domain of dengue type 2 virus expressed in the yeast *Pichia pastoris*. [M.Sc. Thesis in Molecular Genetic-Genetic Engineering]. Bangkok: Faculty of Graduate Studies, Mahidol University; 2001

Jean-Marc D, Dannau M, Gilsoul JJ, Mejdoub TE, Destain J, Portetelle D, Thonart P, Haubruge E, Vandenbol M. Expression of a synthetic gene encoding a Tribolium castaneum carboxylesterase in *Pichia pastoris*. Protein Expr and Purif 2005; 42: 286-294.

Kavi HH, Fernandez HR, Xie W, Birchler JA. RNA silencing in *Drosophila*. FEBS 2005; 579: 5940-5949.

Ketting R, Haverkamp T. van Luenen H, Plasterk R. *mut-7* of *C. elegans*, required for transposon silencing and RNA interference, is a homolog of Werner syndrome helicase and RNaseD. Cell 1999; 99: 133-141.

Ketting RF, Fischer SE, Bernstein E, Sijen T, Hannon GJ, Plasterk RH. Dicer functions in RNA interference and in synthesis of small RNA involved in developmental timing in *C. elegans*. Genes Dev 2001; 15: 2654-2659.

Khvorova A, Reynolds A, Jayasana SD. Functional siRNAs and miRNAs exhibit strand bias. Cell 2003; 115: 209-216.

Kiatpathomchai W, Jitrapakdee S, Panyim S, Boonsaeng V. RT-PCR detection of yellow head virus (YHV) infection in *Penaeus monodon* using dried haemolymph spots. J. Virol Methods 2004; 119: 1-5.

Kim VN. MicroRNA biogenesis: coordinated cropping and dicing. Nature 2005; 6: 376-385.

Knight SW, Bass BL. A role for the RNase III enzyme DCR-1 in RNA interference and germ line development in *Caenorhabditis elegans*. Science 2001; 293: 2269-2271.

Kristie, TM, Roizman B. A4, the major regulatory protein of herpes simplex virus type 1, is stably and specifically associated with promoter-regulatory domains of a gene and/or selective viral gene. Proc Nat Acad Sci U.S.A. 1986; 83: 3218-3222.

Kurtz J, Franz K. Evidence for memory in invertebrate immunity. Nature 2003; 425: 37-38.

Lecellier CH, Dunoyer P, Arar K, Lehmann-Che J, Eyquem S, Himber C, Saib A, Vionnet O. A cellular microRNA mediates antiviral defense in human cells. Science 2005; 308: 557-560.

Lee Y, Ahn C, Choi, Kim J, Yim J, Lee Junho, Provost P, Radmark O, Kim S and Kim VN. The nuclear RNase III Drosha initiates microRNA processing. Nature 2003; 425: 415-419

Lee YS, Nakahara K, Pham JW, Kim K, He Z, Sontheimer EJ, Carthew RW. Distinct roles for *Drosophila* Dicer-1 and Dicer-2 in the siRNA/miRNA silencing pathway. Cell 2004; 117: 69-81.

Li HW and Ding SW. Antiviral silencing in animals. FEBS 2005; 579: 5965-5973.

Li Z, Xiong F, Lin Q, d'Anjou M, Daugulis AJ, Yang DS. Low temperature increases the yield of biologically active herring antifreeze protein in *Pichia pastoris.* Protein Expr Purif 2001; 21: 438-445.

Lingel A, Izaurralde E. RNAi: finding the elusive endonuclease. RNA 2004; 10: 1675-1679.

Lingel A, Simon B, Izaurralde E, Sattler M. Nucleic acid 3'-end recognition by the Argonaute 2 PAZ domain. Nat Struct Mol Biol 2004; 11: 576-577

Lingel A, Simon B, Izaurralde E, Sattler M. Structure and nucleic-acid binding of the *Drosophila* Argonaute 2 PAZ domain. Nature 2003; 426: 465-469.

Little TJ, Hultmark D, Read A. Invertebrate immunity and the limits of mechanistic immunology. Nature Immunology 2005; 6; 651-654.

Liu J, Camell MA, Rivas FV, Marsden CG, Thomson M, Song JJ, Hammond SM, Joshua-Tor L, Hannon GJ. Argonaute 2 is the catalytic engine of mammalian RNAi. Science 2004; 305: 1437-1441.

Liu Q, Rand TA, Kalidas S, Du F, Kim HE, Smith DP, Wang X. R2D2, a bridge between the initiation and effector steps of the *Drosophila* RNAi pathway. Science 2003; 301: 1921-1925.

Lu R, Maduro M, Li F, Li HW, Broitman-Maduro G, Li WX, Ding SW. Animal virus replication and RNAi-mediated antiviral silencing in *Caenorhabditis elegans*. Nature 2005; 436:1040-1043.

Lund E, Gottinger S, Calado A, Dahlberg JE, Kutay U. Nuclear export of microRNA precursors. Science 2004; 303: 95-98.

Ma JB, Ye K, Patek DJ. Structure basis for overhang specific small interfering RNA recognition by the PAZ domain. Nature 2004; 429: 318-322.

Ma JB, Yuan YR, Meister G, Pei Y, Tuschl T, Patel DJ. Structural basis for 5' –end-specific recognition of guide RNA by the *A. fulgidus* Piwi protein. Nature 2005; 434: 666-671.

Macrae IJ, Zhou K, Li F, Repic A, Brooks AN, Cande WZ, Adams PD, Doudna JA. Structural basis for double-stranded RNA processing by Dicer. Science 2006; 311: 195-198.

Martinez J, Patkaniowska A, Urlaub H, Luhrmann R and Tuschl T. Single-stranded antisense siRNAs guide target RNA cleavage in RNAi. Cell 2002; 110: 563-574.

Martinez J, Tuschl T. RISC is a 5' phosphomonoester-producing RNA endonuclease. Genes Dev 2004; 18: 975-980.

Meister G, Landthaler M, Dorsett Y, Tuschl T. Sequence-specific inhibition of microRNA- and siRNA-induced RNA silencing. RNA 2004; 10: 544-550.

Meister G, Landthaler M, patkaniowska A, Dorsett Y, Teng G, Tuschl T. Human Argoaute 2 mediates RNA cleavage targeted by miRNAs and siRNAs. Mol Cell 2004; 15: 158-197.

Meister G, Landthaler M, Peters L, Chen PY, Urlaub H, Luhrmann R, Tuschl T. Identification of novel Argonaute-associated proteins. Curr Biol 2005; 15: 1-7.

Meister G, Tuschl T. Mechanisms of gene silencing by double-stranded RNA. Nature 2004; 431: 343-349.

Mette MF, Aufsatz W, van der Winden J, Matzke MA, Matzke AJ. Transcriptional silencing and promoter methylation triggered by double-stranded RNA. EMBO 2000; 19: 5194-5201.

Miyoshi K, Tsukumo H, Nagami T, Siomi H and Siomi MC. Slicer function of *Drosophila* Argonautes and its involvement in RISC formation. Genes dev 2005; 19: 2837-2848.

Morel JB, Godon C, Mourrain P, Beclin C, Boutet S, Feuerbach F, Proux F, Vaucheret H. Fertile hypomorphic ARGONAUTE (ago1) mutants impaired in post-transcriptional gene silencing and virus resistance. Plant Cell 2002; 14: 629-639.

Napoli C, Lemieux C, Jorgensen R. Introduction of a chalcone synthase gene into Petunia results in reversible co-suppression of homologous genes *in trans*. Plant Cell 1990; 2: 279-289.

Novina CD, Sharp PA. The RNAi revolution. Nature 2004; 430: 161-164.

Nykanen A, B Haley, Zamore PD. ATP requirement and small interfering RNA structure in the RNA interference pathway. Cell 2001; 107: 309-321.

Ohler U, Yekta S, Lim LP, Bartel DP, Burge CB. Patterns of flanking sequence conservation and a characteristic upstream motif for microRNA gene identification. RNA 2004; 10: 1309-1322.

Okamura K, Ishizuka A, Siomi H, Siomi MO. Disinct roles for Argonaute proteins in small RNA-directed RNA cleavage pathways. Gene Dev 2004; 18: 1655-1666.

Pal-Bhadra M, Bhadra U, Birchler JA. RNAi related mechanisms affect both transcriptional and posttranscriptional transgene silencing in *Drosophila.* Mol Cell 2002; 9: 315-327.

Parker JS, Roe SM, Barford D. Crystal structure of a PIWI protein suggests mechanisms for siRNA recognition and slicer activity. EMBO 2004; 23: 4727-4737.

Parker JS, Roe SM, Barford D. Structural insights into mRNA recognition from a PIWI domain-siRNA guide complex. Nature 2005; 434: 663-666.

Pasquinelli AE, Ruvkun G. Control of developmental timing by microRNA and their targets. Annu Rev Cell Biol 2002; 18: 495-513.

Pasquinelli AE, Reinhart BJ, Slack F, Martindale MQ, Kuroda MI, Maller B, Hayward DC, Ball EE, Degnan B, Muller P, Spring J, Srinivasan A, Fishman M, Finnerty J, Corbo J, Levine M, Leahy P, Davidson E, Ruvkun G. Conservation of the sequence and temporal expression of let-7 heterochronic regulatory RNA. Nature 2000; 408: 86-89.

Pham JW, Sontheimer EJ. Molecular requirements for RNA-induced silencing complex assembly in the *Drosophila* RNA interference pathway. J Biol Chem 2005; 280: 39278-39283.

Plasterk RH. RNA silencing: The genome's immune system. Science 2002; 296: 1263-1265.

Provost P, Silverstein RN, Dishart D, Walfridsson J, Djupedal I,Kniola B, Wright A, Samuelsson B, Radmark P, Ekwall K. Dicer is required for chromosome segregation and gene silencing in fission yeast cells. Proc Natl Acad Sci USA 2002; 99: 16648-16653.

Provost P, Dishart D, Doucet J, Frendewey D, Samuelsson B, Radmark O. Ribonuclease activity and RNA binding of recombinant human Dicer. EMBO 2002; 21: 5864-5874.

Rand TA, Ginalski K, Grishin N, Wang X. Biochemical identification of Argonaute 2 as the sole protein required for RNA-induced silencing complex activity. PNAS 2004; 101: 14385-14389.

Rand TA, Petersen S, Du F and Wang X. Argonaute 2 cleaves the anti-guide strand of siRNA during RISC activation. Cell 2005; 123: 621-629.

Reinhart BJ, Bartel DP. Small RNAs correspond to centromeric heterochromatin repeats. Science 2002; 297: 1831.

Rivas FB, Tolia NH, Song JJ, Aragon JP, Liu J, Hannon GJ, Joshua-Tor L. Purified Argonaute 2 and an siRNA form recombinant human RISC. Nature 2005; 12: 340-349.

Romanos M, Scorer C, Clare J. Expression on cloned gene in yeast. In: Glover DM, Hames BD, eds. A practical approach series: DNA cloning II. Expression system.2nd ed. New York: Oxford University. 1995.

Sasaki T, Shiohama A, Minoshima S, Shimizu N. Identification of eight members of the Argonaute family in the human genome. Genomics 2003; 82: 323-330.

Schwarz D, Tomari Y, Zamore P. The RNA-induced silencing complex is a Mg-dependent Endonuclease. Current Biology 2004; 14: 787-791.

Sigova A, Rhind N, Zamore PD. A single Argonaute protein mediates both transcriptional and posttranscriptional silencing in *Schizosaccharomyces pombe*. Genes Dev 2004; 18: 2359-2367.

Sigova A, Rhind N, Zamore PD. A single Argonaute protein mediates both transcriptional and posttranscriptional silencing in *Schizosaccharomyces pombe*. Genes Dev 2004; 18: 2359-2367.

Sijen T and Plasterk RHA. Transposon silencing in the *Caenorhabditis elegans* germ line by natural RNAi. Nature 2003; 426: 310-314.

Singh H, Sen R, Baltimore D and Sharp PA. A nuclear factor that binds to a conserved sequence motif in transcriptional control elements of immunoglobulin gene. Nature 1986; 319: 154-158.

Sithigorngul P, Chauychuwong P, Sithigorngul W, Longyant S, Chaivisuthangkura P and Menasveta P. Development of a monoclonal antibody specific to yellow heas virus (YHV) from *Penaeus monodon*. Disease of Aquatic organisms 2000; 42: 27-34.

Soderhall K and Thornqvist PO. Crustacean immunity- a short review. Fish Vaccinol. 1997; 90: 45-51

Song JJ, Liu J, Tolia NH, Schneiderman J, Smith SK, Martienssen RA, Hannon GJ, Joshua-Tor L. The crystal structure of the Argonaute PAZ domain reveals an RNA binding motif in RNAi effector complexes. Nature 2003; 10: 1026-1032.

Song JJ, Smith SK, Hannon GJ, Joshua-Tor L. Crystal Structure of Argonaute and Its Implications for RISC Slicer Activity. Science 2004; 305: 1434-1437.

Sontheimer EJ. Assembly and function of RNA silencing complexes. Nat Rev Mol Cell Biol 2005; 6: 1434-1437.

Stram Y, Kuzntzova L. Inhibition of viruses by RNA interference. *Virus Genes* 2006; 32(3):299-306.

Tabara H, Sarkissian M, Kelly WG, Fleenor J, Grishok A, Timmons L, Fire A and Mello CC. The rde-1 gene, RNA interference, and transposon silencing in *C. elegans*. Cell 1999; 99: 123-132.

Tang G. siRNA and miRNA: an insight into RISCs. Trends Biochem Sci. 2005; 30: 106-114.

Tang KFJ, Lightner DV. A yellow head virus gene probe: nucleotide sequence and application for in situ hybridization. Disease of Aquatic Organisms 1999; 35: 165-173.

Theobld DL, Mitton-Fry RM, Wuttke DS. Nucleic acid recognition by OB-fold proteins. Annu. Rev Biophys Biomol. Stuct. 2003; 32: 115-133

Thepparit C. Molecular cloning and sequencing of cDNA's of black tiger shrimp haemocytes. [M.Sc. Thesis in Molecular Genetic-Genetic Engineering]. Bangkok: Faculty of Graduate Studies, Mahidol University; 2001

Tirasophon W, Roshom Y, Panyim S. Silencing of yellow head virus replication in penaeid shrimp cells by dsRNA. BBRC 2005; 334: 102-107

Tomari Y, Zamore PD. Perspective: machines for RNAi. Genes Dev 2005; 19: 517-529.

Traci M and Tanaka H. Structure and Function of Argonaute Protein. Structure 2005; 13: 1403-1408.

Treerattrakool S, Eurwilaichitr L, Udomkit A, Panyim S. Secretion of Pem-CMG, a peptide in the CHH/MIH/GIH family of *Penaeus monodon*, in *Pichia pastoris* is detected by secretion signal of the a-mating factor from *Saccharomyces cerevisiae*. J Biochem Mol Biol 2002; 35: 476-481.

Tuschl T, Meister G. Mechanisms of gene silencing by double-stranded RNA. Nature 2004; 431: 343-349.

Tuschl T, Zamore PD, Lehmann R, Bartel DP, Sharp PA. Targeted mRNA degradation by double-stranded RNA in vitro. Gene Dev 1999; 13: 3191-3197.

Uprichard SL. The therapeutic potential of RNA interference. FEBS 2005; 579: 5996-6007.

Verdel A, Jia S, Gerber S, Sugiyama T, Gygi S, Grewal SI, Moazed D. Size selective recognition of siRNA by and RNA silencing suppressor. Cell 2003; 115: 799-811.

Verdel A, Moazed D. RNAi-directed assembly of heterochromatin in fission yeast. FEBS 2005; 579: 5872-5878.

Voinnet O. RNA silencing as a plant immune system against viruses. Trends Genet 2001; 17: 449-459.

Volpe TA, Kidner C, Hall IM, Teng G, Grewal SI, Martienssen RA. Regulation of heterochromatin silencing and histone H3 lysine-9 methylation by RNAi. Science 2002; 297: 1833-1837.

Wassenegger M, Heimes S, Riedel L, Sanger HL. RNA-directed de novo methylation of genomic sequences in plants. Cell 1994; 76: 567-576.

Wassenegger M, Krczal G. Nomenclature and functions of RNA-directed RNA polymerases. Trends Plant Sci 2006; 11: 142-151.

Wassenegger M. The role of the RNAi machinery in heterochromatin formation. Cell 2005; 122: 13-16.

Waterhouse PM, Wang MB, Lough T. Gene silencing as an adaptive defence against viruses. Nature 2001; 411: 834-842.

Wienholds E, Plasterk RHA. MicroRNA function in animal development. FEBS Lett 2005; 579: 5911-5922.

Wightman B, Ha I, Ruvkun G. Posttranscriptional regulation of the heterochronic gene lin-14 by lin-14 mediates temporal pattern formation in *C. elegans*. Cell 1993; 75: 855-862.

Williams RW, Rubin GM. ARGONAUTE 1 is required for efficient RNA interference in *Drosophila* embryos. PNAS 2002; 99: 6889-6894.

Witteveldt J, Cifuentes CC, Vlak JM, Van Hulten MCW. Protection of *Penaeus monodon* against white spot syndrome virus by oral vaccination. J. Virol 2004; 78: 2057-2061.

Yadava A, Ockenhouse CF. Effect of codon optimization on expression levels of a functionally folded malaria vaccine candidate in Prokaryotic and Eukaryotic expression systems. Infection and Immunity 2003; 71: 4961-4969.

Yan KS, Yan S, Farooq A, Han A, Zeng L, Zhou MM. Structure and conserved RNA binding of the PAZ domain. Nature 2003; 426: 469-474.

Yang D, Lu H, Erickson JW. Evidence that processed small dsRNAs may mediate sequence-specific mRNA degradation during RNAi in *Drosophila* embryos. Curr Biol 2000; 10: 1191-1200.

Ye Keqiong, Malinina L, Patel DJ. Recognition of small interfering RNA by a viral suppressor of RNA silencing. Nature 2003; 426: 874-877.

Yi R, Qin Y, Macara IG, Cullen BR. Exportin-5 mediates the nuclear export of pre-microRNAs and short hairpin RNAs. Genes Dev. 2003; 17: 3011-3016.

Yodmuang S, Tirasophon W, Roshom Y, Chinnirunvong W, Panyim S. YHV-protease dsRNA inhibits YHV replication in *Penaeus monodon* and prevent mortality. Biochem Biophys Res Commun. 2006; 341: 351-356.

Yodnuang S. Molecular characterization and biological assays of a putative Molt-Inhibiting Hormone of *Penaeus monodon.* [M.Sc. Thesis in Molecular Genetic-Genetic Engineering]. Bangkok: Faculty of Graduate Studies, Mahidol University; 200Faculty of Graduate Studies, Mahidol University. 2003

Yuan YR, Pel Y, Ma JB, Kuryavyl V, Zhadina M, Meister G, Chen HY, Dauter Z, Tuschl T, Patel D. Crystal structure of. *aeolicus* Argonaute, a site-specific DNA-guided endoribonuclease, provides insights into RISC-mediated mRNA cleavage. Molecular Cell 2005; 19: 405-419.

Zamore PD, Haley B. Ribo-gnome: the big world of small RNAs. Science 2005; 309: 1519-1524.

Zamore PD, Tuschl T, Sharp PA, Bartel DP. RNAi: Double-stranded RNA directs the ATP-dependent cleavage of mRNA at 21 to 23 nucleotides intervals. Cell 2000; 101: 25-33.

Zeng Y and Cullen BR. Efficient processing of primary microRNA hairpins by Drosha requires flanking non-structured RNA sequences. J Biol Chem 2005; 280: 27595-27603.

Zeng Y, Yi R, Cullen BR. Recognition and cleavage of primary microRNA precursors by the nuclear processing enzyme Drosha. EMBO J 2005; 24: 138-148.

Zhang H, Kolb FA, Brondani V, Billy E, Filipowicz W. Human Diver preferentially cleaves dsRNAs at their termini without a requirement for ATP. EMBO 2002; 21: 5875-5885.

Zhang H, Kolb FA. Jaskiewicz L, Westhof E, Filipowicz W. Single processing center models for human Dicer and bacterial RNase III. Cell 2004; 118: 57-68.

APPENDIX

APPENDIXS

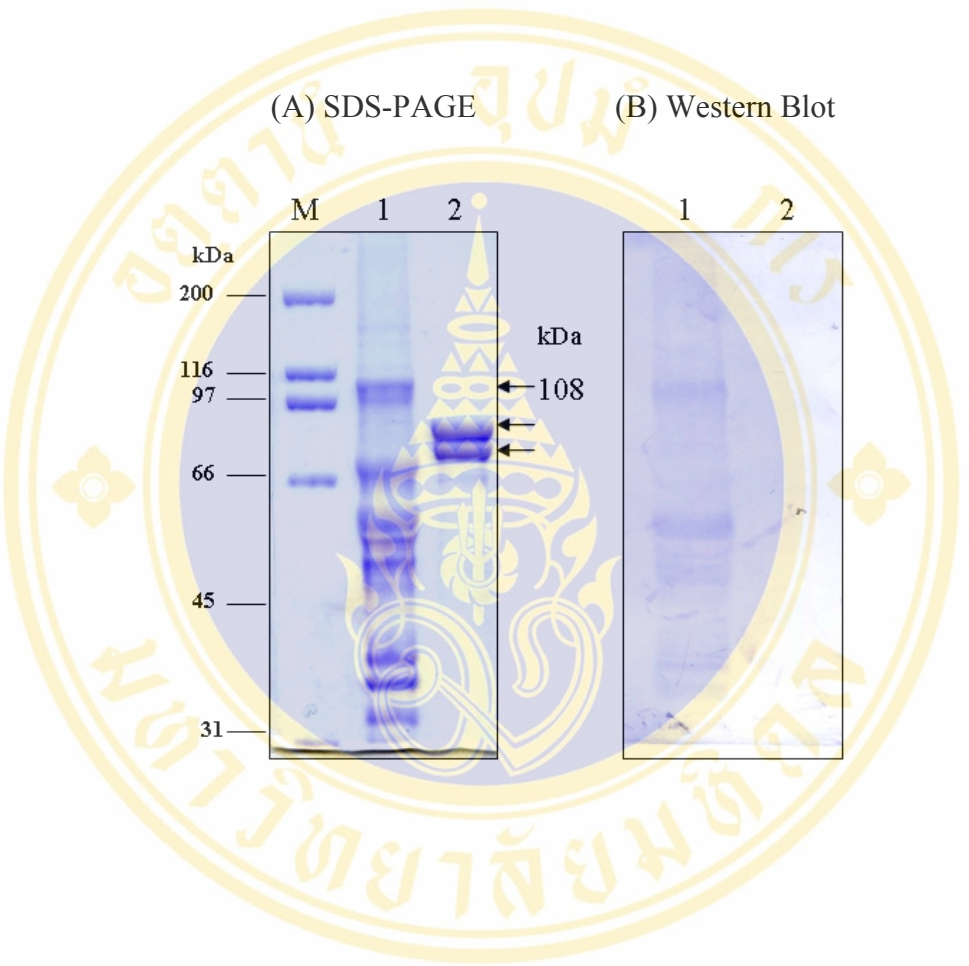

Appendix 1. SDS-PAGE and Western Blot Analysis of *P. monodon*'s Lymphoid Protein Extract

The figures represent 10 % SDS-PAGE (A) and Western Blot analysis with anti-PAZ antibody (B).

Lane M : Standard broad range protein marker

Lane 1 : 15 μg of purified proteins from Ni^{2+} column

Lane 2 : 10 μg of *P. monodon*'s lymphoid extract

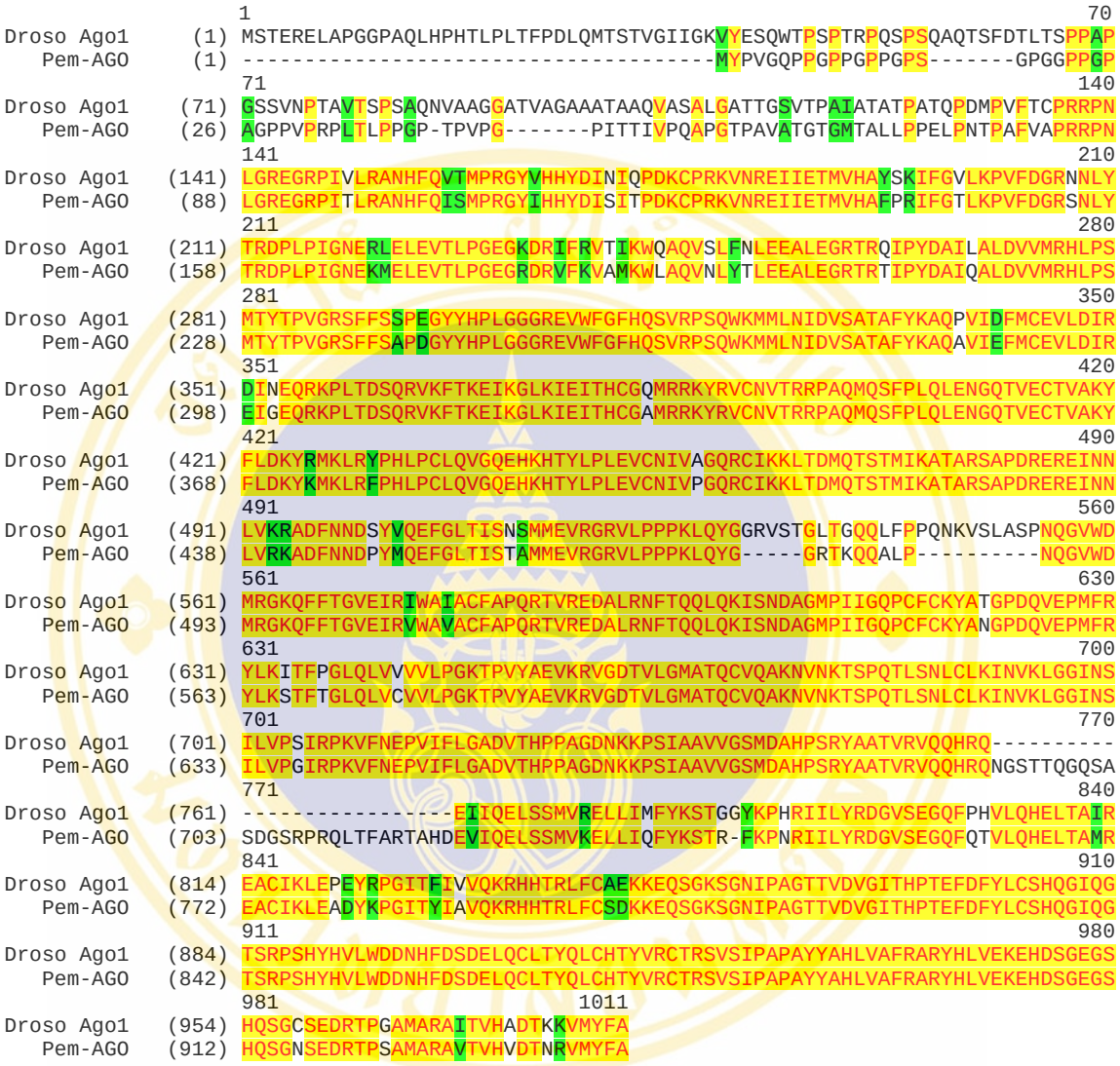

Appendix 2. The alignment between amino acid sequences of *Drosophila* Ago1 and Pem-AGO

The alignment result illustrates that the deduced amino acid sequence of Pem-AGO exhibits 77.2 % identity to a corresponding amino acid sequence of *Drosophila* Ago1 (Droso Ago1). The amino acid residues that are identical are highlight in pale gray whereas the dark gray highlights indicate charge similarity.

```
                1                                                                                                   70
Droso Ago2      (1) MGKKDKNKKGGQDSAAAPQPQQQQKQQQQRQQQPQQLQQPQQLQQPQQLQQPQQQQQQQPHQQQQQSSRQ
   Pem-AGO      (1) ------------------------------------------------------------------------
                   71                                                                                              140
Droso Ago2     (71) QPSTSSGGSRASGFQQGGQQQKSQDAEGWTAQKKQGKQQVQGWTKQGQQGGHQQGRQGQDGGYQQRPPGQ
   Pem-AGO      (1) ------------------------------------------------------------------------
                  141                                                                                              210
Droso Ago2    (141) QQGGHQQGRQGQEGGYQQRPPGQQQGGHQQGRQGQEGGYQQRPSGQQQGGHQQGRQGQEGGYQQRPPGQQ
   Pem-AGO      (1) ------------------------------------------------------------------------
                  211                                                                                              280
Droso Ago2    (211) QGGHQQGRQGQEGGYQQRPSGQQQGGHQQGRQGQEGGYQQRPPGQQQGGHQQGRQGQEGGYQQRPPGQQQ
   Pem-AGO      (1) ----------------MYPVGQPPG----------------PPG--------------------PPG---
                  281                                                                                              350
Droso Ago2    (281) GGHEQGRQGQEGGYQQRPSGQQQGGHQQGRQGQEGGYQQRPSGQQQGGHQQGRQGQEGGYQQRPSGQQQG
   Pem-AGO     (16) -----------------PSG--------------------PGGPP---------GPAGPPVPRPLTLPPG
                  351                                                                                              420
Droso Ago2    (351) GHQQGRQGQEGGYQQRPPGQQPNQTQSQGQYQSRGPPQQQQAAPLPLPPQPAGSIKRGTIGKPGQ-VGIN
   Pem-AGO     (40) -----PTPVPGPITTIVPQAPGTPAVATGTGMTALLPPELPNTPAFVAP------RRPNLGREGRPITLR
                  421                                                                                              490
Droso Ago2    (420) YLDLDLSKMPSVAYHYDVKIMPER-PKKFYRQAFEQFR---VDQLGGAVLAYDGKASCYSVDKLPLNSQN
   Pem-AGO     (99) ANHFQISMPRGYIHHYDISITPDKCPRKVNREIIETMVHAFPRIFGTLKPVFDGRSNLYTRDPLPIGNEK
                  491                                                                                              560
Droso Ago2    (486) PEVTVTDRNGRTLRYTIEIKETGDSTIDLKSLTTYMNDRIFDKPMRAMQCVEVVLASPCHNKAIRVGRSF
   Pem-AGO    (169) MELEVTLP-GEGRDRVFKVAMKWLAQVNLYTLEEALEGRTRTIPYDAIQALDVVMRHLPSMTYTPVGRSF
                  561                                                                                              630
Droso Ago2    (556) FKMSDPNNRHELDDGYEALVGLYQAFMLG-DRPFLNVDISHKSFPISMPMIEYLERFSLKAKINNTTN--
   Pem-AGO    (238) FSAPDG-YYHPLGGGREVWFGFHQSVRPSQWKMMLNIDVSATAFYKAQAVIEFMCEVLDIREIGEQRKPL
                  631                                                                                              700
Droso Ago2    (623) LDYSRRFLEPFLRGINVVYTPPQSFQSAPRVYRVNGLSRAPASSETFEHDG-----KKVTIASYFHSR-N
   Pem-AGO    (307) TDSQRVKFTKEIKGLKIEITHCG---AMRRKYRVCNVTRRPAQMQSFPLQLENGQTVECTVAKYFLDKYK
                  701                                                                                              770
Droso Ago2    (687) YPLKFPQLHCLNVGSSIKSILLPIELCSIEEGQALNRKDGATQVANMIKYAATSTNVRKRKIMNLLQYFQ
   Pem-AGO    (374) MKLRFPHLPCLQVGQEHKHTYLPLEVCNIVPGQRCIKKLTDMQTSTMIKATARSAPDRERIINNLVRKAD
                  771                                                                                              840
Droso Ago2    (757) HNLDPTISRFGIRIANDFIVVSTRVLSPPQVEYHSKRFTMVK--NGSWRMDGMKFLEPKPKAHKCAVLYC
   Pem-AGO    (444) FNNDPYMQEFGLTISTAMMEVRGRVLPPPKLQYGGRTKQQALPNQGVWDMRGKQFFTGVEIRVWAVACFA
                  841                                                                                              910
Droso Ago2    (825) DPRSGRKMNYTQLNDFGNLIISQGKAVNISLDSDVTYRPFTDDERSLDTIFADLKR--SQHDLAIVIIPQ
   Pem-AGO    (514) PQRTVR---EDALRNFTQQLQKISNDAGMPIIGQPCFCKYANGPDQVEPMFRYLKSTFTGLQLVCVVLPG
                  911                                                                                              980
Droso Ago2    (893) FRISYDTIKQKAELQHGILTQCIKQFTVERKCNNQTIGNILLKINSKLNGINHKIKDDPRLPMMKN-TMY
   Pem-AGO    (581) KTPVYAEVKRVGDTVLGMATQCVQAKNVN-KTSPQTLSNLCLKINVKLGGINSILVPGIRPKVFNEPVIF
                  981                                                                                             1050
Droso Ago2    (962) IGADVTHPSPDQREIPSVVGVAASHDPYGASYNMQYRLQRG-------------------------AL
   Pem-AGO    (650) LGADVTHPPAGDNKKPSIAAVVGSMDAHPSRYAATVRVQQHRQNGSTTQGQSASDGSRPRQLTFARTAHD
                 1051                                                                                             1120
Droso Ago2   (1005) EEIEDMFSITLEHLRVYKEYRNAYPDHIIYYRDGVSDGQFPKIKNEELRCIKQACDKVG--CKPKICCVI
   Pem-AGO    (720) EVIQELSSMVKELLIQFYKSTRFKPNRIILYRDGVSEGQFQTVLQHELTAMREACIKLEADYKPGITYIA
                 1121                                                                                             1190
Droso Ago2   (1073) VVKRHHTRFFPSGDVTTSNKFNNVDPGTVVDRTIVHPNEMQFFMVSHQAIQGTAKPTRYNVIENTGNLDI
   Pem-AGO    (790) VQKRHHTRLFCSDKKEQSGKSGNIPAGTTVDVGITHPTEFDFYLCSHQGIQGTSRPSHYHVLWDDNHFDS
                 1191                                                                                             1260
Droso Ago2   (1143) DLLQQLTYNLCHMFPRCNRSVSYPAPAYLAHLVAARGRVYLTG-----------TNRFLDLKKEYAKRTI
   Pem-AGO    (860) DELQCLTYQLCHTYVRCTRSVSIPAPAYYAHLVAFRARYHLVEKEHDSGEGSHQSGNSEDRTPSAMARAV
                 1261     1273
Droso Ago2   (1202) VPEFMKKNPMYFV
   Pem-AGO    (930) TVHVDTNRVMYFA
```

Appendix 3. The alignment between amino acid sequences of *Drosophila* Ago2 and Pem-AGO

The alignment result illustrates that the deduced amino acid sequence of Pem-AGO exhibits 21.8 % identity to a corresponding amino acid sequence of *Drosophila* Ago2 (Droso Ago2). The amino acid residues that are identical are highlight in pale gray whereas the dark gray highlights indicate charge similarity.

BIOGRAPHY

NAME Miss. Narakorn Khunweeraphong

DATE OF BIRTH 12 March 1980

PLACE OF BIRTH Chumphon, Thailand

INSTITUTIONS ATTENDED Mahidol University, 1997-2001
Bachelor of Science
(Medical Technology)

Mahidol University, 2004-2006
Master of Science
(Molecular Genetics and Genetic Engineering)

HOME ADDRESS 78 M.2 Chontheethawara Rd.
Paknam, Muang,
Chumphon, Thailand 86120

E-MAIL narakorntom@gmail.com